WA School of Mines: Minerals, Energy and Chemical Engineering

Curtin University

Advanced downhole geophysical monitoring of subsurface changes with fibre-optic sensors.

Evgenii Sidenko

This thesis is presented for the Degree of
Doctor of Philosophy
of
Curtin University of Technology

December 2022

Declaration

To the best of my knowledge and belief this thesis contains no material previously published by any other person except where due acknowledgement has been made. This thesis contains no material which has been accepted for the award of any other degree or diploma in any university.

Evgenii Sidenko

Signature:

Date: 13/12/2022

Abstract

Distributed Fibre-Optic Sensing is a fast-developing technology and is being actively used in geophysical monitoring applications. The technology is based on continuous measurements along a fibre-optic cable. Distributed temperature sensing (DTS) is used for measuring and monitoring temperature while distributed acoustic sensing (DAS) can record seismic waves/signals that induce axial strain in the cable.

Compared to 4D surface seismic monitoring, repeated Vertical Seismic Profiling (VSP) surveys with DAS receivers reduce the cost and invasiveness of time-lapse CO_2 monitoring considerably, but have limited spatial coverage around the borehole. This coverage can be extended by interferometric imaging that utilises free-surface multiples. Synthetic and field studies demonstrate that interferometric imaging is a viable method to extend the subsurface image beyond the coverage of standard VSP imaging. Comparison of the standard and engineered fibers shows that both fibers are sensitive to free-surface multiples, but the engineered fiber provides much higher signal to noise ratio, and thus is preferable for interferometric imaging with multiples. The results obtained with the engineered DAS cable show that in the depth range suitable for both methods, the VSP interferometric image of reflectors is comparable to the surface seismic image.

Borehole-based DTS and DAS utilized for continuous monitoring of borehole decommissioning operations reveal an abundance of valuable information about the course of the decommissioning process and the quality of the cement job. DAS has detected vibrational disturbances during the cement's setting up, while

DTS was used to assess setting up of the cement and curing times as well as uniformity of cementation from the distribution of temperature along the borehole. Passive DAS data recorded a year later with the same array shows an abundance of seismic events in a wide frequency range from below 1 mHz to over 200 Hz and includes earthquakes, mine blasts, ocean microseisms, and local human activity. The amplitudes of waves from distant seismic events can be used to estimate and monitor physical properties of the media along the entire extent of the well. Spectral analysis of low frequency microseisms shows a strong correlation between passively recorded DAS and local weather observations. Detected peculiar in-hole reverberations are likely caused by crossflows of groundwater behind the intermediate casing, which may indicate imperfections of the cement job. The results demonstrate that downhole fibre-optic array installed in an abandoned well represents an opportunity to establish a permanent facility for continuous recording of passive and active geophysical data and for exploring various applications.

DAS measurements are also sensitive to temperature changes. Laboratory and field tests of DAS sensitivity to changing temperature demonstrate that DAS is sensitive to long-period temperature changes and its response is proportional to the time derivative of temperature. Induced fiber strain is linearly related to slow temperature change and this dependency can be estimated for a particular cable. The results can help compensate for the effect of temperature on low-frequency DAS signal and show that DAS can be used as a distributed temperature sensor if direct temperature measurements are not available.

Most DAS systems are designed to measure signals higher than 1 Hz; however some DAS systems are sensitive to low-frequency (< 1 Hz) signals such as reservoir pressure variations. During CO_2 injection within the CO2CRC Otway Project, pressure related strain-rate DAS signals were observed in two monitoring wells. These signals are highly correlated with the pressure signals measured by borehole pressure gauges above the perforations in monitoring wells. Analysis of the data shows that DAS is able to detect reservoir pressure variations higher than 10^{-4}

psi/s. Analysis of pressure variations and strain calculated from DAS strain rate values allows estimation of the elastic modulus of the reservoir formation. Obtained results show that DAS systems can be utilised not only as seismic sensors, but also as continuous pressure sensors that can help track possible CO_2 leakages into the overburden. In contrast to traditional pressure gauges, DAS is capable of tracking the pressure profile along the entire well. DAS pressure sensing capabilities open up many new applications to complement subsurface reservoir pressure monitoring, CCUS and hydrogeological studies.

Acknowledgements

First of all, I would like to acknowledge my main Supervisor, Prof. Roman Pevzner, who has been guiding me through my entire Ph.D. studies. I thank Roman for the support, for the organisation of the fieldtrips, for improving my IT related skills, for the freedom to implement my own ideas, and for constructed criticism that was always aimed to improve the quality of the research. I am also very grateful to my co-supervisors – Prof. Andrej Bona and Dr. Konstantin Tertyshnikov. I thank Prof. Andrej Bona, who was helping me to design workflows, implement geophysical theory in the research and help in gaining practical skills in preparation of optical fibres. I thank Dr. Konstantin Tertyshnikov for organisation of data collection and field trips, for useful advice on many aspects of my research, and for reviewing my publications.

I want to sincerely thank Prof. Boris Gurevich for the help in publication of all my written work, for the proofreading of all my written work, for the significant improvement of my scientific writing skills, for interesting and helpful discussions of the research matters and for being a major driving force of science in our school.

I thank Prof. Maxim Lebedev for the help in organising the laboratory study and acquiring laboratory data. I thank Dr. Stanislav Glubokovskikh for valuable help and for our work together. I thank Dr. Sinem Yavuz for her support and many organisational matters. I thank Dr. Ludovic Ricard from CSIRO for his help with DTS data. I thank Murray Hehir and Dominic Howman for the help in gaining practical fieldwork skills and for making the geophysical data collection

possible, fun, and easy.

I wish to thank other Curtin University staff members - Prof. Milovan Urosevic, Robert Verstandig, Lee Ignacio, Nichole Sik, Dr. Vasilii Michalevitch, Pavel Shashkin; and students - Dr. Anton Egorov, Dr. Dmitry Popik, Dr. Alexey Yurikov, Roman Isaenkov, Sana Zulic, Dr. Jiabin Liang for their help in different occasions.

I want to acknowledge Prof. Claus Otto and Curtin Oil and Gas Innovation Centre for the Ph.D. scholarship. Also, I would like to acknowledge CO2CRC for providing financial support towards this Ph.D. program. Funding for CO2CRC Otway Project is provided through its industry members and research partners, the Australian Government under the CCS Flagships Programme, the Victorian State Government and the Global CCS Institute. CO2CRC received financial assistance provided through Australian National Low Emissions Coal Research and Development. ANLEC R&D is supported by Low Emission Technology Australia (LETA) and the Australian Government through the Department of Industry, Science, Energy and Resources. Stage 3 of the Project was additionally funded by BHP. Landowners and the Moyne Shire community (Victoria, Australia) are also acknowledged for the support of the Project.

Finally, I want to thank my wife – Sofya Popik, for always being there to help and support.

This research is supported by an Australian Government Research Training Program (RTP) Scholarship.

List of Publications included in this thesis

1. Sidenko, E., Tertyshnikov, K., Bona, A. and Pevzner, R. (2021). DAS-VSP interferometric imaging: CO2CRC Otway Project feasibility study. *Interpretation, 9*(4), SJ1-SJ12.

2. Sidenko, E., Tertyshnikov, K., Gurevich, B., Isaenkov, R., Ricard, L.P., Sharma, S., Van Gent, D. and Pevzner, R. (2022). Distributed fibre-optic sensing transforms an abandoned well into a permanent geophysical monitoring array: a case study from Australian South West. *The Leading Edge, 41*(2), 140-148.

3. Sidenko, E., Tertyshnikov, K., Lebedev, M. and Pevzner, R. (2022). Experimental study of temperature change effect on distributed acoustic sensing continuous measurements. *Geophysics, 87*(3), D111-D122.

4. Sidenko, E., Tertyshnikov, K., Gurevich, B. and Pevzner, R. (2022). DAS signature of reservoir pressure changes caused by a CO_2 injection: experience from the CO2CRC Otway Project. *International Journal Of Greenhouse Gas Control, 119*, 103735.

Statement of candidate about the contribution of co-authors

I am the first author of all the publications included in this thesis. Each of these publications were based on the work in which I was the principle researcher, but which included collaboration with my co-authors. I wrote the papers independently, but receiving technical advice and review comments from my co-authors. Please see comments of my co-authors in Appendix A.

Contents

Chapter 1

Introduction and Overview

1.1 Background and motivation

Industries such as Oil and Gas, Geothermal Energy, Carbon Capture and Storage (CCS) often require monitoring of changes in the subsurface caused by extraction or injection of fluids. Oil and Gas industry traditionally implements monitoring of underground gas storages (Forgues et al., 2007; Mari et al., 2011) or oil and gas reservoirs to improve the efficiency of the production wells (Djuraev et al., 2017) and monitoring of gas. Geothermal industry uses subsurface monitoring as a reservoir management and safety management tool (Darnet et al., 2020; Edwards et al., 2015; Pankow et al., 2020). CCS industry, being focused on the injection of CO_2 deep underground, needs the monitoring to control the injected underground gas behavior and to prevent possible leaks (Eiken et al., 2011).

In order to address all the mentioned problems, industries implement various monitoring technologies. One of them is geophysical monitoring.

1.1.1 Geophysical monitoring

Geophysical monitoring includes several geophysical techniques that measure or estimate changes of physical properties of the subsurface over time. Monitoring methods vary with the type of wavefield utilised for the measurements (electro-magnetic, magnetic, gravimetric, seismic) and with the type of geophysical sources and receivers utilised to create or measure the response from the subsurface.

Geophysical land monitoring surveys can be implemented on the surface – surface methods, or in the borehole – downhole methods. Surface methods are more widespread as they do not require drilling monitoring boreholes, which can be very expensive.

Monitoring that utilises reflected seismic waves emitted by surface seismic sources and recorded by surface receivers is called 4D seismic (Lumley, 2001, 2010). 4D seismic is the most reliable geophysical method for the exploration and

monitoring of sedimentary basins as it can provide the highest possible spatial resolution compared to other geophysical methods. Land 4D seismic typically uses Vibroseis as the seismic source and geophones as seismic receivers. 4D seismic monitoring has become an important geophysical tool to monitor injected CO_2 due to its superior spatial resolution.

1.1.2 Limitation of land seismic monitoring

Even though time-lapse surface seismic is the most reliable geophysical method for monitoring of injected CO_2, this method has certain limitations. The main limitations of 4D surface seismic are:

- high cost of data acquisition compared to other geophysical techniques,
- long intervals between surveys due to the high cost and time required for data acquisition and processing,
- relatively high-level of invasiveness and, as a result, difficulties with access to sensitive areas to conduct multiple surveys,
- high level of noise caused by environmental processes and human activity on the surface.

The necessity to reduce the cost of frequent data acquisition motivates development of alternative techniques that would overcome or mitigate these issues and provide sufficient-quality images of the subsurface changes. Various improvements, for example buried receiver arrays (Shulakova et al., 2015), were introduced into the monitoring programs to increase repeatability of seismic surveys, decrease cost of monitoring program and reduce the impact on landowners.

1.1.3 Downhole monitoring

The need to overcome limitations of 4D surface seismic has resulted in the development of alternative monitoring strategies, such as borehole monitoring

using 3D vertical seismic profiling technique (VSP) (Correa et al., 2018; Lumley, 2010).

VSP is often implemented with surface seismic sources and borehole geophones (Hardage, 1985). VSP surveys with borehole sources and surface receivers are less common; this technique is called reverse VSP. VSP surveys have several advantages over the surface seismic: higher vertical resolution; smaller wavefield attenuation (as seismic waves travel shorter distances); less contamination with surface waves. In the standard VSP, the receivers are placed in the borehole and only seismic source effort required on the surface. Thus, the VSP method does not require any cable systems on the surface, and reduces the surface footprint of seismic monitoring (compared to surface seismic) and therefore makes seismic monitoring much less invasive, as there is no need to install seismic receivers (cables or node systems) on the surface.

However, traditional VSP requires frequent access to the borehole. This is the biggest challenge of the VSP method as the borehole operation time is usually very limited and expensive. Borehole geophones are relatively expensive (compared to surface geophones), so it is common to use a string of several geophones and move it along the borehole, repeating data acquisition at different levels to cover the entire length of the wellbore. This, of course, requires significant time effort. Another downside of VSP is that, like any other borehole method, it has limited reach away from the borehole, and illumination of the target varies strongly with the distance from the borehole. In addition, it is also impossible to use the same borehole as a receiver array and as the injector well (of CO_2, for example) if you need constantly move receivers along the well. This problem can be overcome by installing geophones behind the casing (Deflandre et al., 1995; Van Dok et al., 2016), but such installations are extremely expensive, and increase the well integrity risk, and hence used very rarely.

1.1.4 Distributed Acoustic Sensing (DAS)

The limitations of geophone VSP described above are largely overcome with the recent development of new seismic acquisition technology known as distributed acoustic sensing (DAS). DAS measures and records perturbations that induce dynamic strain (strain rate) in the fibre-optic cable. The measured strain rate can be converted into strain by integration over time. Dynamic strain measurements are different from static strain measurements that are used to track long-term slow strain variations.

Most DAS systems measure changes in differential phase of the backscattered light. These measurements can be implemented using different techniques – phase unwrapping, dual-pulse, interferometric phase recovery and others (Hartog, 2017). In seismic applications a DAS cable can act as an array of receivers replacing an array or geophones or hydrophones (Parker et al., 2014).

The use of fibre-optic cables as downhole sensors has substantial advantages over conventional downhole receivers. Most fibre-optic cables are very robust and reliable for long-term installations as they have no electronics or moving parts. Also, deployment of such cables in a well distributes sensors over its entire length at small spacing intervals. Fibre-optic cables can also be manufactured to withstand considerable pressure and temperature (up to 250 °C). The most sensitive and valuable instrument equipment – an optical interrogator unit – is always located at the surface and can be easily connected to the downhole cable and reconfigured to satisfy the measurement requirements. Such benefits make this technology a perfect option for borehole seismic monitoring applications and building permanent surveillance arrays in harsh environments like deep wells. Once deployed, fibre-optic cables can be used for Distributed Acoustic Sensing (DAS), Distributed Temperature Sensing (DTS) and other sensing applications. Permanently installed DAS receivers can make borehole monitoring even more flexible and cost-effective (Daley et al., 2013; Correa et al., 2019; Yurikov et al., 2021), because relatively inexpensive, and highly durable fibre optic cables enable

acquisition of seismic data of the quality similar to that of geophones (Correa et al., 2017). Permanently deployed optical fibre cables as receiver arrays in borehole reservoir surveillance considerably reduce the invasiveness of the seismic monitoring, and allow more frequent surveys, which is essential for the early detection of CO_2 leaks.

Permanent borehole DAS receivers coupled with surface orbital vibrators or SOVs (Dou et al., 2016; Freifeld et al., 2016), can be automated to collect and process seismic data continuously. Such monitoring system does not require any surface operations, except for maintenance (Isaenkov et al., 2021). Continuously recorded data allow tracking the subsurface changes without any time gaps.

1.1.5 Review of state of the art in downhole DAS monitoring

The most common implementations of downhole DAS monitoring are offset VSP and 3D VSP. Offset VSP involves only one source position (single source-receiver azimuth and offset), while 3D VSP involves multiple source positions around the well (which gives many combinations of source-receiver azimuths and offsets).

Despite many advantages of DAS VSP for subsurface monitoring, VSP subsurface coverage is limited by the half-offset between the well and surface source location (Galperin, 1985). Furthermore, it is hard to use traditional VSP monitoring for the shallow part of the well, as there are not enough reflections needed for imaging.

A significant advantage of DAS compared to traditional sensors such geophones and hydrophones is its very broad frequency range. DAS recordings are often used to study natural phenomena at frequencies far below 1 Hz such as distant earthquakes (Ajo-Franklin et al., 2019), oceanic microseisms (Lindsey et al., 2019; Glubokovskikh et al., 2021), or earth tides (Becker and Coleman, 2019). Low-frequency DAS is also being utilised in different industrial applica-

tions, such as hydraulic fractures geometry characterisation (Jin and Roy, 2017), low-frequency strain measurements (Becker et al., 2019), multiphase flow characterisation (Titov et al., 2020; Sharma et al., 2020), wellbore gas influx detection (Feo et al., 2020; Sharma et al., 2021), fluid pressure sensing (Becker et al., 2017), monitoring of well integrity (Raab et al., 2019) and borehole decommissioning operations (Ricard et al., 2019). DAS is also sensitive to slow strain variations, for instance, those caused by both natural and industrial processes such as diurnal atmospheric temperature variations, hydraulic fracturing treatments (Bakku et al., 2014; Karrenbach et al., 2017, 2019), borehole fluids flows (Sharma et al., 2020; Titov et al., 2020), temperature variations in geothermal reservoirs (Miller and Coleman, 2018) or pressure changes (Becker et al., 2017). These variations can distort low-frequency seismic records and thus need to be corrected for. Furthermore, the temperature or pressure response on DAS maybe useful in themselves. If these effects are well understood on DAS recordings, they can be extracted to provide useful additional information about subsurface processes. In some situations, for example, when there is no separate temperature measurements, such as distributed temperature sensing (DTS), DAS can be utilized for relative temperature monitoring as well (Koyamada et al., 2009; Bao and Wang, 2021).

As DAS technology is relatively new, its application for geophysical monitoring purposes is not fully studied yet. There are different research topics to be still covered such as: DAS directivity patterns, DAS sensitivity to passive seismic wavefield including low frequencies (< 1 Hz), effect of temperature variation on DAS measurements, ability of DAS systems to record reservoir pressure variations. Additionally, DAS recording abilities can vary between different manufacturers, as different engineering designs (optical path designs) affect the DAS response to disturbances applied to the fibre. Nevertheless, distributed fibre-optic sensing is gaining its popularity in the field of geophysical monitoring. It opens up many potential applications for geophysical exploration and CCUS industry.

The thesis addresses four different problems related to the borehole monitoring

using DAS:

1) Utilization of secondary wavefield, such as free-surface multiples, for improved borehole imaging – can we use multiples to extend subsurface coverage?

2) Continuous borehole monitoring of the well cementation process and analysis of ambient wavefield components – can we use borehole DAS to monitor borehole itself such as cementation process?

3) Effect of temperature variations on DAS measurements – can we compensate temperature related signal on DAS measurements and/or use DAS to estimate temperature variations?

4) Reservoir pressure signature on DAS – can we utilise DAS for reservoir pressure monitoring such as during CO_2 injection?

1.2 Objectives and outline

The general objective of this thesis is to study DAS capabilities to enhance VSP survey subsurface illumination using multiple reflections, to study DAS capabilities to record passive seismic signals (from natural and human-related sources) including low frequency signal, and to study temperature and pressure signatures on DAS in the borehole environment. These topics are covered in four published papers. Here I outline the main objectives from each paper.

Objective 1. Explore a possibility to improve subsurface illumination of VSP method using borehole DAS and free-surface multiples.

As discussed in the section 1.1, uneven illumination of the subsurface is a limitation factor for VSP monitoring. However, the illumination can be improved with interferometric migration of free-surface multiple reflections (Schuster, 2009; Yu and Schuster, 2004). Such interferometric migration was previously used for drill-bit source data or reverse VSP data acquired with surface receivers, as reverse VSP geometry provides better well coverage compared to standard VSP. Paired with DAS VSP technology, interferometric imaging can considerably increase the effectiveness and reliability of subsurface monitoring that is impossible to achieve with geophones. Thus, it is interesting to explore if the interferometric technique paired with DAS can be effectively utilized to extend seismic images around wellbores.

The outlined problem is addressed in *Paper 1* - ***DAS-VSP interferometric imaging: CO2CRC Otway Project feasibility study***. In this paper, we explore the feasibility of interferometric imaging by conducting a synthetic and field experiments. The synthetic walkaway VSP data were computed using the 3D model of the CO2CRC Otway site (Glubokovskikh et al., 2016). We also tested the technique on the field walkaway VSP data acquired at the same research site using conventional borehole geophones and DAS cables as receiver arrays (DAS data were acquired with two sets of DAS equipment). Finally, we compared the results of DAS VSP interferometric imaging to the 3D surface seismic migrated

image obtained within the same area.

Objective 2. Investigate the capabilities of DAS for recording passive borehole data during borehole plug and abandonment operations and investigate the components of passive seismic data recorded in the abandoned well.

As outlined in the section 1.1, DAS is able to record many types of passive data in the borehole environment. Most installations of fibre-optics are in open and active monitoring and production wells. In addition to these common applications, passive DAS can be utilised for unusual tasks, such as monitoring of well cementation process during plug and abandon operation. Installation of a DAS cable during decommissioning has a potential to transform an abandoned well into a permanent sensor array. This deployment can be used to control the cementation process and monitor subsequent changes in the subsurface by recording such parameters as strain, temperature and vibration caused by natural or induced seismicity. Besides, such wells can be utilised to conduct active borehole seismic surveys such as Vertical Seismic Profiling (VSP).

During the P&A operations of Harvey-3 well (drilled as a part of the South West Hub CO_2 geosequestration project in Western Australia), a comprehensive dataset was acquired using DAS and DTS to monitor cement flow and curing (Ricard et al., 2019). One year after completion of the decommissioning operations, the Harvey-3 fibre-optic cable was used for a week-long acquisition of passive seismic data (Pevzner et al., 2020). Although one week is a relatively short time to record a representative dataset for analysis of noise patterns and seismicity in the area, many valuable observations and revelations were obtained. In particular, the results demonstrate that ambient seismic signals can reveal information about the well's conditions a year after cementation, distribution of elastic properties along the well and natural processes such as seismicity and oceanic wave climate.

The problem is addressed in *Paper 2* - ***Distributed fibre-optic sensing transforms an abandoned well into a permanent geophysical moni-***

toring array: A case study from Australian South West. A systematic and complete analysis of the experiment and data is presented in this paper. The paper also provides the examples of the useful information that can be extracted from the acquired data.

Objective 3. Investigate the effect of temperature on DAS measurements in field and laboratory conditions.

As discussed in the section 1.1, DAS measurements can be affected by temperature variations caused by both natural and industrial processes such as diurnal atmospheric temperature variations, hydraulic fracturing treatments, borehole fluids flows or temperature variations in geothermal reservoirs. Such temperature variations can be considered as a low–frequency signal (< 0.1 Hz). This frequency range is far below typical frequencies utilized in seismic exploration. However, DAS applications often include passive broadband monitoring of the subsurface. But DAS response to temperature variations is still poorly understood and needs to be studied in a controlled environment.

The problem is addressed in *Paper 3* - ***Experimental study of temperature change effect on distributed acoustic sensing continuous measurements***. The main objective of this study is to learn experimentally about the DAS response caused by the temperature variation. We acquired DAS data from different experimental and in-situ setups along with temperature data to analyse relation between DAS signal and temperature variation.

Objective 4. Investigate reservoir pressure signature recorded with borehole DAS during CO_2 injections.

As discussed above, being sensitive to slow strain variations, DAS can be utilised for pressure monitoring at reservoir conditions. However, despite the extensive research on DAS in recent years, its' pressure sensing capabilities are not fully understood. The real project demonstrations can provide a deeper insight into pressure sensing capabilities of optical fibres in reservoir conditions, and potentially help the DAS technology to be recognized as a continuous pressure

sensor that can be efficiently utilised in different areas such as CO_2 injection monitoring, hydrogeological studies, borehole leakage detection. Being relatively inexpensive and reliable, DAS can be very cost-effective for these applications as it covers the entire borehole length, unlike traditional pressure sensors bases on transducers. For example, it can be used to assess the real-time reservoir pressure changes during the CO_2 injection. It is important to mention the availability of distributed fibre optic strain sensors (DFOSS), which measure frequency shifts of Rayleigh backscattering for estimation of static strain variations (Xue et al., 2018; Zhang et al., 2020). DFOSS technology can be a better choice for measuring long-term changes, such as reservoir deformations caused by fluid injection/pumping (Lei et al., 2019; Zhang and Xue, 2019) than DAS systems based on dynamic strain measurements. However, DFOSS equipment might not be available for a particular reservoir monitoring setup that utilises DAS as a primary sensor.

The pressure sensitivity of DAS is explored in *Paper 4* - ***DAS signature of reservoir pressure changes caused by a CO_2 injection: Experience from the CO2CRC Otway Project***. Our main objective here is to learn about pressure sensing capabilities of borehole DAS in in-situ environment and demonstrate the capabilities of DAS technology as a continuous pressure sensor in a real-live application in a CCUS project. To this end, we describe the DAS response to the reservoir pressure change during CO_2 injection in CO2CRC Otway site.

1.3 Thesis publications and their relation to the thesis topic

1. Sidenko, E., Tertyshnikov, K., Bona, A. and Pevzner, R. (2021). DAS-VSP interferometric imaging: CO2CRC Otway Project feasibility study. *Interpretation, 9*(4), SJ1-SJ12.

We have analysed feasibility of interferometric imaging using a synthetic walkaway VSP data set, followed by its application to field walkaway VSP data recorded by conventional borehole geophones and two types of DAS (standard and engineered fibres). Both experiments (synthetic and field) demonstrate that interferometric imaging is a viable method to extend the subsurface image beyond the coverage of standard VSP imaging. Specifically, the interferometry approach provides a more detailed upper section of the subsurface, whereas standard migration of primary reflections provides a more detailed bottom part of the image. Comparison of the standard and engineered fibres indicates that both fibres are sensitive to free-surface multiples, but the engineered fibre provides a much higher signal-to-noise ratio; thus, it is preferable for interferometric imaging with multiples. The result obtained with the engineered DAS cable indicates that in the depth range suitable for both methods, the VSP interferometric image of the reflectors is comparable to the surface seismic image. The experiment on the field DAS data proves that DAS is sensitive enough to record the non-primary wavefield for imaging and monitoring of the subsurface.

2. Sidenko, E., Tertyshnikov, K., Gurevich, B., Isaenkov, R., Ricard, L.P., Sharma, S., Van Gent, D. and Pevzner, R. (2022). Distributed fibre-optic sensing transforms an abandoned well into a permanent geophysical monitoring array: a case study from Australian South West. *The Leading Edge, 41*(2), 140-148.

Distributed temperature sensing (DTS) and distributed acoustic sensing (DAS) data recorded by a fibre-optic array installed during the decommissioning opera-

tions of the 1550 m Harvey 3 well in Western Australia reveal an abundance of valuable information about the course of the decommissioning process and the quality of the cement job. The DAS monitoring has detected vibrational disturbances during the cement's setting up, while DTS was used to assess setting up of the cement and curing times as well as uniformity of cementation from the distribution of temperature along the borehole. A weeklong trial acquisition of passive seismic data with the same array a year later shows an abundance of seismic events in a wide frequency range from below 1 mHz to above 200 Hz. The downhole DAS array provides traveltimes and amplitudes of these events, which include earthquakes, mine blasts, ocean microseisms, and local human activity. The amplitudes of waves from distant seismic events can be used to estimate and monitor physical properties of the media along the extent of the well. When used in combination with information from active vertical seismic profiling, these events can help obtain independent estimates of velocities and densities. Spectral analysis of low-frequency microseisms shows a strong correlation between passively recorded DAS and local weather observations. This shows that the ability to continuously record oceanic microseisms at low frequencies opens opportunities to employ such arrays for wave climate studies. In addition, the data contain peculiar in-hole reverberations likely caused by crossflow of groundwater behind the intermediate casing, which may indicate imperfections of the cement job. The results demonstrate that a downhole fibre-optic array installed in an abandoned well represents an opportunity to establish a permanent facility for continuous recording of passive and active geophysical data and for exploring various applications.

3. Sidenko, E., Tertyshnikov, K., Lebedev, M. and Pevzner, R. (2022). Experimental study of temperature change effect on distributed acoustic sensing continuous measurements. *Geophysics, 87*(3), D111-D122.

To understand and quantify the DAS signature of temperature changes during

water injections at CO2CRC Otway site, a series of experiments have been conducted at the Curtin University/National Geosequestration Laboratory (NGL) well research facility and Curtin rock-physics laboratory. Overall, three DAS cables are examined. Two fibres are tested in the laboratory and one cable, which is installed behind the casing in the Curtin/NGL well, is examined in the well. Laboratory measurements and observations made during analysis of passive DAS and DTS field data recorded in four Otway wells demonstrate that DAS is sensitive to long-period temperature changes, and its response is proportional to the time derivative of temperature. Induced fibre strain is linearly related to slow temperature change, and this dependency can be estimated for a particular cable. Obtained proportionality constants between strain and temperature change indicate some dependency on the cable type/design and acquisition setup, but they are all of the same order of magnitude. DAS measurements also can be affected by low-frequency noise possibly associated with the effect of temperature on the DAS acquisition unit itself. The results can help compensate for the effect of temperature on low-frequency DAS signals and show that DAS can be used as a distributed temperature sensor if direct temperature measurements are not available.

4. Sidenko, E., Tertyshnikov, K., Gurevich, B. and Pevzner, R. (2022). DAS signature of reservoir pressure changes caused by a CO_2 injection: experience from the CO2CRC Otway Project. *International Journal Of Greenhouse Gas Control, 119*, 103735.

At the time of CO_2 injection within the CO2CRC Otway Project, pressure related strain-rate DAS signals were observed in two monitoring wells. These signals are highly correlated with the pressure signals measured by borehole pressure gauges above the perforations in monitoring wells.

Comparison of DAS measurements and pressure measurements shows a linear relationship between the two datasets. Analysis of data shows that DAS is able to detect reservoir pressure variations higher than 10^{-4} psi/s. Analysis of pressure

variations and strain calculated from DAS strain rate values allows estimation of the elastic modulus of the reservoir formation.

Obtained results show that DAS systems can be utilised not only as seismic sensors, but also as continuous pressure sensors that can help track possible CO_2 leakages into the overburden. In contrast to traditional pressure gauges, DAS is also capable of tracking the pressure profile along the entire well. DAS pressure sensing capabilities open up many new applications to complement subsurface reservoir pressure monitoring, CCUS and hydrogeological studies.

1.4 The sources of data: CO2CRC Otway Project, South West Hub Project, Curtin NGL Well, Curtin Rock-Physics Laboratory

The data used in publications were acquired in different projects and experiments. We outline the origins of datasets below.

1.4.1 CO2CRC Otway Project

Borehole DAS data (used in *papers 1, 3, 4*) were acquired as part of the CO2CRC Otway Project, a pilot research initiative of onshore CO_2 geosequestration in Australia (Cook, 2014). The project started in the beginning of 2000's and included a number of experiments dedicated to demonstrate the effectiveness and safety of the geosequestration methodology. The Otway Site is located about 240 km southwest from Melbourne (Victoria) in an active farming area. Because of the CO_2-rich natural gas source and depleted Naylor gas reservoir located in the area (Underschultz et al., 2011), the Otway site was suitable for CO_2 geosequestration and had been chosen for the pilot research CO_2 geosequestration site in Australia.

To date, the Otway project included three main stages, all of which have been completed. Seismic monitoring was one of the major components of each stage and included 4D surface seismic, passive surface and borehole seismic, 4D VSP, time-lapse walkaway VSP, time-lapse offset VSP with traditional geophones and Vibroseis trucks geophones, time-lapse offset VSP with permanently installed borehole DAS receivers and Surface Orbital Vibrators (SOV).

Stage 1 mainly included the 4D surface seismic and 4D VSP to monitor 66 kt of CO_2/CH_4 supercritical gas mixture being injected through the CRC-1 well (Jenkins et al., 2012).

Stage 2 focused on the geosequestration of 15 kt of supercritical CO_2 at the

depth of 1500 m. The monitoring component of the Stage 2C focused primarily on the time-lapse surface seismic conducted using a permanently deployed receiver array (Pevzner et al., 2017). Stage 2C also included a time-lapse borehole seismic monitoring program using geophones and DAS receivers and trials of continuous seismic monitoring.

The most recent stage of the Otway Project, Stage 3, has a major focus on well-based monitoring techniques. Borehole DAS arrays are installed in several monitoring wells (Pevzner et al., 2020). One of the primary goals of this stage is to carry out active and passive continuous monitoring: active seismic using permanently installed SOVs and passive seismic using human-related and environmental noise. In addition to the continuous monitoring, Stage 3 involves time-lapse 3D VSP surveys using vibroseis sources (acquired before, during, and after the injection).

The walkaway datasets (synthetic and experimental) from CRC-3 (used in *paper 1*) were acquired as a part of Stage 2C. The monitoring component of Stage 2C focused primarily on the time-lapse surface seismic conducted using a permanently deployed receiver array (Pevzner et al., 2017). Stage 2C also included a time-lapse borehole seismic monitoring program using geophones and DAS receivers and trials of continuous seismic monitoring.

The continuous datasets from CRC-3, CRC-4, CRC-5, CRC-6 and CRC-7 (used for *papers 3 and 4*) were acquired during water and CO_2 injections as a part of Stage 3. Stage 3 has a major focus on well-based monitoring techniques aimed to monitor a small (15 kt) injection of supercritical CO_2 into a saline aquifer through the CRC-3 (Isaenkov et al., 2021; Jenkins et al., 2017). Borehole DAS arrays are installed in several monitoring wells (Pevzner et al., 2020). One of the primary goals of this stage is to carry out active and passive continuous monitoring: active seismic using permanently installed Surface Orbital Vibrators (SOV) and passive seismic using human-related and environmental noise. This injection well (CRC-3) and four monitoring wells (CRC-4, 5, 6, 7) are being used

for the seismic, temperature and pressure monitoring. All the wells are equipped with fibre-optic sensing equipment: fibre-optic cables are cemented behind casings and connected to DAS (Silixa Carina systems) and DTS (Silixa Ultima DTS) interrogators.

1.4.2 South West Hub Project

Other passive borehole DAS datasets were acquired in the scope of The South West Hub CCS Project (*paper 2*). The project was the first initiative in Western Australia supported by the Australian Government's CCS Flagships program (Sharma et al., 2017; Sharma and Van Gent, 2018). The site is located approximately 120 km south of state capital Perth. Data were acquired in the Harvey-3 well that was drilled between December 2014 and June 2015 as a stratigraphic well for geological characterisation of the South West Hub project area (Nims and Pollock, 2015). The total depth of the well is 1,550 m. The well was left suspended shortly after drilling with van Ruth plugs at the bottom. Planned decommissioning of the well presented an excellent opportunity to conduct the first trial of transforming an abandoned well into a deep vertical permanent seismic array using the fibre-optic sensing technology. The deployed fibre-optic cable acts as a receiver array providing in-situ measurements of the subsurface at thousands of points along the well during and after the P&A process.

1.4.3 Curtin NGL Well

Additional experimental datasets (DAS and DTS datasets used in *paper 3*) were acquired using a 900 m deep well which is a part of the Curtin/NGL research facility and located at the Curtin University main campus in Perth, Western Australia. A fibre-optic cable is installed behind the casing along the entire well. The cable contains a set of single-mode and multi-mode fibres. The facility is being used to test, re-test and calibrate equipment as well as to carry out geophysical experiments.

1.4.4 Curtin Rock Physics Laboratory

To study the effect of changing temperature on DAS measurements in controlled temperature conditions (*paper 3*), we designed a heating/cooling laboratory setup and conducted a series of experiments in the Curtin Rock Physics laboratory to estimate this effect as well as to gain insights on the influence of different fibre-optic cables on such temperature response.

1.5 Conclusions and outlook

1.5.1 DAS-VSP interferometric imaging

The study of the interferometric imaging approach on synthetic, field VSP geophone and field VSP DAS data within the geological setting of the Otway research site leads to the following conclusions:

(1) Tests on synthetic data for the Otway site show that the interferometric imaging can greatly complement the standard seismic borehole processing. Utilization of secondary wavefield (free-surface multiples) significantly increases illumination of the subsurface and, unlike standard VSP imaging, can provide subsurface coverage above the shallowest borehole receiver. This can be critical for any project that focuses on VSP monitoring.

(2) Application of interferometric migration to field geophone data of the Otway Project demonstrated a significant increase of the subsurface coverage compared to the standard VSP imaging strategy. The method allowed to extract reflectivity information above the shallowest receiver and to widely expand the final VSP image section even with only eight geophones installed in the borehole.

(3) The enhanced backscattering fibre can significantly improve DAS sensitivity, providing a considerably higher SNR ratio of the final image than the standard fibre. The test shows that DAS with engineered fibres is sensitive enough to record free-surface VSP multiples and can provide an image of reflectors comparable to the surface seismic image in the depth range suitable for both methods ($\sim$ 300-700 m in our case).

(4) The interferometric imaging methodology paired with DAS technology can considerably increase reliability of the reservoir monitoring programs based on the borehole measurements. All experiments demonstrate that the trialed methodology provides a significant lateral and vertical extension of

the subsurface image obtained with borehole receivers. This can be highly valuable for the correlation of geological horizons at the stage of data interpretation.

(5) To detect any possible changes in the subsurface caused by CO_2, it is extremely important for CCS projects to have a time-lapse image over the overburden as well as the reservoir. Introduction of such methodology into borehole seismic processing and imaging significantly increases the value of monitoring based on borehole observations.

The presented workflow of DAS-VSP interferometry is based on the P-waves only, however seismic interferometry can also be used to take advantage of shear waves (both source-generated and converted). In the future, it would be important to implement the method in 3D and explore time-lapse and repeatability of the such data.

1.5.2 Analysis of data from a DAS cable cemented into an abandoned well

Installation of a fibre-optic cable in the Harvey-3 well provided a unique opportunity to monitor P&A operations, verify the quality of the cement job, and created a permanent seismic and temperature sensor for future passive and active geophysical surveys. The main conclusions drawn:

(1) Fibre-optic-sensing data recorded during the cementing operations reveal an abundance of valuable information about the course of the decommissioning process and the quality of the cement job. The DAS monitoring has detected vibrational disturbances during the cement's setting up, while DTS helped to assess setting up of the cement and curing times as well as uniformity of the cementation. However, DTS has relatively coarse temporal sampling; using finer sampling in DTS might be useful to help identify the origin of some anomalies recorded at the same time by DAS.

(2) A subsequent week-long trial acquisition of passive seismic data using the previously installed vertical sensing array shows an abundance of seismic events in a wide frequency range including the ultra-low part of the spectrum of less than 1 mHz. The downhole DAS array allows an analysis of the depth variation of travel times and amplitudes of these events, which include earthquakes, mine blasts, ocean microseisms, and local human activity.

(3) The amplitudes of waves from distant seismic events can be used to estimate and monitor physical properties of the media along the entire extent of the well. When used in combination with active vertical seismic profiling acquired using either controlled or a random source of energy located near the well, these events can help obtain independent estimates of velocities and densities.

(4) Spectral analysis of low frequency microseisms shows a strong correlation between passively recorded DAS and local weather observations. This shows that the ability to continuously record oceanic microseisms at low frequencies opens up opportunities to employ such arrays for wave climate studies.

(5) Detected peculiar in-hole reverberations likely caused by crossflow of groundwater behind the intermediate casing, which may indicate imperfections of the cement job. This information can be used to better understand fluid flows and potentially identify pockets of bypassed oil, as well as identify any early onsets of corrosion or other damage, which may be useful as preventive measure in producing wells. Such information can also be considered in a future well design.

The Harvey-3 site is located not far from a population centre in an extensively studied area away from urban noise. Thus, the downhole fibre-optic array represents an opportunity to establish an excellent diagnostic facility for continuous recording of passive and active geophysical data and for exploring various applications. For example, a group of wells instrumented with fibre-optic sensors can

be utilised for multilateration of regional earthquakes and mine blasts. Overall, the variety of observations made during Harvey-3 study indicates a strong potential of such installations for many applications. The bigger picture is that any onshore well coming for P&A can be equipped with a fibre-optic cable. This can provide an opportunity to build a continent-scale network of vertical sensing arrays gathering information about seismic events, global heat flow and crustal state of stress.

1.5.3 Temperature effect on DAS measurements

The series of field and laboratory studies of the temperature effect on DAS data leads to the following conclusions:

(1) Phase based DAS is sensitive to temperature time derivative and is able to register very low-frequency signals (< 0.01 Hz). The results demonstrate a linear relationship between DAS response and temperature change. The proportionality constant in theses linear relationships have different values for different types of DAS cables and installations but are all of the same order of magnitude (from 2.9 to 10.5 $\mu\epsilon/^{\circ}$C).

(2) The rapid temperature change has a significant effect on DAS measurements and must be taken into account in time-lapse DAS seismic monitoring applications and especially in passive monitoring with the utilisation of low frequencies.

(3) Knowing a linear dependency between strain and temperature we can potentially remove low-frequency temperature related noise from DAS data or use DAS records to estimate temperature variations along the fibre-optic cable. Thus, DAS can be potentially utilised to track temperature changes in the absence of DTS or other direct temperature measurements. However, utilisation of DAS and DTS together can be very beneficial, as it

would allow estimating the thermal effect on DAS measurements and can help separate the temperature effect from the acoustic (seismic) signal.

(4) The data analysis shows that DAS measurements can be affected by the arifical common mode noise that should be removed from data before low-frequency data analysis. It can be caused by temperature variations in the room housing the acquisition unit and affects the interrogator itself. This noise appears as a common-mode signal which is closely correlated with the room temperature.

The common mode noise presented in DAS low-frequency data can be interrogator specific. This noise possibly appears because of internal measurements processing (common-mode subtraction). The described noise can be estimated using a reference (not affected by any signals) piece of fibre and subtracted from the data. I suggest that different interrogators and different setups should be studied separately.

In this study I used Raman-based DTS. While DTS can be based on both Raman and Rayleigh backscattering, DAS is based only on Rayleigh backscattering. Thus, there can be uncertainty between different scatterings or different interrogators when comparing the temperature effect on DAS with Raman-based temperature measurements.

Many other aspects such as DAS acquisition parameters (gauge length and pulse length), types of interrogators, type of cable, cable installation designs, etc. influence the DAS measurements. Overall, it is apparent that the combination of a particular fibre optic cable, specific interrogator unit and deployment strategy should be considered, assessed and operated as a single acquisition system in which each component has its own contribution to the data quality.

1.5.4 DAS signature of reservoir pressure changes caused by CO_2 injection

Analysis of the effect of pressure on the DAS response leads to the following conclusions:

(1) Results of the study show that DAS can record local pressure changes in a borehole environment. During the Stage 3 of Otway Project a pressure response was recorded using DAS in two monitoring wells from CO_2 injection in the injection well.

(2) Comparison of pressure gauge and DAS data shows that the DAS response is proportional to pressure time derivative and is sensitive to 10^{-4} psia/s pressure rates.

(3) Capability of DAS to record such minor pressure deviations opens up a perspective to utilize DAS for CO_2 monitoring not only as a seismic sensor, but as a continuous pressure sensor, which can help track possible CO_2 leakages into the overlying formations (leakage detection). While borehole pressure gauges provide response only from certain depth points, DAS is capable of tracking the pressure profile along the entire well (at 1m spacing).

(4) The data analysis of strain-pressure relationship provided an estimation of the ratio of the induced pressure to DAS strain of about 8 GPa. The corresponding theoretical value from the measured moduli is 23 GPa, i.e., three times higher. The theoretical values are derived from measured velocities and correspond to the dynamic moduli. Dynamic moduli are typically higher than static, and the observed difference is reasonable for soft sandstones.

Pressure sensing capabilities open up many new applications for DAS technology in subsurface reservoir pressure monitoring, CCS and hydrogeological studies. As the DAS system examined in this study responds to pressure change (pressure

time derivative), its sensitivity can be limited by the rate of pressure variations, thus, it can be insensitive to very small and long period signals. This is the major limitation of DAS compared to traditional borehole pressure gauges. Nevertheless, DAS can be utilised in monitoring systems and setups that are not designed to have a dense pressure gauge coverage. In such situations DAS can be used to interpolate pressure data between high sensitivity pressure sensors.

References

Ajo-Franklin, J., S. Dou, N. J. Lindsey, I. Monga, C. Tracy, M. Robertson, V. Rodriguez Tribaldos, C. Ulrich, B. Freifeld, T. Daley, and X. Li (2019). Distributed acoustic sensing using dark fiber for near-surface characterization and broadband seismic event detection. *Scientific Reports 9*(1), 1–14.

Bakku, S. K., M. Fehler, P. Wills, J. Mestayer, A. Mateeva, and J. Lopez (2014). Vertical seismic profiling using distributed acoustic sensing in a hydrofrac treatment well. pp. 5024–5028. Society of Exploration Geophysicists.

Bao, X. and Y. Wang (2021). Recent advancements in rayleigh scattering-based distributed fiber sensors. *Advanced Devices & Instrumentation 2021*.

Becker, M., C. Ciervo, and T. Coleman (2019). Laboratory testing of low frequency strain measured by distributed acoustic sensing. *2018 SEG International Exposition and Annual Meeting, SEG 2018*, 4963–4966.

Becker, M., T. Coleman, C. Ciervo, M. Cole, and M. Mondanos (2017). Fluid pressure sensing with fiber-optic distributed acoustic sensing. *The Leading Edge 36*(12), 1018–1023.

Becker, M. and T. I. Coleman (2019). Distributed acoustic sensing of strain at earth tide frequencies. *Sensors (Switzerland) 19*(9).

Cook, P. (2014). *Geologically storing carbon: Learning from the Otway Project experience*. CSIRO PUBLISHING.

Correa, J., A. Egorov, K. Tertyshnikov, A. Bona, R. Pevzner, T. Dean, B. Freifeld, and S. Marshall (2017). Analysis of signal to noise and directivity characteristics of das vsp at near and far offsets — a co2crc otway project data example. *The Leading Edge 36*(12), 994a1–994a7.

Correa, J., R. Pevzner, A. Bona, K. Tertyshnikov, B. Freifeld, M. Robertson, and T. Daley (2019). 3d vertical seismic profile acquired with distributed acoustic sensing on tubing installation: A case study from the co2crc otway project. *Interpretation 7*(1), SA11–SA19.

Correa, J., R. Pevzner, S. Popik, K. Tertyshnikov, A. Bona, and B. Freifeld (2018). Application of 3d vsp acquired with das and 3c geophones for site characterization and monitoring program design: preliminary results from stage 3 of the co2crc otway project. In *2018 SEG International Exposition and Annual Meeting*. OnePetro.

Daley, T. M., B. M. Freifeld, J. Ajo-Franklin, S. Dou, R. Pevzner, V. Shulakova, S. Kashikar, D. E. Miller, J. Goetz, J. Henninges, and S. Lueth (2013). Field testing of fiber-optic distributed acoustic sensing (das) for subsurface seismic monitoring. *The Leading Edge 32*(6), 699–706.

Darnet, M., P. Wawrzyniak, N. Coppo, S. Nielsson, E. Schill, and G. Fridleifsson (2020). Monitoring geothermal reservoir developments with the controlled-source electro-magnetic method—a calibration study on the reykjanes geothermal field. *Journal of Volcanology and Geothermal Research 391*, 106437.

Deflandre, J., J. Laurent, D. Michon, and E. Blondin (1995). Microseismic surveying and repeated vsps for monitoring an underground gas storage reservoir using permanent geophones. *First Break 13*(4).

Djuraev, U., S. R. Jufar, and P. Vasant (2017). A review on conceptual and practical oil and gas reservoir monitoring methods. *Journal of Petroleum Science and Engineering 152*, 586–601.

Dou, S., J. Ajo-Franklin, T. Daley, M. Robertson, T. Wood, B. Freifeld, R. Pevzner, J. Correa, K. Tertyshnikov, M. Urosevic, and B. Gurevich (2016). Surface orbital vibrator (sov) and fiber-optic das: Field demonstration of economical, continuous-land seismic time-lapse monitoring from the australian co 2 crc otway site. Volume 35, pp. 5552–5556. Society of Exploration Geophysicists.

Edwards, B., T. Kraft, C. Cauzzi, P. Kästli, and S. Wiemer (2015). Seismic monitoring and analysis of deep geothermal projects in st gallen and basel, switzerland. *Geophysical Journal International 201*(2), 1022–1039.

Eiken, O., P. Ringrose, C. Hermanrud, B. Nazarian, T. A. Torp, and L. Høier (2011). Lessons learned from 14 years of ccs operations: Sleipner, in salah and snøhvit. *Energy procedia 4*, 5541–5548.

Feo, G., J. Sharma, D. Kortukov, W. Williams, and T. Ogunsanwo (2020). Distributed fiber optic sensing for real-time monitoring of gas in riser during offshore drilling. *Sensors (Switzerland) 20*(1).

Forgues, E., J. Meunier, C. Hubans, and J. Gelot (2007). Innovative low cost 4d seismic technology: Cggveritas seismovie technology. In *GeoSiberia 2007-International Exhibition and Scientific Congress*, pp. cp–59–00493. European Association of Geoscientists & Engineers.

Freifeld, B. M., R. Pevzner, S. Dou, J. Correa, T. M. Daley, M. Robertson, K. Tertyshnikov, T. Wood, J. Ajo-Franklin, M. Urosevic, and B. Gurevich (2016). The co2crc otway project deployment of a distributed acoustic sensing network coupled with permanent rotary sources. pp. 2–6.

Galperin, E. I. (1985). *Vertical seismic profiling and its exploration potential*, Volume 1. Springer Science & Business Media.

Glubokovskikh, S., R. Pevzner, T. Dance, E. Caspari, D. Popik, V. Shulakova, and B. Gurevich (2016). Seismic monitoring of co2geosequestration: Co2crc

otway case study using full 4d fdtd approach. *International Journal of Greenhouse Gas Control 49*(2016), 201–216.

Glubokovskikh, S., R. Pevzner, E. Sidenko, K. Tertyshnikov, B. Gurevich, S. Shatalin, A. Slunyaev, and E. Pelinovsky (2021). Downhole distributed acoustic sensing provides insights into the structure of short-period ocean-generated seismic wavefield. *Journal of Geophysical Research: Solid Earth 126*.

Hardage, B. A. (1985). Vertical seismic profiling. *The Leading Edge 4*(11), 59–59.

Hartog, A. H. (2017). *An introduction to distributed optical fibre sensors*. CRC press.

Isaenkov, R., R. Pevzner, S. Glubokovskikh, S. Yavuz, A. Yurikov, K. Tertyshnikov, B. Gurevich, J. Correa, T. Wood, B. Freifeld, M. Mondanos, S. Nikolov, and P. Barraclough (2021). An automated system for continuous monitoring of co2 geosequestration using multi-well offset vsp with permanent seismic sources and receivers: Stage 3 of the co2crc otway project. *International Journal of Greenhouse Gas Control 108*(December 2020), 103317–103317.

Jenkins, C., P. J. Cook, J. Ennis-King, J. Undershultz, C. Boreham, T. Dance, P. de Caritat, D. M. Etheridge, B. M. Freifeld, and A. Hortle (2012). Safe storage and effective monitoring of co2 in depleted gas fields. *Proceedings of the National Academy of Sciences 109*(2), E35–E41.

Jenkins, C., S. Marshall, T. Dance, J. Ennis-King, S. Glubokovskikh, B. Gurevich, T. La Force, L. Paterson, R. Pevzner, E. Tenthorey, and M. Watson (2017). Validating subsurface monitoring as an alternative option to surface m&v - the co2crc's otway stage 3 injection. *Energy Procedia 114*(November 2016), 3374–3384.

Jin, G. and B. Roy (2017). Hydraulic-fracture geometry characterization using low-frequency das signal. *The Leading Edge 36*(12), 975–980.

Karrenbach, M., S. Cole, A. Ridge, K. Boone, D. Kahn, J. Rich, K. Silver, and D. Langton (2019). Fiber-optic distributed acoustic sensing of microseismicity, strain and temperature during hydraulic fracturing. *GEOPHYSICS 84*(1), D11–D23.

Karrenbach, M., A. Ridge, S. Cole, K. Boone, J. Rich, K. Silver, and D. Langton (2017). Das microseismic monitoring and integration with strain measurements in hydraulic fracture profiling. American Association of Petroleum Geologists.

Koyamada, Y., M. Imahama, K. Kubota, and K. Hogari (2009). Fiber-optic distributed strain and temperature sensing with very high measurand resolution over long range using coherent otdr. *Journal of Lightwave Technology 27*(9), 1142–1146.

Lei, X., Z. Xue, and T. Hashimoto (2019). Fiber optic sensing for geomechanical monitoring: (2)- distributed strain measurements at a pumping test and geomechanical modeling of deformation of reservoir rocks. *Applied Sciences 9*(3).

Lindsey, N. J., T. Craig Dawe, and J. B. Ajo-Franklin (2019). Illuminating seafloor faults and ocean dynamics with dark fiber distributed acoustic sensing. *Science 366*(6469), 1103–1107.

Lumley, D. (2001). Time-lapse seismic reservoir monitoring. *GEOPHYSICS 66*(1), 50–53.

Lumley, D. (2010). 4d seismic monitoring of co2 sequestration. *The Leading Edge 29*(2), 150–155.

Mari, J., F. Huguet, J. Meunier, and M. Becquey (2011). Natural gas storage seismic monitoring. *Oil & Gas Science and Technology–Revue d'IFP Energies nouvelles 66*(1), 9–20.

Miller, D. E. and T. Coleman (2018). Das and dts at bradyhot springs: Ob-

servations about coupling and coupled interpretations. *Stanford Geothermal Workshop* (March 2016), 1–13.

Nims, P. and M. Pollock (2015). Harvey-3 final well report department of mines and petroleum. Report.

Pankow, K., M. Mesimeri, J. McLennan, P. Wannamaker, and J. Moore (2020). Seismic monitoring at the utah frontier observatory for research in geothermal energy. In *Proceedings of the 45th Workshop on Geothermal Reservoir Engineering, Stanford, CA, USA*, pp. 10–12.

Parker, T., S. Shatalin, and M. Farhadiroushan (2014). Distributed acoustic sensing – a new tool for seismic applications. *First Break 32*(2010), 61–69.

Pevzner, R., K. Tertyshnikov, E. Sidenko, R. Isaenkov, S. Glubokovskikh, L. Ricard, B. Gurevich, S. Sharma, and D. Van Gent (2020). Underground sounds from an abandoned well: Forensic analysis of distributed acoustic sensing data. In *EAGE Workshop on Fiber Optic Sensing for Energy Applications in Asia Pacific*, Volume 2020, pp. 1–5. European Association of Geoscientists & Engineers.

Pevzner, R., K. Tertyshnikov, E. Sidenko, and S. Yavuz (2020). Effects of cable deployment method on das vsp data quality: Study at co2crc otway in-situ laboratory. Volume 2020, pp. 1–5. European Association of Geoscientists & Engineers.

Pevzner, R., M. Urosevic, K. Tertyshnikov, B. Gurevich, V. Shulakova, S. Glubokovskikh, D. Popik, J. Correa, A. Kepic, B. Freifeld, M. Robertson, T. Wood, T. Daley, and R. Singh (2017). Stage 2c of the co2crc otway project: Seismic monitoring operations and preliminary results. *Energy Procedia 114*(November 2016), 3997–4007.

Raab, T., T. Reinsch, S. R. Aldaz Cifuentes, and J. Henninges (2019). Real-time

well-integrity monitoring using fiber-optic distributed acoustic sensing. *SPE Journal 24*(05), 1997–2009.

Ricard, L., R. Pevzner, E. Sidenko, K. Tertyshnikov, S. Sharma, D. Van Gent, and R. Isaenkov (2019). Transforming an abandoned well into a permanent downhole receiver array: Harvey-3 case study. *ASEG Extended Abstracts 2019*(1), 1–4.

Schuster, G. T. (2009). *Seismic Interferometry*, Volume 9780521871. Cambridge: Cambridge University Press.

Sharma, J., T. Cuny, O. Ogunsanwo, and O. Santos (2021). Low-frequency distributed acoustic sensing for early gas detection in a wellbore. *IEEE Sensors Journal 21*(5), 6158–6169.

Sharma, J., O. L. A. Santos, G. Feo, O. Ogunsanwo, and W. Williams (2020). Well-scale multiphase flow characterization and validation using distributed fiber-optic sensors for gas kick monitoring. *Optics Express 28*(26), 38773–38773.

Sharma, S. and D. Van Gent (2018). The australian south west hub project: Developing confidence in migration assisted trapping in a saline aquifer – understanding uncertainty boundaries through scenarios that stress the models. *SSRN Electronic Journal* (October), 1–21.

Sharma, S., D. Van Gent, M. Burke, and L. Stelfox (2017). The australian south west hub project: Developing a storage project in unconventional geology. *Energy Procedia 114*, 4524–4536.

Shulakova, V., R. Pevzner, J. Christian Dupuis, M. Urosevic, K. Tertyshnikov, D. E. Lumley, and B. Gurevich (2015). Burying receivers for improved time-lapse seismic repeatability: Co2crc otway field experiment. *Geophysical Prospecting 63*(1), 55–69.

Titov, A., Y. Fan, G. Jin, A. Tura, K. Kutun, and J. Miskimins (2020). Experimental investigation of distributed acoustic fiber-optic sensing in production logging: Thermal slug tracking and multiphase flow characterization. SPE.

Underschultz, J., C. Boreham, T. Dance, L. Stalker, B. Freifeld, D. Kirste, and J. Ennis-King (2011). Co2 storage in a depleted gas field: An overview of the co2crc otway project and initial results. *International Journal of Greenhouse Gas Control 5*(4), 922–932.

Van Dok, R., B. Fuller, L. Walter, N. Kramer, P. Anderson, and T. Richards (2016). *Permanent borehole sensors for CO2 injection monitoring–Hastings Field, Texas*, pp. 5511–5515. Society of Exploration Geophysicists.

Xue, Z., J.-Q. Shi, Y. Yamauchi, and S. Durucan (2018). Fiber optic sensing for geomechanical monitoring: (1)-distributed strain measurements of two sandstones under hydrostatic confining and pore pressure conditions. *Applied Sciences 8*(11).

Yu, J. and G. T. Schuster (2004). Enhancing illumination coverage of vsp data by crosscorrelogram migration. In *2004 SEG Annual Meeting*. OnePetro.

Yurikov, A., K. Tertyshnikov, R. Isaenkov, E. Sidenko, S. Yavuz, S. Glubokovskikh, P. Barraclough, P. Shashkin, and R. Pevzner (2021). Multi-well 3d distributed acoustic sensing vertical seismic profile imaging with engineered fibers: Co2crc otway project case study. *Geophysics 86*(6), D241–D248.

Zhang, Y., X. Lei, T. Hashimoto, and Z. Xue (2020). In situ hydromechanical responses during well drilling recorded by fiber-optic distributed strain sensing. *Solid Earth 11*(6), 2487–2497.

Zhang, Y. and Z. Xue (2019). Deformation-based monitoring of water migration in rocks using distributed fiber optic strain sensing: A laboratory study. *Water Resources Research 55*(11), 8368–8383.

Chapter 2

Published Papers

2.1 DAS-VSP interferometric imaging: CO2CRC Otway Project feasibility study.

DAS-VSP interferometric imaging: CO2CRC Otway Project feasibility study

Evgenii Sidenko[1], Konstantin Tertyshnikov[1], Andrej Bona[1], and Roman Pevzner[1]

Abstract

Recent advancements in distributed acoustic sensing (DAS) technology open new ways for borehole-based seismic monitoring of CO_2 geosequestration. Compared to 4D surface seismic monitoring, repeated vertical seismic profiling (VSP) surveys with DAS receivers considerably reduce the cost and invasiveness of time-lapse CO_2 monitoring. However, standard borehole imaging techniques cannot provide the same level of reservoir illumination as 3D surface seismic. The performance of VSP imaging can be significantly improved with interferometric utilization of free-surface multiples. We have developed a feasibility study of interferometric imaging with a synthetic walkaway VSP data set, followed by its application to field walkaway VSP data recorded by conventional borehole geophones and two types of DAS (standard and engineered fibers). Both experiments (synthetic and field) demonstrate that interferometric imaging is a viable method to extend the subsurface image beyond the coverage of standard VSP imaging. Specifically, the interferometry approach provides a more detailed upper section of the subsurface, whereas standard migration of primary reflections provides a more detailed bottom part of the image. Comparison of the standard and engineered fibers indicates that both fibers are sensitive to free-surface multiples, but the engineered fiber provides a much higher signal-to-noise ratio; thus, it is preferable for interferometric imaging with multiples. The result obtained with the engineered DAS cable indicates that in the depth range suitable for both methods, the VSP interferometric image of the reflectors is comparable to the surface seismic image. The experiment on the field DAS data proves that DAS is sensitive enough to record the nonprimary wavefield for imaging and monitoring of the subsurface.

Introduction

Carbon capture and storage (CCS) is one of the approaches of the world's cooperative efforts to reduce the emission of greenhouse gases. In CCS operations, it is paramount to have the ability to image and monitor injected CO_2 to provide confidence in the location of a plume within the target depth interval and to identify any possible leakages.

Time-lapse seismic has become one of the principal approaches to assess conformance of the predicted plume behavior and ensure containment of the introduced CO_2 (Lumley, 2010). Despite the fact that time-lapse surface seismic is the most reliable geophysical method for monitoring the injected CO_2, the approach has some challenges: the relatively high cost of frequent data acquisition and the high level of disruption for other land uses (especially onshore), which often make frequent surveys impractical. These factors motivate the development of less invasive seismic techniques, which can provide subsurface images of sufficient quality in a more cost-effective manner compared to the surface seismic.

Technological advancements in source and receiver designs and optimizations in survey practices have led to alternative acquisition approaches (Shulakova et al., 2015; Freifeld et al., 2016; Pevzner et al., 2017a). Development of permanently installed receivers and sources, especially for monitoring purposes, can substantially reduce operational impacts and costs (Pevzner et al., 2015; Dou et al., 2016). In particular, recent improvements in distributed acoustic sensing (DAS) technology have had a significant effect on the seismic monitoring (Miller et al., 2012; Daley et al., 2013; Karrenbach et al., 2019). Indeed, relatively inexpensive and highly durable fiber-optic cables are easy to deploy and enable the acquisition of seismic data of the quality similar to geophones (Correa et al., 2017). Permanently deployed optical fiber cables as receiver arrays in borehole reservoir surveillance considerably reduce the cost and invasiveness of the seismic monitoring, and they allow more frequent surveys, which is essential for early detection of CO_2 leaks.

A further decrease of costs can be achieved through the reduction and optimization of the seismic source effort required to conduct monitoring surveys (Popik et al., 2019). A reduction of the number of sources without compromising the subsurface image quality can be

[1]Curtin University, Western Australia, 6107 and CO2CRC Ltd., Melbourne, Victoria, Australia. E-mail: evgenysidenko@gmail.com (corresponding author); Konstantin. Tertyshnikov@curtin.edu.au; A.Bona@curtin.edu.au; R.Pevzner@curtin.edu.au.

Manuscript received by the Editor 29 January 2021; revised manuscript received 15 June 2021; published ahead of production 31 August 2021; published online 15 October 2021. This paper appears in *Interpretation*, Vol. 9, No. 4 (November 2021); p. SJ1–SJ12, 16 FIGS., 2 TABLES.
http://dx.doi.org/10.1190/INT-2021-0038.1.

achieved by using more effective data analysis, which would maximize the use of information available in the recorded data. One way to achieve this is to use a nonprimary wavefield, such as the first-order free-surface multiples. This can be achieved by interferometric redatuming of vertical seismic profiling (VSP) data to pseudosurface data and subsequent migration of redatumed wavefield (Schuster et al., 2004). Such interferometric migration used to be mainly applied to drill-bit source data or reverse VSP data acquired with surface receivers because reverse VSP geometry provides better well coverage compared to standard VSP. However, the emergence of DAS technology opened new opportunities for borehole acquisitions by introducing robust and dense sensors' coverage in the wells. Thus, the interferometric technique can be effectively used to extend seismic images around wellbores.

In this paper, we explore the feasibility of interferometric imaging by conducting synthetic and field experiments. The synthetic walkaway VSP data were computed using the 3D model of the CO2CRC Otway site (Glubokovskikh et al., 2016). We also tested the technique on the field walkaway VSP data acquired at the same research site using conventional borehole geophones and DAS cables as receiver arrays (DAS data were acquired with two sets of DAS equipment). Finally, we compared the results of DAS VSP interferometric imaging to the 3D surface seismic prestack time migration (PSTM) image obtained within the same area.

CO2CRC Otway Project

The CO2CRC Otway Project is a pilot research initiative of onshore CO_2 geosequestration in Australia. The project started in the early 2000s and included many experiments dedicated to demonstrate the effectiveness and safety of the geosequestration methodology (Cook, 2014). The Otway site is located approximately 240 km southwest of Melbourne (Victoria) in an active farming area.

The monitoring component of a previous stage (Stage 2C) of the project primarily focused on the time-lapse surface seismic conducted using a permanently deployed receiver array (Pevzner et al., 2017a). Stage 2C also included a time-lapse borehole seismic monitoring program using geophones and DAS receivers and trials of continuous seismic monitoring. The use of a buried receiver array demonstrated higher repeatability, noise reduction, and benefits to reduce impacts on landowners (Pevzner et al., 2017b). Other positive outcomes are significant reduction of acquisition time and a relatively small crew required to conduct a seismic survey.

The current stage of the Otway Project, Stage 3, has a major focus on well-based monitoring techniques. Borehole DAS arrays are installed in several monitoring wells (Pevzner et al., 2020). One of the primary goals of this stage is to carry out active and passive continuous monitoring: active seismic using permanently installed surface orbital vibrators and passive seismic using human-related and environmental noise.

In addition to the continuous monitoring, Stage 3 involves time-lapse 3D VSP surveys using vibroseis sources (acquired before, during, and after the injection). To achieve a subsurface coverage comparable to 3D surface seismic, we propose to use free-surface VSP multiples for imaging the subsurface. This approach will complement standard VSP Kirchhoff migration of primary reflections, making the image comparable to a respective 3D PSTM section (Sidenko et al., 2019).

Interferometric imaging for borehole seismic data

The reflected wavefield recorded with surface sources and receivers usually provides a broad subsurface illumination by common-reflection points due to the wide surface distribution of source and receiver locations. However, this is not the case for the VSP geometry. Figure 1a shows subsurface reflection points for a single-receiver offset VSP in a homogeneous and horizontally layered medium. In Figure 1a, the green curve and straight lines correspond to primary reflections, whereas the blue ones correspond to the first-order free-surface multiple reflections. In conventional VSP methods, the subsurface area illuminated by the primary reflections is constrained by a half-offset between the well and surface source locations. In cases in which the well is not fully covered by the receivers (especially in the near-surface part), the subsurface illumination will be even more limited: No reflections will be above the shallowest receiver. Thus,

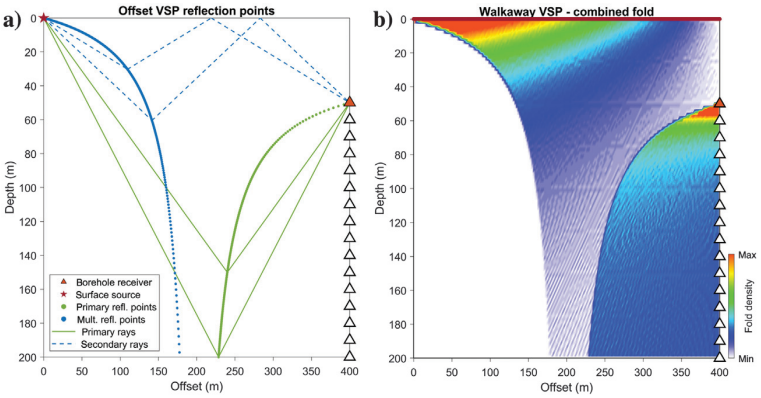

Figure 1. Schematic of VSP imaging illumination for horizontal reflectors. (a) Offset VSP reflections; the green color indicates illumination by primary reflections, and the blue color indicates illumination by free-surface multiples. (b) The combined reflections' fold distribution is shown for walkaway VSP with a single receiver.

due to geometry constraints, conventional VSP methods cannot provide the same image of the subsurface as surface seismic, which normally provides illumination of an entire section under the acquisition array. However, as indicated by Figure 1a, the imaging area of the VSP can be significantly increased by using free-surface multiple reflections (the blue curve). Figure 1b shows the combined primary and multiple (first order) reflection fold distribution for the walkaway VSP with a single receiver.

Figure 2 shows reflection fold distribution of a walkaway VSP with a dense (1 m interval) source and receiver coverage. The distribution of the primary reflection points is shown in Figure 2a, multiple reflection points in Figure 2b, and combined fold distribution in Figure 2c. The combined fold distribution indicates that the joint use of primary and secondary reflection fields can significantly increase the subsurface illumination area.

To use the free-surface multiples and thus increase the subsurface illumination of the VSP approach, one can apply the interferometric (crosscorrelation) migration to the VSP data (Yu and Schuster, 2004). In general, seismic interferometry is a group of techniques that applies convolution or correlation methods to redatum the seismic wavefield (Wapenaar, 2004; Bakulin and Calvert, 2006). Afterward, the redatumed (transformed) wavefield can be migrated to obtain the reflectivity distribution (image) of the subsurface or to map source locations for passively acquired seismic data (Schuster et al., 2004).

The concept of seismic interferometry method was introduced by Claerbout (1968), who suggests that the reflection trace of a surface source can be obtained by the autocorrelation of a trace acquired on the surface from an unknown depth source. Rickett and Claerbout (1996) show that a crosscorrelation of two noise traces recorded at different surface locations can provide a response of the underlying media, which would be recorded if a source and receiver were deployed at those two locations.

Schuster et al. (2004) demonstrate that reflectivity distribution of media can be obtained by migration of VSP free-surface multiples after redatuming. Yu and Schuster (2004) show that interferometric migration of free-surface multiples can significantly increase the illumination of VSP data. Application of interferometric imaging for VSP free-surface multiples is described in detail in Schuster (2009), and the principle is illustrated in Figure 3. The method is also called the vertical seismic profile to surface seismic profile (VSP-SSP) transform.

The black arrows in Figure 3a and 3b show schematic raypaths from two different surface sources to a single borehole receiver for which the physical raypaths "BC" of the downgoing direct and surface multiple waves coincide. Correlation of the downgoing direct wave (BC) with the downgoing wavefield ("AoBC") leads to a reflection response ("AoB") between points "A" and "B." A priori, it is not known which of the receivers will record this physical ray. To address this

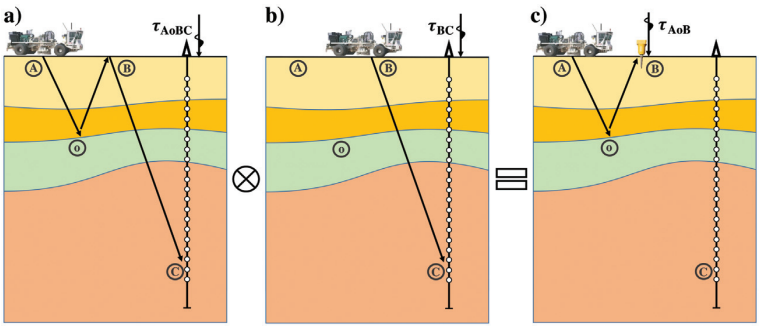

Figure 3. VSP-SSP transform visualization (adapted from Schuster, 2009).

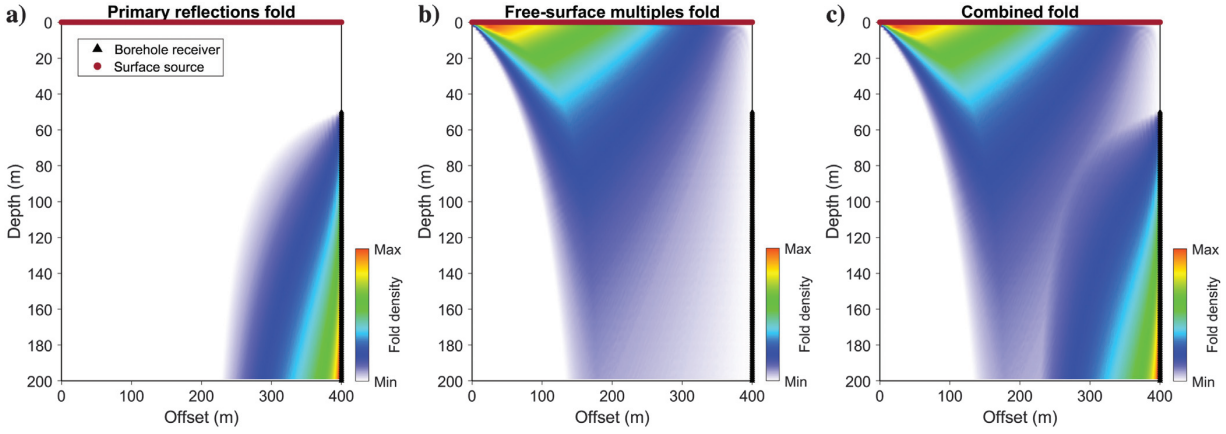

Figure 2. The reflections' fold distribution of the walkaway VSP method in a case of a dense source and receiver coverage. (a) Primary reflections, (b) free-surface multiples, and (c) combined field.

issue, we compute this correlation for all borehole receivers; then, the result of crosscorrelations is summed across the receivers. Due to the principle of the stationary phase, the sum over different receivers will constructively add only for physical rays (stationary points) common for direct and multiple waves. After creating the equivalent of the surface trace AoB, we can migrate it using any migration method.

The implemented workflow consists of the following major steps:

1) extraction of up- and downgoing wavefields from walkaway VSP data
2) S-wave elimination (muting)
3) VSP-SSP (interferometric) transform
4) migration.

Besides the interferometric imaging of VSP multiples, we also performed standard Kirchhoff migration of primary reflections. We combined the results of the primary and multiple wavefields to obtain the maximum outcome from the walkaway VSP data.

Results

Synthetic data: Walkaway VSP

First, we computed a walkaway VSP synthetic data set to test the interferometric VSP migration approach. Acoustic and elastic data sets were simulated using an open-source SOFI-2D software (Bohlen et al., 2015) and a model of the Otway site built by geologists using numerous 3D seismic data sets of the area (Glubokovskikh et al., 2016). Figure 4 shows a sample cross section of the compressional velocity; the black triangles represent the locations of the receivers, and the red dots represent subsampled locations of the source points. The geometry parameters are shown in Table 1. Because the presence of free-surface multiples (ghosts) is essential for the VSP interferometric workflow, a free-surface boundary was implemented on the top of the model, whereas other boundaries form high-absorbing frames. We calculated 176 VSP shot gathers with 700 receivers placed in the borehole for the acoustic and elastic cases. Examples of raw VSP gathers are presented in Figure 5. An initial workflow was built and tested on the acoustic synthetic data because it has a simpler wavefield to adjust the parameters of the processing routine.

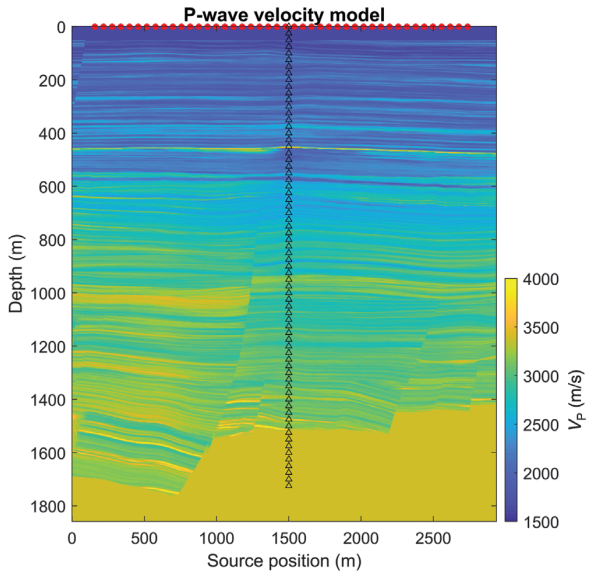

Figure 4. Otway P-wave velocity model used for synthetic wavefield simulations. The red dots represent the subsampled source locations. The black triangles show the positions of the receiver locations. The corresponding modeling parameters are presented in Table 1.

The elastic data are more complex due to the presence of S- and PS-waves, which can be treated as noise for our workflow, especially if we focus on the data that correspond to the shallowest part of the borehole receiver array and near offsets (Figure 5). It is difficult to separate S-waves from other wavefield components due to crosstalk between shear waves in the common-receiver domain and the kinematic similarity between the P- and S-waves in the common-source domain for middle and far offsets. Thus, we decided to mute the shear waves for the middle- and far-offset shot gathers. For the near offsets, we suppressed the shear waves using frequency-wavenumber filtering.

To redatum data from the borehole to the surface domain, we applied the VSP-SSP transform. An example of the resulting virtual shot gather is shown in Figure 6a, and a corresponding surface seismic shot gather is shown in Figure 6b for comparison. Figure 6 indicates that virtual and surface synthetic shot gathers are likely to have different amplitudes because the virtual gather is obtained by correlation of wavefields, which is a nonlinear operation; hence, it does not preserve the amplitudes. Thus, standard analysis of amplitudes might not be applicable to virtual images. The S-wave removal prior to the transform minimizes false reflection events attributed to the presence of strong S-waves in raw data. After the VSP-SSP transform, we migrated the crosscorrelograms (Figure 7a). In the standard VSP processing workflow, we extracted the upgoing P-wave wavefield and applied Kirchhoff migration to obtain a primary reflection image (Figure 7b). For imaging purposes, we used a smoothed velocity wavefield.

The results presented in Figure 7 demonstrate that interferometric imaging of free-surface multiples (ghosts) provides a more detailed upper section of the subsurface image, whereas the standard migration of primary reflections provides a more detailed lower section of the image. This result is consistent with the conceptual framework illustrated in Figure 1. Combining the images from both methods can provide a more detailed representation of the subsurface (Figure 7c). Before merging the two images, we normalized the amplitudes for both methods and applied additional

DOI:10.1190/INT-2021-0038.1

muting to remove the "stretch" noise. Overall, the synthetic test confirms that the presented approach is feasible for the Otway settings and provides additional benefits in imaging. In the next section, we evaluate the method on the field VSP data sets.

Table 1. Geometry parameters for synthetic walkaway VSP data modeling.

Parameters	Value
Number of sources	176
Number of receivers	700
Source interval	15 m
Receiver interval	2.5 m
Trace length	6 s
Time sampling	2 ms
Model cell size	2.5 m

Field data: Walkaway VSP with 3C geophones

Stage 2C of the Otway Project involved acquisition of one baseline and five monitoring surveys (M1-M5). Apart from the 3D surface seismic data sets recorded with a buried receiver array (Pevzner et al., 2017c), borehole 3D VSP vintages were recorded for every survey over the same set of source locations (Popik et al., 2020). Here, we apply interferometric imaging to borehole data recorded during the M5 monitor survey (Figure 8). To acquire 3D VSP data, downhole conventional sensors were deployed in the CRC-1 well (eight shuttles with 3C geophones over the depth interval of 760–865 m measured depth). The shuttles were separated by 15 m intervals.

To test the interferometric imaging approach on the Otway geophone data, we chose VSP gathers acquired with source locations along a long transect highlighted in Figure 8. The chosen source line crosses the CRC-1 well with the installed geophone array. Using a similar workflow as for the synthetic data, we separated the up- and downgoing wavefields and then applied standard Kirchhoff and interferometric migration workflows.

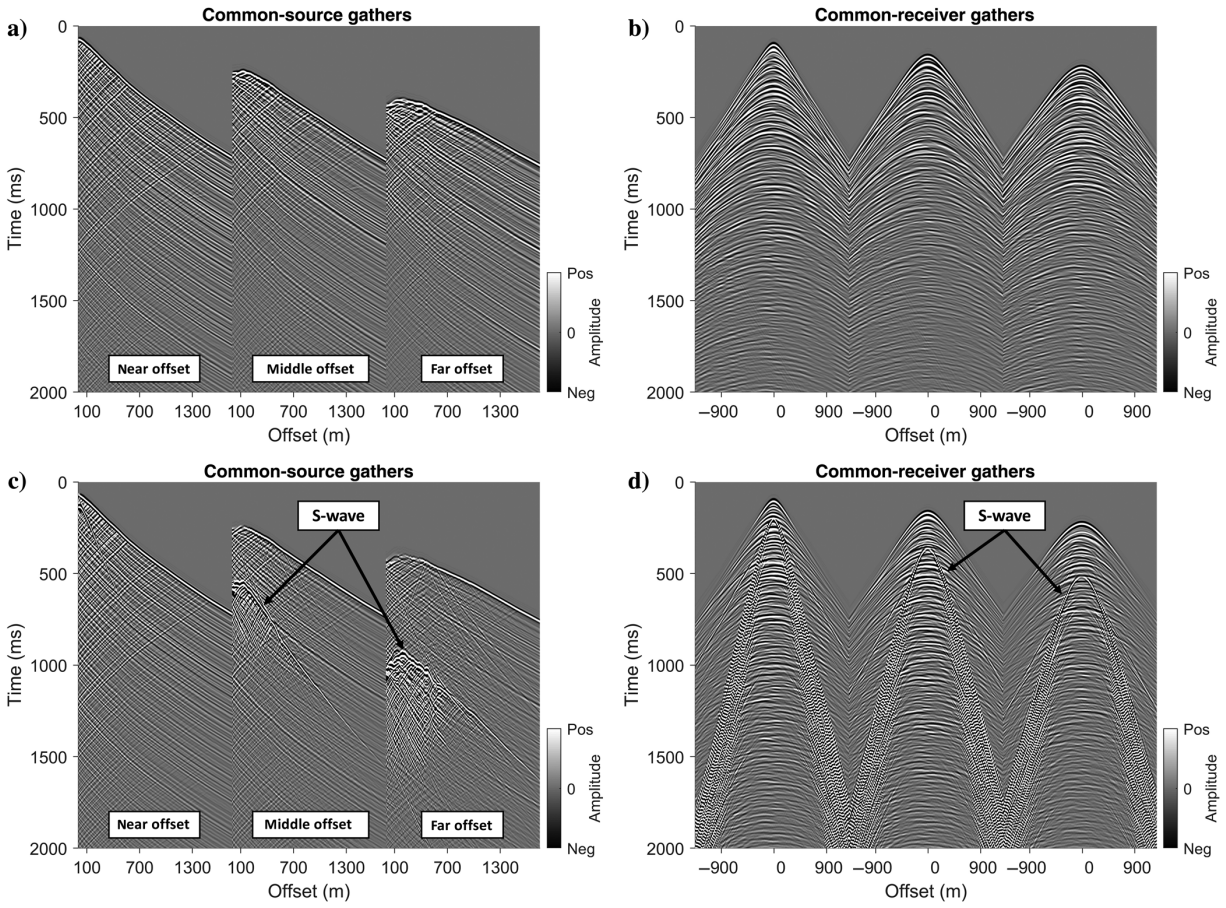

Figure 5. Example of raw synthetic data: (a) acoustic common-source gathers; (b) acoustic common-receiver gathers; (c) elastic common-source gathers; (d) elastic common-receiver gathers.

A virtual shot gather is shown in Figure 9a, and a borehole common-receiver gather (760 m measured depth) is shown in Figure 9b for reference. The final combined subsurface image for the M5 survey is shown in Figure 10. Here, the green dashed line separates the standard (below) and interferometric (above) images, the yellow dots show the locations of geophones in the CRC-1 well, and the red dots represent the source locations on the surface. The test of the interferometric approach on the geophone data shows that the free-surface multiples provide substantially increased illumination of the subsurface and that a much more complete image was obtained by combining the multiples and primaries. Even in this situation with a constrained receiver configuration (only eight geophones), the use of multiples provides additional information and extends the final image. The laterally extended image can provide a more reliable horizon tracking for seismic interpretation. The method also allows us to extract the information above the shallowest receiver in the borehole. This can be important if a receiver array does not fully cover the upper part of the well. When the source offset increases, the image resolution decreases because large incidence angles and low geophone sensitivity (poor signal-to-noise ratio [S/N]) affect the imaging quality. Beyond the half-offset distance from the receivers, the image is constructed only by the presence of the multiple events. A more complete image can be obtained if receivers cover a larger part of the length of the well. This can be achieved using DAS as discussed in the next section.

Field data: Walkaway VSP with DAS

Compared to geophones, DAS provides a broader range of illumination angles for subsurface imaging due to better borehole sensor coverage and a good coupling if cemented behind the casing. On the other hand, standard DAS cables can be less sensitive than geophones, especially for recording weak secondary wavefields.

The test of the interferometry imaging workflow on DAS VSP data was performed on a data set acquired using fiber-optic cables installed behind the casing in the CRC-3 well. CRC3 is the injector well for stage 3 of the Otway Project (injection target depth — 1500 m). The data set was acquired to improve seismic characterization of the subsurface and test the capability of the fiber-optic system (Correa et al., 2017). Data were simultaneously recorded with two DAS systems: a standard single-mode fiber connected to the Silixa's iDASv2 interrogator and an enhanced backscatter (engineered) constellation fiber connected to the iDASv3 interrogator. Overall, the survey consisted of several walkaway lines (Figure 11); interferometric analysis was applied to 31 common-shot VSP gathers acquired from shot points located along a 2D line that, if extended, would pass through the CRC-3 wellhead. The offsets range

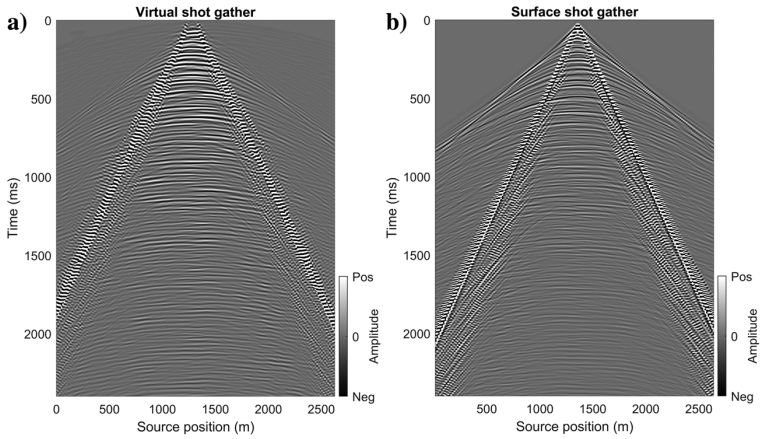

Figure 6. (a) Virtual shot gather and (b) surface seismic shot gather.

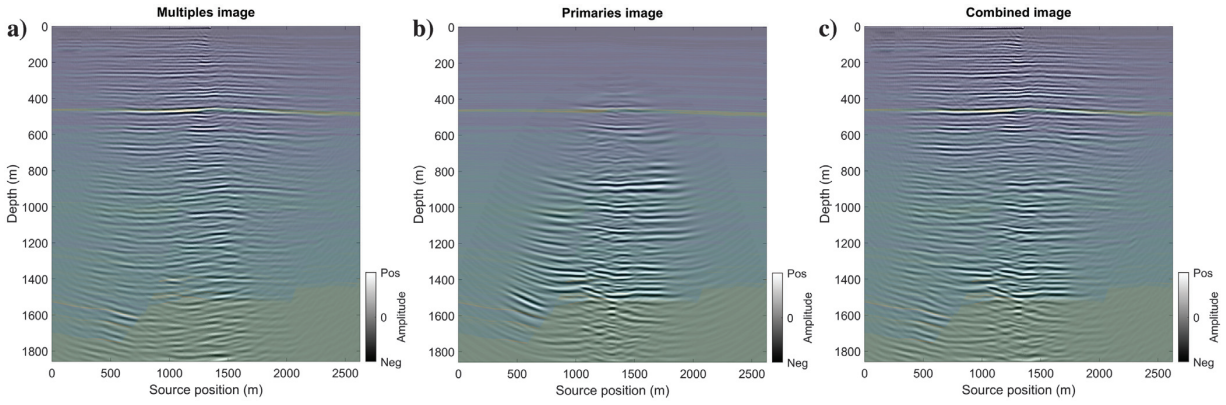

Figure 7. Synthetic data images overlayed with the velocity model. (a) Interferometric image of the free-surface multiples, (b) Kirchhoff migrated image of the primary VSP reflections, and (c) their combination.

from 435 to 885 m. Figure 11 shows the survey map, and Table 2 shows the acquisition parameters. Only sensors deeper than 275 m were used for imaging to avoid tube waves related to the surface casing.

The secondary wavefield, such as free-surface multiples, can be much weaker compared to the primary reflected wavefield. Therefore, fibers with higher sensitivity can be beneficial for interferometric imaging

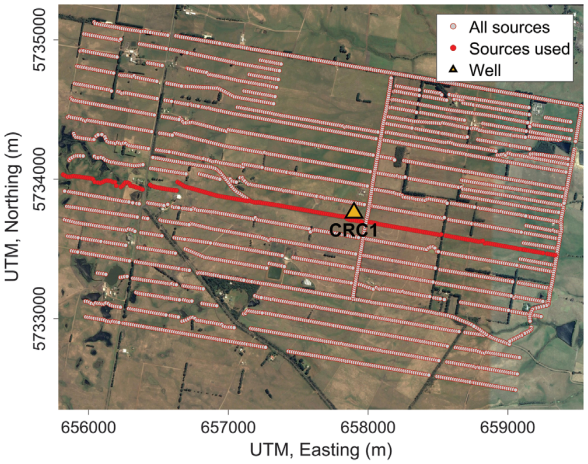

Figure 8. Stage 2C-M5 survey acquisition map. The source line taken for the interferometry test is highlighted in red; the location of the well is indicated by a yellow triangle.

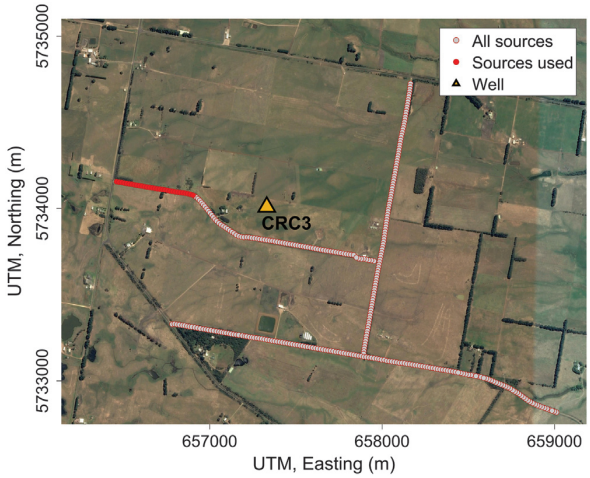

Figure 11. Stage 3 walkaway DAS-VSP acquisition basemap. The corresponding geometry parameters are presented in Table 2.

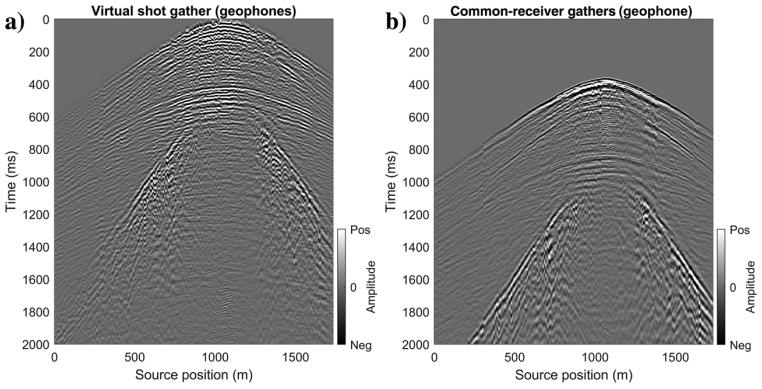

Figure 9. (a) Borehole geophone virtual shot gather and (b) borehole common-receiver gather.

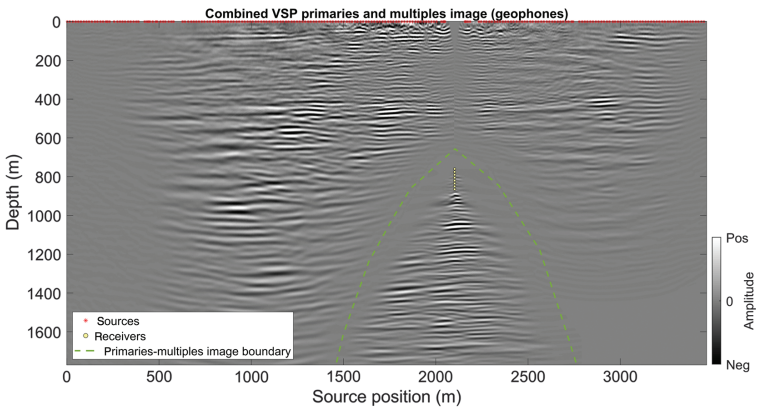

Figure 10. Standard Kirchhoff image of the VSP primaries combined with an interferometric image of VSP free-surface multiples for the Otway geophone data. The yellow dots indicate the location of the geophones; the green line shows the boundary between the standard VSP and interferometric images.

Table 2. Geometry parameters of walkaway DAS-VSP field data.

Parameters	Value
Number of sources	31
Number of receivers	273
Source interval	15 m
Receiver interval	5 m
Min offset	435 m
Max offset	885 m
Min receiver depth	275 m
Max receiver depth	1635 m
Trace length	4000 ms
Time sampling	2 ms

using surface multiples. The engineered fiber generates a stronger backscattered signal than the standard fiber and hence provides a higher S/N. Figure 12 shows raw DAS VSP shot gathers acquired with the two DAS systems. The detailed analysis of S/N between the two data sets was performed by Correa et al. (2017). The significant difference in S/Ns between the two systems is even more pronounced when comparing the results of cross-correlation interferometry (VSP-SSP transform) shown in Figure 13.

The imaging of DAS data was done with the same workflow as for the synthetic and geophone data. Interferometric images are shown in Figure 14a and 14b. Figure 14a corresponds to the engineered fiber and Figure 14b to the standard fiber. The S/N plots for both DAS systems are shown in Figure 14c and 14d. The S/N plots are calculated using the method described in Pevzner et al. (2011). Figure 14 shows that the overall

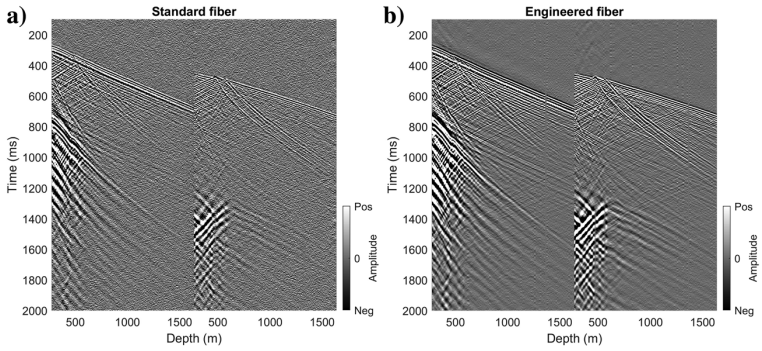

Figure 12. Raw DAS-VSP shot gathers: (a) standard DAS and (b) DAS with an enhanced fiber. The surface offsets from the wellhead are 850 and 430 m.

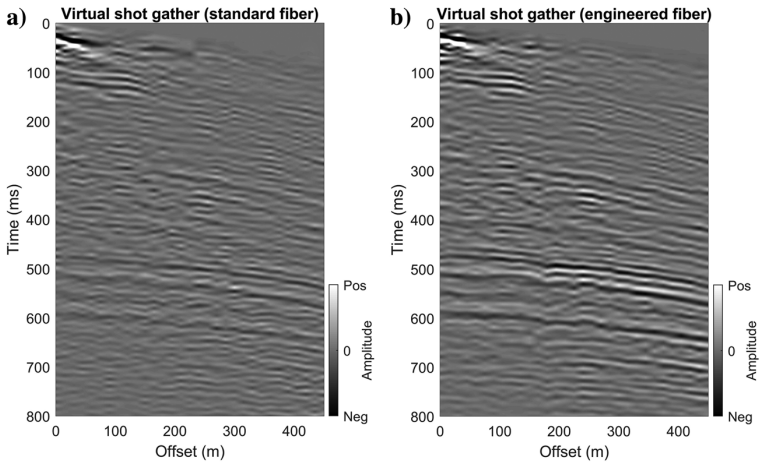

Figure 13. Virtual surface shot gathers obtained with the (a) standard fiber and (b) engineered fiber.

DOI:10.1190/INT-2021-0038.1

S/N is considerably higher for the engineered fiber, indicating that engineered fibers with higher sensitivity are more suitable for recording free-surface multiples.

Figure 15 shows the results of interferometric and standard imaging using the engineered fiber. The results demonstrate that interferometric imaging of DAS data gives the same benefits as shown in the tests on synthetic and field geophone data. Interferometric imaging provides better illumination of the near-surface part away from the well, whereas standard imaging illuminates the bottom part that is close to the borehole. The two images complement each other, and the combined image produces a more detailed picture of the subsurface next to the well.

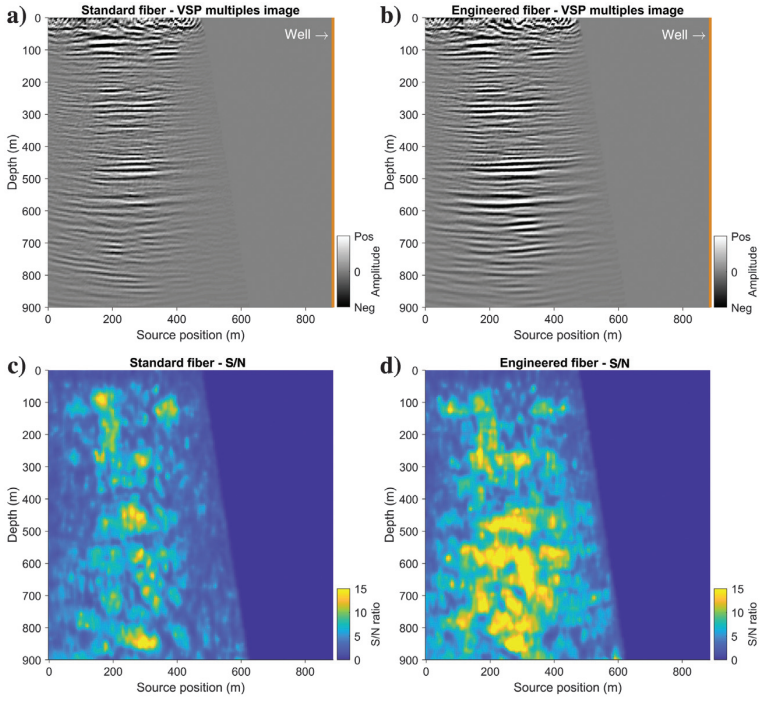

Figure 14. DAS-VSP interferometric images and S/Ns calculated for the image sections for the (a and c) standard fiber and (b and d) engineered fiber.

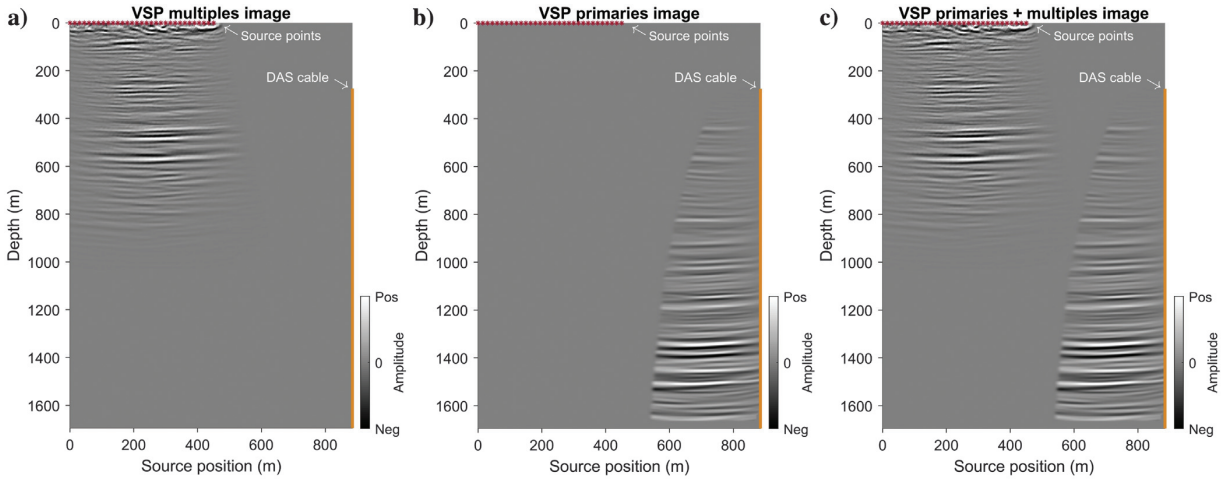

Figure 15. Result of DAS VSP imaging (engineered fiber). (a) Interferometric image of multiples, (b) standard Kirchhoff image of primaries, and (c) combined image of multiples and primaries.

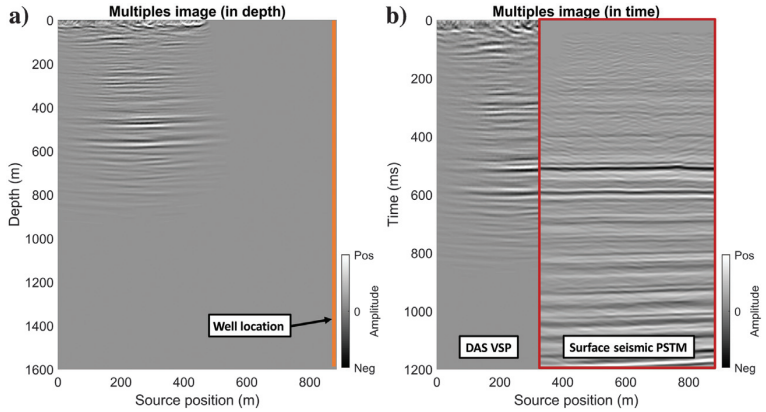

Figure 16. (a) Interferometric image of DAS VSP multiples and (b) comparison of the interferometric image of the DAS VSP multiples and PSTM surface seismic stack in time.

To examine the result of interferometric imaging approach, Figure 16 shows the DAS interferometric image converted to the time domain in comparison with a PSTM surface seismic section. The surface section was extracted from the 3D PSTM cube of the M5 survey (Popik et al., 2020). The main reflectors in Figure 16 match well between VSP and surface seismic images. The interferometric image defines the general structure properly and provides additional details in the near-surface part, which are absent on the conventional surface seismic image. A more detailed near-surface part in the interferometric image can be explained by the differences in the ranges of source-receiver offsets in the two data sets. The 3D surface seismic data are represented by the offset range of 200–1800 m, whereas the virtual shot gathers are represented by a 15–400 m offset range, which is more suitable for imaging of the near surface. These results show that the interferometric workflow can significantly improve the resolution of the shallow section of the subsurface imaging, which cannot be achieved with the standard VSP imaging alone.

Conclusions

We trialed the interferometric imaging approach on synthetic, field VSP geophone, and field VSP DAS data within the geologic setting of the Otway research site. Tests on synthetic data for the Otway site show that interferometric imaging can greatly complement standard seismic borehole processing. The method uses secondary wavefield (free-surface multiples), which significantly increases illumination of the subsurface and, unlike standard VSP imaging, can provide subsurface coverage above the shallowest borehole receiver. This can be critical for any project that focuses on VSP monitoring. To detect any possible changes in the subsurface caused by CO_2, it is extremely important for CCS projects to have a time-lapse image over the overburden as well as the reservoir. Introduction of such a methodology into borehole seismic processing and imaging significantly increases the value of monitoring based on borehole observations. The presented workflow is based on P-waves only; however, seismic interferometry can also be used to take advantage of shear waves (source-generated and converted), but this is beyond the scope of this paper.

Application of interferometric migration to field geophone data of the Otway Project demonstrated a significant increase of the subsurface coverage compared to the standard VSP imaging strategy. The method allowed us to extract reflectivity information above the shallowest receiver and to widely expand the final VSP image section even with only eight geophones installed in the borehole. This field test suggests that interferometric imaging is a promising method for seismic monitoring with receiver arrays covering an entire length of the well.

Such well coverage is almost impossible to achieve with geophones, but it can be easily achieved with DAS, which results in a wider range of illumination angles for interferometric data redatuming. On the other hand, standard DAS sensors are less sensitive than geophones, which can impede imaging using a weak secondary wavefield. However, the enhanced backscattering fiber can significantly improve DAS sensitivity, providing a considerably higher S/N ratio of the final image than the standard fiber. Our test shows that DAS with engineered fibers is sensitive enough to record free-surface VSP multiples and can provide an image of the reflectors comparable to the surface seismic image in the depth range suitable for both methods (approximately 300–700 m in our case).

The interferometric imaging methodology paired with DAS technology can considerably increase the reliability of reservoir monitoring programs based on borehole measurements. All of the experiments demonstrate that the trialed methodology provides a significant lateral and vertical extension of the subsurface image obtained with borehole receivers. This can be highly valuable for the correlation of geologic horizons at the stage of data interpretation.

The presented workflow is designed for 2D implementations only. A possibility of a 3D implementation as well as time-lapse and repeatability analysis will be the subjects of future work.

Acknowledgments

The authors would like to acknowledge CO2CRC for their leadership in the conceptualization, design, and field operations associated with the Otway Project. This project received CO2CRC funding through its industry members and research partners, the Australian government under the CCS Flagships Programme, the Victorian

state government, and the Global CCS Institute. The authors wish to acknowledge the financial assistance provided through the Australian National Low Emissions Coal Research and Development (ANLEC R&D). ANLEC R&D is supported by Australian Coal Association Low Emissions Technology Limited and the Australian government through the Clean Energy Initiative. E. Sidenko thanks Curtin Oil and Gas Innovation Centre for the Ph.D. scholarship. The authors are grateful to the sponsors of the Curtin Reservoir Geophysics Consortium for the financial support. We also thank A. Egorov and S. Popik for their help (both of Curtin University). Special thanks go to B. Gurevich (Curtin University) for his useful advice and for help with manuscript preparation.

Data and materials availability

Data associated with this research are confidential and cannot be released.

References

Bakulin, A., and R. Calvert, 2006, The virtual source method: Theory and case study: Geophysics, **71**, no. 4, SI139–SI150, doi: 10.1190/1.2216190.

Bohlen, T., K. Daniel, and S. Jetschny, 2015, SOFI2D, seismic modeling with finite differences, 2D — Acoustic and viscoelastic version, Users Guide: Karlsruhe Institute of Technology, 1–54.

Claerbout, J. F., 1968, Synthesis of a layered medium from its acoustic transmission response: Geophysics, **33**, 264–269, doi: 10.1190/1.1439927.

Cook, P., 2014, Geologically storing carbon: Learning from the Otway Project experience: CSIRO Publishing.

Correa, J., A. Egorov, K. Tertyshnikov, A. Bona, R. Pevzner, T. Dean, B. Freifeld, and S. Marshall, 2017, Analysis of signal to noise and directivity characteristics of DAS VSP at near and far offsets — A CO2CRC Otway Project data example: The Leading Edge, **36**, 994a1–994a7, doi: 10.1190/tle36120994a1.1.

Daley, T. M., B. M. Freifeld, J. Ajo-Franklin, S. Dou, R. Pevzner, V. Shulakova, S. Kashikar, D. E. Miller, J. Goetz, J. Henninges, and S. Lueth, 2013, Field testing of fiber-optic distributed acoustic sensing (DAS) for subsurface seismic monitoring: The Leading Edge, **32**, 699–706, doi: 10.1190/tle32060699.1.

Dou, S., J. Ajo-Franklin, T. Daley, M. Robertson, T. Wood, B. Freifeld, R. Pevzner, J. Correa, K. Tertyshnikov, M. Urosevic, and B. Gurevich, 2016, Surface orbital vibrator (SOV) and fiber-optic DAS: Field demonstration of economical, continuous-land seismic time-lapse monitoring from the Australian CO 2 CRC Otway site: 86th Annual International Meeting, SEG, Expanded Abstracts, 5552–5556, doi: 10.1190/segam2016-13974161.1.

Freifeld, B. M., R. Pevzner, S. Dou, J. Correa, T. M. Daley, M. Robertson, K. Tertyshnikov, T. Wood, J. Ajo-Franklin, M. Urosevic, and B. Gurevich, 2016, The CO2CRC Otway Project deployment of a distributed acoustic sensing network coupled with permanent rotary sources: 78th Annual International Conference and Exhibition : Efficient Use of Technology — Unlocking Potential, EAGE, Extended Abstracts, 2–6, doi: 10.3997/2214-4609.201600577.

Glubokovskikh, S., R. Pevzner, T. Dance, E. Caspari, D. Popik, V. Shulakova, and B. Gurevich, 2016, Seismic monitoring of CO_2 geosequestration: CO2CRC Otway case study using full 4D FDTD approach: International Journal of Greenhouse Gas Control, **49**, 201–216, doi: 10.1016/j.ijggc.2016.02.022.

Karrenbach, M., S. Cole, A. Ridge, K. Boone, D. Kahn, J. Rich, K. Silver, and D. Langton, 2019, Fiber-optic distributed acoustic sensing of microseismicity, strain and temperature during hydraulic fracturing: Geophysics, **84**, no. 1, D11–D23, doi: 10.1190/geo2017-0396.1.

Lumley, D., 2010, 4D seismic monitoring of CO_2 sequestration: The Leading Edge, **29**, 150–155, doi: 10.1190/1.3304817.

Miller, D., T. Parker, S. Kashikar, M. Todorov, and T. Bostick, 2012, Vertical seismic profiling using a fibre-optic cable as a distributed acoustic sensor: 74th Annual International Conference and Exhibition Incorporating SPE EUROPEC: Responsibly Securing Natural Resources, EAGE, Extended Abstracts, 17–21, doi: 10.3997/2214-4609.20148799.

Pevzner, R., V. Shulakova, A. Kepic, and M. Urosevic, 2011, Repeatability analysis of land time-lapse seismic data: CO2CRC Otway pilot project case study: Geophysical Prospecting, **59**, 66–77, doi: 10.1111/j.1365-2478.2010.00907.x.

Pevzner, R., K. Tertyshnikov, V. Shulakova, M. Urosevic, A. Kepic, B. Gurevich, and R. Singh, 2015, Design and deployment of a buried geophone array for CO_2 geosequestration monitoring: CO2CRC Otway Project, Stage 2C: 85th Annual International Meeting, SEG, Expanded Abstracts, 266–270, doi: 10.1190/segam2015-5902309.1,

Pevzner, R., K. Tertyshnikov, E. Sidenko, and S. Yavuz, 2020, Effects of cable deployment method on DAS VSP data quality: Study at CO2CRC Otway in-situ Laboratory: 82nd Annual International Conference and Exhibition, EAGE, Extended Abstracts, 1–5, doi: 10.3997/2214-4609.202010765.

Pevzner, R., M. Urosevic, D. Popik, V. Shulakova, K. Tertyshnikov, E. Caspari, J. Correa, T. Dance, A. Kepic, S. Glubokovskikh, S. Ziramov, B. Gurevich, R. Singh, M. Raab, M. Watson, T. Daley, M. Robertson, and B. Freifeld, 2017b, 4D surface seismic tracks small supercritical CO_2 injection into the subsurface: CO2CRC Otway Project: International Journal of Greenhouse Gas Control, **63**, 150–157, doi: 10.1016/j.ijggc.2017.05.008.

Pevzner, R., M. Urosevic, D. Popik, V. Shulakova, K. Tertyshnikov, E. Caspari, J. Correa, T. Dance, A. Kepic, S. Glubokovskikh, S. Ziramov, B. Gurevich, R. Singh, M. Raab, M. Watson, T. Daley, M. Robertson, and B. Freifeld, 2017c, 4D surface seismic tracks small supercritical CO_2 injection into the subsurface: CO2CRC Otway Project: International Journal of Greenhouse Gas Control, **63**, 150–157, doi: 10.1016/j.ijggc.2017.05.008.

Pevzner, R., M. Urosevic, K. Tertyshnikov, B. Gurevich, V. Shulakova, S. Glubokovskikh, D. Popik, J. Correa, A. Kepic, B. Freifeld, M. Robertson, T. Wood, T. Daley, and R. Singh, 2017a, Stage 2C of the CO2CRC Otway Project: Seismic monitoring operations and preliminary results: Energy Procedia, **114**, 3997–4007, doi: 10.1016/j.egypro.2017.03.1540.

Popik, S., R. Pevzner, K. Tertyshnikov, D. Popik, M. Urosevic, V. Shulakova, S. Glubokovskikh, and B. Gurevich, 2020, 4D surface seismic monitoring the evolution of a small CO2 plume during and after injection: CO2CRC Otway Project study: Exploration Geophysics, **51**, 570–580. 10.1080/08123985.2020.1735934.

Popik, S., D. Popik, and R. Pevzner, 2019, Effect of density of seismic sources on the quality of the 4D seismic data: 81st Annual International Conference and Exhibition, EAGE, Extended Abstracts, 1–5, doi: 10.3997/2214-4609.201901581.

Rickett, J., and J. Claerbout, 1996, Passive seismic imaging applied to synthetic data: SEP Report, **92**, 83–90.

Schuster, G. T., 2009, Seismic interferometry: Cambridge University Press.

Schuster, G. T., J. Yu, J. Sheng, and J. Rickett, 2004, Interferometric/daylight seismic imaging: Geophysical Journal International, **157**, 838–852, doi: 10.1111/j.1365-246X.2004.02251.x.

Shulakova, V., R. Pevzner, J. Christian Dupuis, M. Urosevic, K. Tertyshnikov, D. E. Lumley, and B. Gurevich, 2015, Burying receivers for improved time-lapse seismic repeatability: CO2CRC Otway field experiment: Geophysical Prospecting, **63**, 55–69, doi: 10.1111/1365-2478.12174.

Sidenko, E., R. Pevzner, A. Bona, and K. Tertyshnikov, 2019, Seismic interferometry using walkaway DAS VSP data: CO2CRC Otway project feasibility study: 81st Annual International Conference and Exhibition, EAGE, Extended Abstracts, 1–5, doi: 10.3997/2214-4609.201900694.

Wapenaar, K., 2004, Retrieving the elastodynamic Green's function of an arbitrary inhomogeneous medium by cross correlation: Physical Review Letters, **93**, 254301, doi: 10.1103/PhysRevLett.93.254301.

Yu, J., and G. T. Schuster, 2004, Enhancing illumination coverage of VSP data by crosscorrelogram migration: 74th Annual International Meeting, SEG, Expanded Abstracts, 2501–2504, doi: 10.1190/1.1845235.

Biographies and photographs of the authors are not available.

2.2 Distributed fibre-optic sensing transforms an abandoned well into a permanent geophysical monitoring array: a case study from Australian South West.

Distributed fiber-optic sensing transforms an abandoned well into a permanent geophysical monitoring array: A case study from Australian South West

Evgenii Sidenko[1], Konstantin Tertyshnikov[1], Boris Gurevich[1], Roman Isaenkov[1], Ludovic P. Ricard[2], Sandeep Sharma[3], Dominique Van Gent[4], and Roman Pevzner[1]

https://doi.org/10.1190/tle41020140.1

Abstract

Distributed temperature sensing (DTS) and distributed acoustic sensing (DAS) data recorded by a fiber-optic array installed during the decommissioning operations of the 1550 m Harvey 3 well in Western Australia reveal an abundance of valuable information about the course of the decommissioning process and the quality of the cement job. The DAS monitoring has detected vibrational disturbances during the cement's setting up, while DTS was used to assess setting up of the cement and curing times as well as uniformity of cementation from the distribution of temperature along the borehole. A weeklong trial acquisition of passive seismic data with the same array a year later shows an abundance of seismic events in a wide frequency range from below 1 mHz to above 200 Hz. The downhole DAS array provides traveltimes and amplitudes of these events, which include earthquakes, mine blasts, ocean microseisms, and local human activity. The amplitudes of waves from distant seismic events can be used to estimate and monitor physical properties of the media along the extent of the well. When used in combination with information from active vertical seismic profiling, these events can help obtain independent estimates of velocities and densities. Spectral analysis of low-frequency microseisms shows a strong correlation between passively recorded DAS and local weather observations. This shows that the ability to continuously record oceanic microseisms at low frequencies opens opportunities to employ such arrays for wave climate studies. In addition, the data contain peculiar in-hole reverberations likely caused by crossflow of groundwater behind the intermediate casing, which may indicate imperfections of the cement job. The results demonstrate that a downhole fiber-optic array installed in an abandoned well represents an opportunity to establish a permanent facility for continuous recording of passive and active geophysical data and for exploring various applications.

Introduction

New wells give an opportunity to gather new information about the subsurface through wireline logging, coring, and borehole geophysical studies. Wells also provide room for installing dedicated sensors to monitor subsurface changes such as those related to oil production or CO_2 geosequestration. Abandonment of previously drilled wells is a costly operation and involves plugging with cement and removal of all infrastructure. As a result, the well, an expensive and formerly precious asset, is lost. However, installation of distributed fiber-optic sensors during decommissioning has potential to transform an abandoned well into a permanent sensor array. This deployment can be used to control the cementation process and monitor subsequent changes in the subsurface by recording such parameters as strain, temperature, and vibration caused by natural or induced seismicity. Such wells also can be utilized to conduct active borehole seismic surveys such as vertical seismic profiling (VSP).

The use of fiber-optic cables as downhole sensors has substantial advantages over conventional downhole receivers. Most fiber-optic cables are robust and reliable for long-term installations as they have no electronics or moving parts. Also, deployment of such cables in a well distributes sensors over its entire length at small spacing intervals. Fiber-optic cables can also be manufactured to withstand considerable pressure and temperature (up to 250°C). The most sensitive and valuable instrument equipment — an optical interrogator unit — is always located at the surface and can be connected easily to the downhole cable and reconfigured to satisfy the measurement requirements. Such benefits make this technology a perfect option for plug and abandon (P&A) monitoring applications and building permanent surveillance arrays in harsh environments such as deep wells. Once deployed, fiber-optic sensing systems can be used for distributed acoustic sensing (DAS) and distributed temperature sensing (DTS).

DTS measures temperature distribution along the fiber-optic cable. Borehole temperature monitoring helps with wellbore and reservoir characterization. Continuous DTS recording can characterize downhole flow operations (Patterson et al., 2017; Miller et al., 2018). DTS can also be used to monitor the cement curing process, which provides near real-time information about the cement injection process, and verify the quality of the cement binding a posteriori (Ricard, 2020).

DAS is designed to measure dynamic strain and uses a single optical fiber as an array of optical vibrational sensors with a dense receiver spacing that could be as small as 0.25 cm (Silixa, 2018). It is capable of acquiring data in a broad frequency range

[1]Centre for Exploration Geophysics, Curtin University, Perth, Western Australia. E-mail: evgenysidenko@gmail.com; konstantin.tertyshnikov@curtin.edu.au; b.gurevich@curtin.edu.au; roman.isaenkov@postgrad.curtin.edu.au; r.pevzner@curtin.edu.au.
[2]CSIRO Energy, Perth, Western Australia. E-mail: ludovic.ricard@csiro.au.
[3]Carbon Projects Pty. Ltd., Perth, Western Australia. E-mail: sandeep_sharma1@outlook.com.
[4]Department of Mines, Industry Regulation and Safety, Perth, Western Australia. E-mail: dvangent54@gmail.com.

from below 1 mHz to hundreds of hertz (Becker et al., 2017; Lindsey et al., 2019). DAS can be used to monitor local and regional seismicity and detect distant seismic events (Ajo-Franklin et al., 2019), record ambient seismic noise, and monitor any borehole-related vibrational signals (Miller et al., 2018; Karrenbach et al., 2019).

Most installations of fiber optics are in open and active monitoring and production wells. Here, we use fiber-optic sensing for monitoring of P&A operations of a deep well and its subsequent transformation into a permanent seismic monitoring array. The study was done during and after decommissioning of the Harvey 3 well drilled as a part of the South West Hub CO_2 geosequestration project in Western Australia (Sharma et al., 2017).

The proposed initiative to cement a fiber-optic cable inside the Harvey 3 well as a part of the decommissioning procedure was supported by the Department of Mines, Industry Regulation and Safety of Western Australia, and the installation was conducted in January 2019. The Harvey 3 well site is located about 120 km south of the state capital of Perth and about 10 km from the coast. Such close proximity to a major city yet away from industrial and traffic noise makes the site an optimal location for establishing a permanent facility for passive seismic data acquisition. During P&A operations, a comprehensive data set was acquired using DAS and DTS to monitor cement flow and curing (Ricard et al., 2019).

One year after completing decommissioning operations, the Harvey 3 fiber-optic cable was used for a weeklong acquisition of passive seismic data (Pevzner et al., 2020b). Although one week is a relatively short time to record a representative data set for analysis of noise patterns and seismicity in the area, many valuable observations and revelations were obtained. In particular, the results demonstrate that ambient seismic signals can reveal information about the well's conditions a year after cementation, distribution of elastic properties along the well, and natural processes such as seismicity and ocean wave climate.

Preliminary results describing installation of the fiber-optic cable DAS and DTS monitoring of P&A operations and one-week passive monitoring conducted a year after the borehole cementation were published in Ricard et al. (2019) and Pevzner et al. (2020b). In this paper, we present a more systematic and complete analysis of the experiment and data.

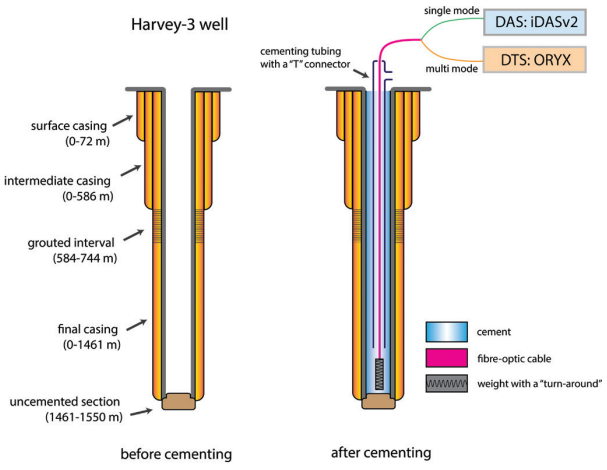

Figure 1. Scheme of Harvey 3 well before and after cementing.

South West Hub project background

The South West Hub Carbon Capture and Storage (CCS) project was the first initiative in Western Australia supported by the Australian Government's CCS Flagships program (Sharma and Van Gent, 2018). The site is located approximately 120 km south of Perth. Several wells were drilled (Harvey 1, 2, 3, and 4) in the project area as part of an extensive program of geologic characterization and uncertainty reduction. The Harvey 1 well was plugged and abandoned in 2011. Harvey 2 is a site of a long-term CSIRO In-Situ Laboratory research facility (Michael et al., 2019). Harvey 3 and Harvey 4 were decommissioned in 2019. Harvey 3 was drilled between December 2014 and June 2015 as a stratigraphic well for geologic characterization of the South West Hub project area. The well reached the top of the target formation for planned CO_2 injections. The well is completed with three stages of casing (Figure 1) including a 4.5 in. production casing. The total depth of the well is 1550 m. The well was left suspended shortly after drilling with van Ruth plugs at the bottom (Nims and Pollock, 2015). The Harvey 3 well and its vicinity area are characterized by a comprehensive suite of data comprising core samples analysis (Singh, 2018), wireline logs, and seismic surveys, including 3D VSP and a dedicated high-resolution 3D surface seismic survey (Urosevic et al., 2017). Availability of such a detailed knowledge base about the site makes it attractive for innovative experiments and trials. Planned decommissioning of the well presented an excellent opportunity to conduct the first trial of transforming an abandoned well into a deep vertical permanent seismic array using fiber-optic sensing technology. The deployed fiber-optic cable acts as a receiver array providing in-situ measurements of the subsurface at thousands of points along the well during and after the P&A process.

Monitoring of the decommissioning process using optical fibers

The fiber-optic cable was installed as a part of Harvey 3 well decommissioning operations on 22 and 23 January 2019. A quarter-inch stainless steel jacketed fiber-optic loose-tube cable has four single-mode and two multimode fiber-optic cores as well as two copper cores.

The fiber-optic cable was terminated with a double-ended configuration for the multimode cores (for DTS measurements) and with attenuators for the single-mode cores (for DAS measurements), while the electrical conductors were connected together to enable heating of the cable (for active DTS measurements). The downhole terminations were inserted inside a 6 m long steel weight for protection and to ease the cable deployment.

Before cementing started, a cementing tubing (2 ⅜ in) was installed to enable the fiber-optic cable deployment inside it. Once the tubing was installed and the fluid swapped, the fiber-optic cable was lowered inside the tubing. A custom-designed T-shaped connection at the wellhead enabled the simultaneous cementing process and its monitoring using distributed fiber-optic sensors.

The tubing was left in the well after the cement injection. A schematic diagram of the Harvey 3 well before and after the cementation is shown in Figure 1.

The primary idea of the experiment was to monitor the borehole P&A (cementing) process using fiber-optic sensing technology.

DTS monitoring. Borehole temperature was monitored for two days including baseline (after cable installation and prior to the cement injection), cement injection, and postinjection (cement curing) using a Sensornet Oryx DTS interrogator with a vertical spacing of 1 m and temporal sampling of 60 s.

Figure 2 shows the DTS data recorded over the P&A operations in the well. Figure 2a shows absolute temperature values measured by DTS; Figure 2b shows the temperature anomaly — absolute temperature minus baseline average (depth temperature distribution). The baseline average was calculated for each depth along the fiber-optic cable and over the time interval before the start of the cement injection (to the left from the first black dashed line in Figure 2). On both plots, the vertical axis corresponds to the length along the fiber-optic cable (measured depth); the horizontal axis corresponds to time. The time interval between the two dashed lines corresponds to the period of the acquired DAS data shown in Figure 3 in the next section. Three different stages can be observed on DTS data plots: (1) baseline, (2) injection and cement settling, and (3) cement curing and equilibration.

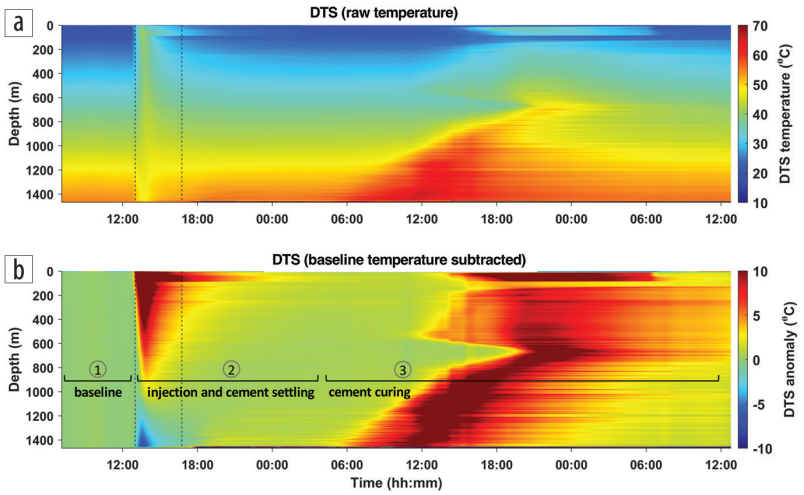

Figure 2. DTS data recorded in Harvey 3 well. (a) Absolute temperature. (b) Temperature change regarding the baseline's average. Dashed interval indicates recorded DAS data time frame.

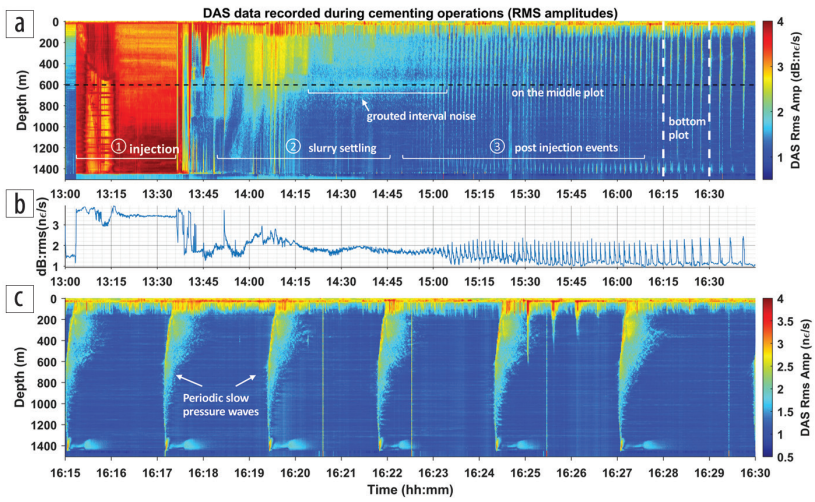

Figure 3. DAS data recorded during Harvey 3 well cementation. (a) DAS root-mean-square amplitudes for the whole well interval starting from the start of the injection; (b) DAS response from a single depth of 600 m (a single trace shown as black dashed line on the upper plot); (c) DAS response from the time interval highlighted by white dashed lines in the upper plot.

Cement temperature was constant over the time of the injection and while it filled the whole well column. From Figure 2 it is clear that the temperature of the cement slurry was equal to the formation temperature at about 1100 m depth (approximately 40°C–45°C). The interval between two dashed lines on the anomaly plot (Figure 2b) shows that the introduction of the cement slurry heated the depth interval above 1100 m and cooled the interval below 1100 m.

After the cement was fully injected, it gradually settled down, and in 12 hours the temperature reversed back to the formation (baseline) values over the entire well length. It took noticeably more time for temperatures in the upper part (0–100 m) to equilibrate, probably because of lower thermal conductivity of the well in this interval due to the presence of the surface casing.

Cement curing started only 18 hours after injection (6:00 to the end of the recording). First, it starts at the bottom of the well, as the formation temperature is the catalyst and it is the highest in the deepest part. Then, the cement curing process starts slowly at each depth all the way up to the wellhead. As cement curing is an exothermic reaction, the DTS data show a clear heat release.

Recorded DTS data help identify two heterogeneities in the well structure. The first occurs between 600 and 800 m as a delay to the start of the curing process in this interval. This depth interval corresponds to the grouted section of the Harvey 3 well (see Figure 1). The second heterogeneity is in the depth interval around 100 m. This section corresponds to a joint between intermediate and surface casings. DTS data acquired in this interval show very little temperature change compared to other parts of the well.

Overall, fiber-optic temperature monitoring data acquired during P&A operations demonstrate that this method is a simple and reliable tool to monitor the process of cement curing along the entire borehole. Real-time DTS data help diagnose cement conditions and better assess the actual cementation time. This is important to ensure that the pipe is not moved before the cement is fully set and reduces the chances of developing of channels allowing flow in cement behind casing.

DAS monitoring. DAS monitoring of the decommissioning process used single-mode fibers and two different interrogators: Fotech Helios Theta and Silixa iDAS v2. Monitoring acquisition started at 10:00 on 23 January and completed by 17:00 on the same day. The recorded DAS data are shown in Figure 3. The time-lapse response from the interrogators over a nearly 4-hour time interval is shown in Figure 3a.

Surface activities near the wellhead are indicated by short red bursts at the 0–200 m depth interval. Cement injection lasted for 30 minutes from 13:05 until 13:35. The injection process is clearly visible on DAS as a red intensive area along the entire length of the well. The response to the injection is uniform along the entire length of the borehole and is hard to interpret as it is primarily related to vibrations of the cementing tubing.

After the cement has been injected, various responses at different parts of the well can be observed (13:45–14:45). In this time interval, the DAS response is not uniform along the borehole and probably is related to the cement slurry settling down in the well. We can observe short-period oscillations in the lower part of the well (below 1000 m) and more long-period signals in the upper part (0–800 m).

To improve borehole integrity, during the well drilling in 2015, the depth interval from 584–744 m was relatively soft and friable and thus was grouted with the cement and redrilled (Nims and Pollock, 2015). We can see the presence of some distinct noise related to this interval around 600 m depth between 14:30 and 15:15.

The final time interval of DAS monitoring between approximately 15:00 and 16:45 shows a completely different behavior compared to the previous parts of the record. During this time, DAS recorded a number of slow periodical events propagating along the fiber-optic cable. The time gap between these events is gradually increasing toward the end of the DAS record from approximately 1–2 to 3–4 minutes. Several events recorded during this time interval, indicated by two white dashed lines in Figure 3a, are shown in Figure 3c. The apparent propagation velocity of these events along the cable up to the wellhead is less than 100 m/s. This is much lower than for any typical body or surface seismic waves. These events are most possibly slow pressure waves occurring in the water-gas mixtures (Boone et al., 2014). The velocity of pressure waves in water-gas mixtures depends on temperature, pressure, and gas void fraction. The presence of air bubbles dramatically decreases the pressure-wave velocity, which can be as low as 20 m/s (Kieffer, 1977).

The character of the observed periodic events was changing with time as shown in Figure 4. At the beginning (Figure 4a), it is mostly shapeless scattered noise with no distinct front. After approximately 15:04, a front gradually appears (first-break arrivals of the events) along the entire length of the well (Figure 4b). After 16:00, the front becomes clear: most of the energy is concentrated around first-break arrivals (Figure 4c). Scattered noise becomes denser in the upper part, and it becomes evident that this noise is related to these periodic events. Traveltime curves are not symmetric along the borehole length. Their zero time corresponds to the depth interval between 800 and 1200 m. The apparent velocity is lower in the upper part of the well as manifested by a more noticeable curvature of first-break arrivals. Such a time evolution of the described events could be caused by varying borehole conditions (pressure, temperature, gas bubbles' fraction). Also, different noise patterns can be observed in the upper half of the cable and in the vicinity of the bottom hole. The noise is much more scattered after first-break arrivals in the upper part of the well. There are second-order events occurring near the bottom hole. These deeper events could occur because of the interaction between the cable and the bottom hole. Temperature variations also causes a signal on DAS (shown in Figure 4b). Such short-period events cannot be validated by DTS as it has a much larger sampling rate (60 s).

The acquired DAS data are quite rich in events but also quite complex and require further studies to gain more understanding and develop an appropriate approach for analysis. Nevertheless, even this qualitative examination provides new insights into the interaction between a fiber-optic cable and injected cement slurry and even into the mechanical behavior of the whole cemented borehole system. It is also important that DAS data are usually acquired with much denser temporal sampling than DTS (1 ms versus 30 s). Thus, DAS can easily track not only seismic vibrations but also signals caused by short-period temperature changes, as DAS is sensitive to the time derivative of the temperature (Miller et al., 2018; Sidenko et al., 2021).

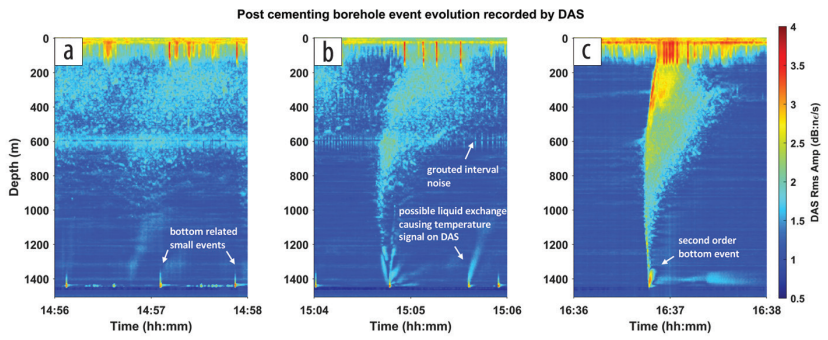

Figure 4. Evolution of the borehole event recorded by DAS after cementing operations were finished.

Passive data acquisition

In May 2020, more than one year after the completion of the P&A operations, passive DAS acquisition was conducted using the fiber-optic array cemented in the Harvey 3 well. The main objective of the experiment was to further explore the feasibility and

potential of passive borehole seismic monitoring using the cable in the abandoned borehole.

The passive DAS survey was acquired using only the Silixa iDAS v2 interrogator. The DAS recording unit was housed in a seismic acquisition truck and powered from a diesel generator on a trailer positioned away from the truck to reduce vibration on the interrogators. The equipment was controlled remotely using a cellular network.

Data acquisition commenced on 21 May and finished on 28 May. No data were acquired for one day around 24 May due to a once-in-a-decade storm (Manfield et al., 2020) passing through the area, which forced suspension of the operation.

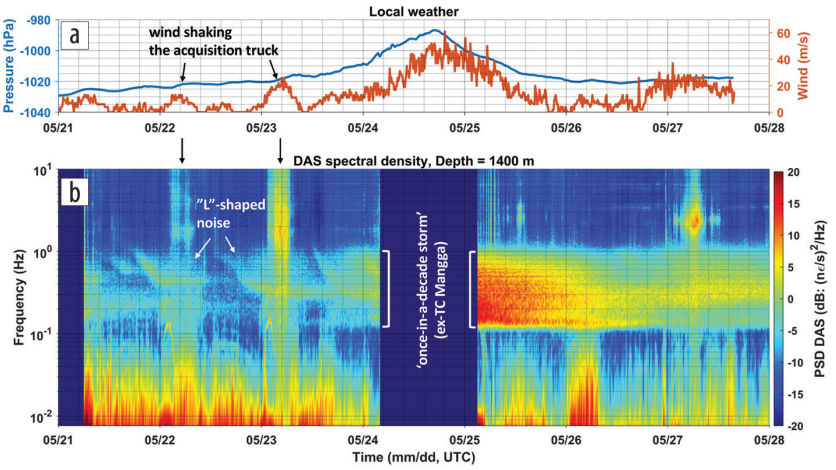

Figure 5. (b) Spectrogram of the DAS record at 1400 m MD compared to (a) weather events.

Passive seismic data analysis consists of identification of site-specific components of the wavefield, which can be used to derive useful information about the subsurface, conditions of the well, or human-related and natural events. As a result, three major groups of events were identified in the recorded data set: (1) ocean-related low-frequency microseisms, (2) distant mine blasting and earthquakes, and (3) local surface human-related activity and in-well repeating events.

Oceanic microseisms. Figure 5 shows a spectrogram of DAS data (Figure 5b) computed for the receiver at 1400 m along with information about the weather in the area (Figure 5a). The frequency range between 0.1 and 1 Hz is dominated by Rayleigh waves corresponding to the oceanic microseisms (Bromirski, 2002; Nishida, 2017; Glubokovskikh et al., 2021) represented by the double frequency of the actual ocean waves spectrum (Lin et al., 2018). They originate from the coastal surface oscillations generated by nonlinear interference between oppositely propagating ocean waves of the same frequency (Hasselmann, 1963). The spectrogram also demonstrates the ability of fiber-optic sensors to record very low frequencies (down to 10 mHz), which can carry useful information about the oceanic climate.

The spectrogram contains clearly pronounced L-shaped spectral associated with a sea breeze on 22 and 23 May as well as clear evidence of a big storm on 24 and 25 May. The increased wideband noise at approximately 2–3 Hz is related to the resonance of the acquisition truck forced by the strong wind with speeds above approximately 25 km/h.

Arrivals of remote storms are characterized by the spectral peak shifting toward the higher frequencies due to the deepwater ocean waves' dispersion and distinguished by L-shaped patterns (Bromirski et al., 1999) of the oceanic noise recorded between 21 and 24 May. In contrast, the development of a large local storm is indicated by the spectral peak shift toward the lower frequencies. It is accompanied by the dramatic increase of wind speed (Figure 5a) as the intensity of the local storm increases.

Mine blasting and earthquakes. Eight blasting events from mines located 40–70 km from the site were detected on

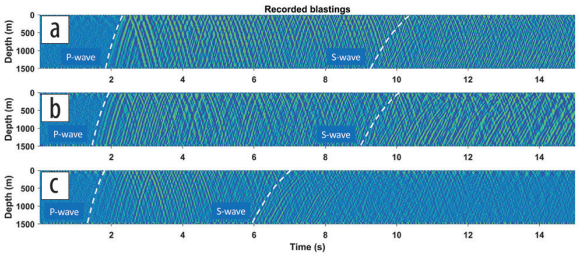

Figure 6. Examples of blasting events recorded by the permanently installed fiber-optic array.

seismograms using a semblance-based algorithm. Three examples of such events are shown in Figure 6. Both P- and S-waves are clearly pronounced on the record and can be identified by the difference in the apparent velocities. The delay between P- and S-wave arrival times allows estimating the distance to the source. To do this, we use a velocity model that was previously calibrated using several regional earthquakes recorded by a training well at the Curtin campus approximately 120 km away from Harvey 3 (Shulakova et al., 2020).

DAS also recorded several earthquakes. To identify earthquakes in data, we matched the times of the events to Geoscience Australia's Earthquake Database (Geoscience Australia, 2020). Figure 7 shows an example of a distant earthquake (the Banda Sea earthquake with magnitude Mw = 5.42). Figure 7 shows the earthquake signal recorded by DAS at 500 m depth; Figure 7b shows the corresponding DAS response spectrogram; Figure 7c shows the signal recorded at the same time by the vertical component of the broadband high-gain seismometer located 10 km from the well in the town of Harvey (Balfour et al., 2014). Both DAS and seismometer data are band-pass filtered to emphasize body waves arrivals. In DAS data, the P-wave first arrival looks more distinct than in the seismometer data as DAS receivers are located in a quiet downhole environment away from surface wave noise.

Recorded waves from distant blasting events and natural earthquakes can be used to monitor variations of elastic properties

along the well over time (Mateeva and Zwartjes, 2017; Pevzner et al., 2020a). The DAS amplitude is inversely proportional to the acoustic quantity

$$(A_{DAS})^{-1} \sim (\rho V_P^3)^{0.5}, \quad (1)$$

where ρ is the density and V_P is the compressional wave velocity. The downhole DAS array records these regularly occurring events (particularly blasting, which has a firm daily schedule) with a very high signal-to-noise ratio and provides a clear path for practical monitoring of the near-well formation properties.

A comparison of elastic properties from wireline log data and DAS amplitude for one of the blasting events is shown in Figure 8. Note that the lower amplitude (higher inverse amplitude) in the section above 586 m corresponds to the intermediate casing and may indicate poorer coupling between borehole and the formation in this section. Each event may have different absolute amplitude and the measurement provides only a relative spatial variation.

Repeating surface events. Several surface seismic events associated with human activity were detected during the trial. Figure 9 shows examples of those events.

Figures 9a and 9b show P- and S-waves whereas Figure 9c has only the S-wave. The shape of the P-waves traveltime curves suggests that these events originated at the surface not too far from the well. Figure 10a shows a stack of eight repeated events found within the recorded data set compared to a single shot (with similar offset) from 3D VSP data acquired in 2017 from the same well using a 26,000 lb vibroseis source and conventional geophones (Figure 10b).

Having small-offset surface events recorded by DAS gives an opportunity to derive a velocity profile of the P- and, potentially, S-waves. Figure 11 shows the comparison between P-wave velocity profiles from the sonic log data and estimated from the passive DAS recordings. Joined analysis of the traveltimes from the near-offset events and amplitudes from distant blasts and earthquakes has a potential to provide independent estimates of both velocities and densities of near-well formations and their variation over time. Quality of the passive VSP data can be improved by stacking more repeating events potentially reaching the point that we can also use reflected waves for imaging purposes.

In-well repeating impulse events. DAS also recorded some unexpected events (Figure 12). Their central frequency is close to 200 Hz, while the symmetrical straight-line traveltime curve indicates that the source is located in the wellbore itself (or very close to

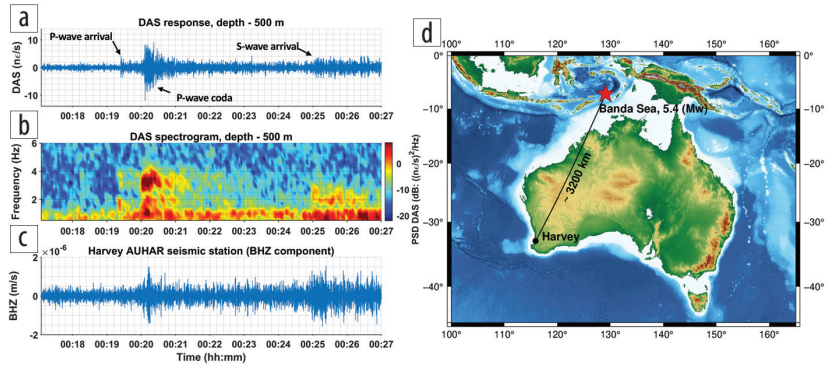

Figure 7. Example of the teleseismic event recorded by fiber optics in the abandoned Harvey 3 well. (d) Earthquake epicenter location relatively to Harvey, WA. (a) Time-series response of a single DAS channel at 500 m depth. (b) Spectrogram of the DAS trace. (c) Vertical component recorded by the local seismic station located in St Anne's School, Harvey, WA.

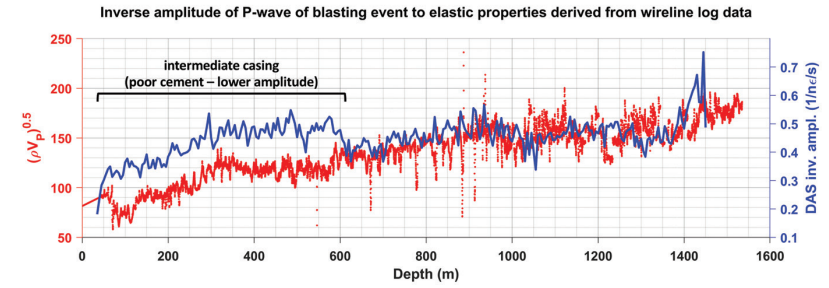

Figure 8. Inverse amplitude of P-wave produced by blasting event on 24 May compared to elastic properties $(\rho V_P^3)0.5$ derived from wireline log data.

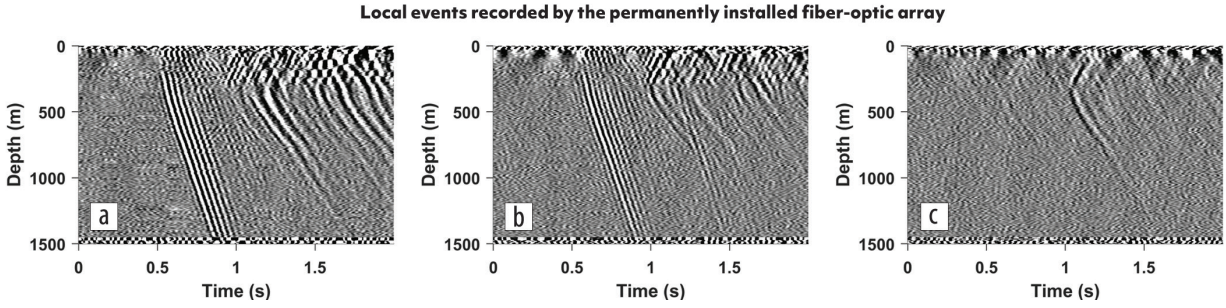

Figure 9. Local events recorded in Harvey 3 well.

DOI:10.1190/tle41020140.1

it). The depth of the sources varies from 200 to 385 m, and the energy propagates up and down the wellbore within the depth interval corresponding to the intermediate casing. The apparent velocity of the propagating wave is 4.5 km/s, which is typical for a tube wave traveling within the casing.

Overall, 14 such events were detected. The existence of the events may indicate some defects in the quality of the cement between the main and intermediate casing strings. Similar events were described by Bakulin and Korneev (2008) in which unwanted cracks and channels lead to fluid exchange through developing conduits in the cement behind the casing (known as "crossflow"). The crossflow is caused by the pressure difference between different formations. This is an important observation for monitoring P&A wells and can be used immediately in similar situations.

Discussion and conclusions

Installation of a fiber-optic cable in the Harvey 3 well provided a unique opportunity to monitor P&A operations, verify the quality of the cement job, and create a permanent seismic and temperature sensor for future passive and active geophysical surveys.

Fiber-optic-sensing data recorded during the cementing operations reveal an abundance of valuable information about the course of the decommissioning process and the quality of the cement job. The DAS monitoring has detected vibrational disturbances during the cement's setting up, while DTS helped to assess setting up of the cement and curing times as well as uniformity of the cementation. However, DTS has relatively coarse temporal sampling; using finer sampling in DTS might be useful to help identify the origin of some anomalies recorded at the same time by DAS.

A subsequent weeklong trial acquisition of passive seismic data using the previously installed vertical sensing array shows an abundance of seismic events in a wide frequency range including the ultra-low part of the spectrum down to at least approximately 10 mHz. The downhole DAS array allows an analysis of the depth variation of traveltimes and amplitudes of these events, which include earthquakes, mine blasts, ocean microseisms, and local human activity.

The amplitudes of waves from distant seismic events can be used to estimate and monitor physical properties of the media along the entire extent of the well. When used in combination with active

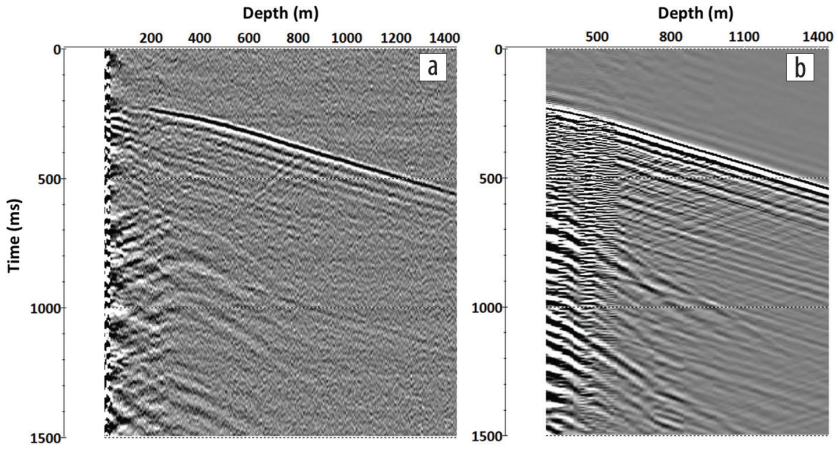

Figure 10. (a) Stack of eight repeating surface events recorded by the cemented fiber-optic array compared to (b) active VSP data acquired in 2017 from the same offset using 26,000 lb vibroseis and 3C geophones.

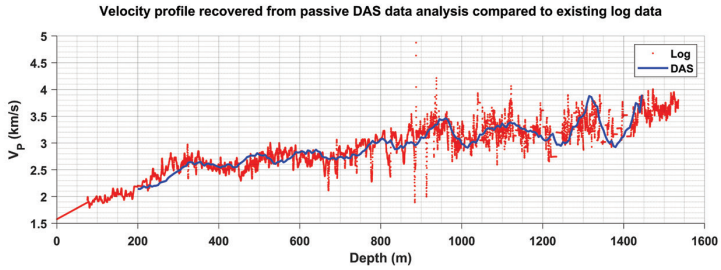

Figure 11. Velocity profile recovered from passive DAS data analysis (blue) compared to existing log data (red).

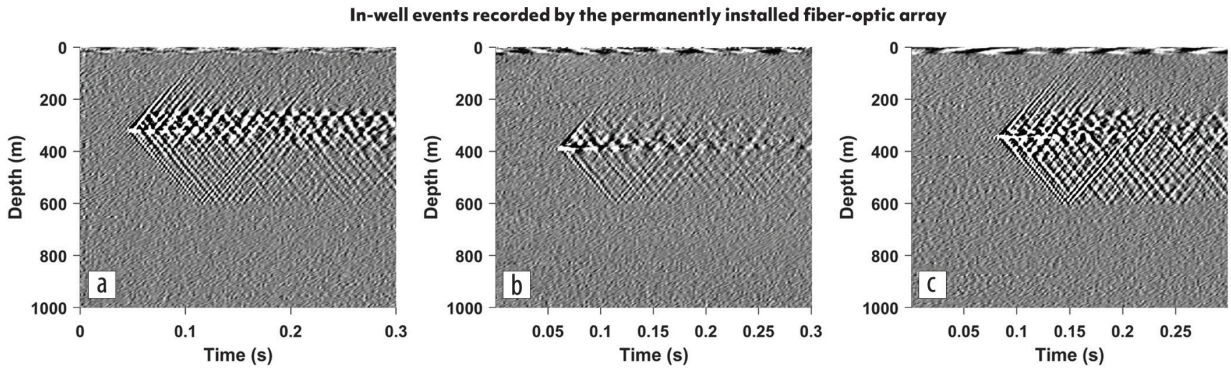

Figure 12. High-frequency in-well events propagating within the intermediate casing section and recorded by the fiber-optic array.

VSP acquired using either controlled or a random source of energy located near the well, these events can help obtain independent estimates of velocities and densities.

Spectral analysis of low-frequency microseisms shows a strong correlation between passively recorded DAS and local weather observations. This shows that the ability to continuously record oceanic microseisms at low frequencies opens up opportunities to employ such arrays for wave climate studies.

In addition, the data contain peculiar in-hole reverberations likely caused by crossflow of groundwater behind the intermediate casing, which may indicate imperfections of the cement job. This information can be used to better understand fluid flows and identify any early onsets of corrosion or other damage, which may be useful as preventive measure in producing wells. Such information can also be considered in a future well design.

The Harvey 3 site is located not far from a population center in an extensively studied area away from urban noise. Thus, the downhole fiber-optic array represents an opportunity to establish an excellent diagnostic facility for continuous recording of passive and active geophysical data and for exploring various applications. For example, a group of wells instrumented with fiber-optic sensors can be utilized for multilateration of regional earthquakes and mine blasts.

Overall, the variety of observations made during this study indicates a strong potential of such installations for many applications. At the moment of writing, we are not aware of another public-domain example with integrated, postabandonment analysis using distributed fiber-optic sensing technology. The bigger picture is that any onshore well coming for P&A can be equipped with a fiber-optic cable. This can provide an opportunity to build a continent-scale network of vertical sensing arrays gathering information about seismic events, global heat flow, and crustal state of stress. TLE

Acknowledgments

The authors are grateful to the Department of Mines, Industry Regulation and Safety of Western Australia for partially funding the work. Parts of this research also have been supported by Curtin Reservoir Geophysical Consortium and the Mineral Exploration Cooperative Research Centre whose activities are funded by the Australian Government's Cooperative Research Centre Program. Seismic data were retrieved from the AusPass archive (http://auspass.edu.au/) under a Creative Commons Attribution 4.0 International license (CC BY 4.0: https://creativecommons.org/licenses/by/4.0/). The data from the AuSIS network were discussed in the "Mine blastings and earthquakes" section. E. S. thanks Curtin Oil and Gas Innovation Centre for providing a PhD scholarship. We are also grateful to Silixa Ltd. for providing iDAS interrogator for our studies.

Data and materials availability

Some data associated with this research are available and can be obtained by contacting the corresponding author.

Corresponding author: evgenysidenko@gmail.com

References

Ajo-Franklin, J. B., S. Dou, N. J. Lindsey, I. Monga, C. Tracy, M. Robertson, V. Rodriguez Tribaldos, et al., 2019, Distributed acoustic sensing using dark fiber for near-surface characterization and broadband seismic event detection: Scientific Reports, **9**, 1328, https://doi.org/10.1038/s41598-018-36675-8.

Bakulin, A., and V. Korneev, 2008, Acoustic signatures of crossflow behind casing in commingled reservoirs: A case study from Teapot Dome: Geophysics, **73**, no. 4, E145–E152, https://doi.org/10.1190/1.2940154.

Balfour, N. J., M. Salmon, and M. Sambridge, 2014, The Australian seismometers in schools network: Education, outreach, research, and monitoring: Seismological Research Letters, **85**, no. 5, 1063–1068, https://doi.org/10.1785/0220140025.

Becker, M., T. Coleman, C. Ciervo, M. Cole, and M. Mondanos, 2017, Fluid pressure sensing with fiber-optic distributed acoustic sensing: The Leading Edge, **36**, no. 12, 1018–1023, https://doi.org/10.1190/tle36121018.1.

Boone, K., A. Ridge, R. Crickmore, and D. Onen, 2014, Detecting leaks in abandoned gas wells with fibre-optic distributed acoustic sensing: International Petroleum Technology Conference, IPTC-17530-MS, https://doi.org/10.2523/IPTC-17530-MS.

Bromirski, P. D., 2002, The near-coastal microseism spectrum: Spatial and temporal wave climate relationships: Journal of Geophysical Research, **107**, no. B8, ESE 5-1–ESE 5-20, https://doi.org/10.1029/2001JB000265.

Bromirski, P. D., R. E. Flick, and N. Graham, 1999, Ocean wave height determined from inland seismometer data: Implications for investigating wave climate changes in the NE Pacific: Journal of Geophysical Research: Oceans, **104**, no. C9, 20753–20766, https://doi.org/10.1029/1999JC900156.

Geoscience Australia, 2020, Earthquakes@GA, https://earthquakes.ga.gov.au, accessed 3 February 2021.

Glubokovskikh, S., R. Pevzner, E. Sidenko, K. Tertyshnikov, B. Gurevich, S. Shatalin, A. Slunyaev, and E. Pelinovsky, 2021, Downhole distributed acoustic sensing provides insights into the structure of short-period ocean-generated seismic wavefield: Journal of Geophysical Research: Solid Earth, **126**, no. 12, e2020JB021463, https://doi.org/10.1029/2020JB021463.

Hasselmann, K., 1963, A statistical analysis of the generation of microseisms: Reviews of Geophysics, **1**, no. 2, 177–210, https://doi.org/10.1029/RG001i002p00177.

Karrenbach, M., S. Cole, A. Ridge, K. Boone, D. Kahn, J. Rich, K. Silver, and D. Langton, 2019, Fiber-optic distributed acoustic sensing of microseismicity, strain and temperature during hydraulic fracturing: Geophysics, **84**, no. 1, D11–D23, https://doi.org/10.1190/geo2017-0396.1.

Kieffer, S. W., 1977, Sound speed in liquid-gas mixtures: Water-air and water-steam: Journal of Geophysical Research, **82**, no. 20, 2895–2904, https://doi.org/10.1029/JB082i020p02895.

Lin, J., S. Fang, X. Li, R. Wu, and H. Zheng, 2018, Seismological observations of ocean swells induced by typhoon Megi using dispersive microseisms recorded in coastal areas: Remote Sensing, **10**, no. 9, 1437, https://doi.org/10.3390/rs10091437.

Lindsey, N. J., T. C. Dawe, and J. B. Ajo-Franklin, 2019, Illuminating seafloor faults and ocean dynamics with dark fiber distributed acoustic sensing: Science, **366**, no. 6469, 1103–1107, https://doi.org/10.1126/science.aay5881.

Manfield, E., G. De Poloni, and J. Hayes, 2020, Ex-Tropical Cyclone Mangga set to bring "once-in-a-decade" storm to Western Australia, https://www.abc.net.au/news/2020-05-23/ex-tropical-cyclone-mangga-brings-one-in-a-decade-storm-to-wa/12279544, accessed 22 December 2021.

Mateeva, A., and P. M. Zwartjes, 2017, Depth calibration of DAS VSP channels: A new data-driven method: 79th Conference and

Exhibition, EAGE, Extended Abstracts, https://doi.org/10.3997/2214-4609.201701201.
Michael, K., A. Avijegon, L. Ricard, M. Myers, K. Tertyshnikov, R. Pevzner, J. Strand, et al., 2019 In-Situ Laboratory for CO_2 controlled-release experiments and monitoring in a fault zone in Western Australia: 2nd Australasian Exploration Geoscience Conference, ASEG Extended Abstracts, https://doi.org/10.1080/22020586.2019.12073207.
Miller, D., T. Coleman, X. Zeng, J. Patterson, E. Reinisch, H. Wang, D. Fratta, et al., 2018, DAS and DTS at Brady Hot Springs: Observations about coupling and coupled interpretations: 43rd Stanford Workshop on Geothermal Reservoir Engineering Stanford Geothermal Workshop.
Nims, P., and M. Pollock, 2015, Harvey-3 final well report: Department of Mines and Petroleum.
Nishida, K., 2017, Ambient seismic wave field: Proceedings of the Japan Academy, Series B, **93**, 423–448, https://doi.org/10.2183/pjab.93.026.
Patterson, J. R., M. Cardiff, T. Coleman, H. Wang, K. L. Feigl, J. Akerley, and P. Spielman, 2017, Geothermal reservoir characterization using distributed temperature sensing at Brady Geothermal Field, Nevada: The Leading Edge, **36**, no. 12, 1024a1–1024a7, https://doi.org/10.1190/tle36121024a1.1.
Pevzner, R., B. Gurevich, A. Pirogova, K. Tertyshnikov, and S. Glubokovskikh, 2020a, Repeat well logging using earthquake wave amplitudes measured by distributed acoustic sensors: The Leading Edge, **39**, no. 7, 513–517, https://doi.org/10.1190/tle39070513.1.
Pevzner, R., K. T. Tertyshnikov, E. Sidenko, R. Isaenkov, S. Glubokovskikh, L. Ricard, B. Gurevich, S. Sharma, and D. Van Gent, 2020b, Underground sounds from an abandoned well: Forensic analysis of distributed acoustic sensing data: EAGE Workshop on Fiber Optic Sensing for Energy Applications in Asia Pacific, https://doi.org/10.3997/2214-4609.202070026.
Ricard, L. P., 2020, Using distributed temperature sensing to inform the quality of cementing operations: SPE Asia Pacific Oil and Gas Conference and Exhibition, SPE-202350-MS, https://doi.org/10.2118/202350-MS.
Ricard, L., R. Pevzner, E. Sidenko, K. Tertyshnikov, S. Sharma, D. Van Gent, and R. Isaenkov, 2019, Transforming an abandoned well into a permanent downhole receiver array: Harvey-3 case study: ASEG Extended Abstracts, https://doi.org/10.1080/22020586.2019.12073043.
Sharma, S., and D. Van Gent, 2018, The Australian South West Hub Project: Developing confidence in migration assisted trapping in a saline aquifer — Understanding uncertainty boundaries through scenarios that stress the models: 14th International Conference on Greenhouse Gas Control Technologies, GHGT-14, https://doi.org/10.2139/ssrn.3366170.
Sharma, S., D. Van Gent, M. Burke, and L. Stelfox, 2017, The Australian South West Hub Project: Developing a storage project in unconventional geology: Energy Procedia, **114**, 4524–4536.
Shulakova, V., K. Tertyshnikov, R. Pevzner, Y. Kovalyshen, A. Bona, and B. Gurevich, 2020, Ambient seismic noise in urban environment: Case study using downhole DAS at Curtin University campus: EAGE Workshop on Fiber Optic Sensing for Energy Applications in Asia Pacific, https://doi.org/10.3997/2214-4609.202070019.
Sidenko, E., R. Pevzner, K. Tertyshnikov, and M. Lebedev, 2021, Effects of temperature on DAS measurements: Second EAGE Workshop on Distributed Fibre Optic Sensing, https://doi.org/10.3997/2214-4609.202131018.
Silixa, 2018, iDAS datasheet, https://silixa.com/wp-content/uploads/iDAS-datasheet-2018-2.pdf, accessed 22 December 2021.
Singh, A., 2018, Final report, special core analysis, selected samples from Wells DMP Harvey-1, DMP Harvey-3 , and DMP Harvey-4 Western Australia: Prepared for Department of Mines and Petroleum, https://www.dmp.wa.gov.au/documents/community-education/Harvey-1-3-4-SCA-Report-Corelab.pdf, accessed 17 January 2022.
Urosevic, M., S. Ziramov, R. Pevzner, K. Tertyshnikov, D. Popik, and D. Van Gent, 2017, CO_2 storage site characterisation at the location of Harvey-3 well, Harvey, Western Australia: EAGE/SEG Research Workshop 2017, https://doi.org/10.3997/2214-4609.201701945.

2.3 Experimental study of temperature change effect on distributed acoustic sensing continuous measurements.

GEOPHYSICS, VOL. 87, NO. 3 (MAY-JUNE 2022); P. D111–D122, 16 FIGS.
10.1190/GEO2021-0524.1

Experimental study of temperature change effect on distributed acoustic sensing continuous measurements

Evgenii Sidenko[1], Konstantin Tertyshnikov[1], Maxim Lebedev[2], and Roman Pevzner[1]

ABSTRACT

Distributed fiber-optic sensing is useful in geophysical exploration and monitoring applications. Distributed temperature sensing (DTS) is used for measuring and monitoring temperature and distributed acoustic sensing (DAS) for recording the seismic wavefield. However, DAS measurements also are sensitive to temperature changes. To understand and quantify the DAS signature of temperature changes during water injections at CO2CRC Otway site, a series of experiments have been conducted at the Curtin University/National Geosequestration Laboratory (NGL) well research facility and Curtin rock-physics laboratory. Overall, three DAS cables are examined. Two fibers are tested in the laboratory and one cable, which is installed behind the casing in the Curtin/NGL well, is examined in the well. Laboratory measurements and observations made during analysis of passive DAS and DTS field data recorded in four Otway wells demonstrate that DAS is sensitive to long-period temperature changes, and its response is proportional to the time derivative of temperature. Induced fiber strain is linearly related to slow temperature change, and this dependency can be estimated for a particular cable. Obtained proportionality constants between strain and temperature change indicate some dependency on the cable type/design and acquisition setup, but they are all of the same order of magnitude. DAS measurements also can be affected by low-frequency noise possibly associated with the effect of temperature on the DAS acquisition unit itself. The results can help compensate for the effect of temperature on low-frequency DAS signals and show that DAS can be used as a distributed temperature sensor if direct temperature measurements are not available.

INTRODUCTION

Fiber-optic (FO) distributed acoustic sensing (DAS) is an emerging technology, which has already found a widespread application in seismic acquisition and reservoir monitoring (Mateeva et al., 2014; Karrenbach et al., 2019; Isaenkov et al., 2021). DAS measurements can be affected by temperature variations caused by natural and industrial processes such as diurnal atmospheric temperature variations, hydraulic fracturing treatments (Bakku et al., 2014; Karrenbach et al., 2017, 2019), borehole fluids flows (Sharma et al., 2020; Titov et al., 2020), or temperature variations in geothermal reservoirs (Miller and Coleman, 2018). Such temperature variations can be considered as a low-frequency signal (<0.1 Hz). This frequency range is far below typical frequencies used in seismic exploration. However, DAS applications often include passive broadband monitoring of the subsurface. Because FO measurements are capable of acquiring data at very low frequencies, passive DAS recording often is used to study natural phenomena at frequencies far below 1 Hz such as distant earthquakes (Ajo-Franklin et al., 2019), oceanic microseisms (Lindsey et al., 2019; Glubokovskikh et al., 2021), and earth tides (Becker and Coleman, 2019). Low-frequency DAS also is being used in different industrial applications, such as hydraulic-fractures geometry characterization (Jin and Roy, 2017), low-frequency strain measurements (Becker et al., 2019), multiphase flow characterization (Titov et al., 2020; Sharma et al., 2021), wellbore gas-influx detection (Feo et al., 2020; Sharma et al., 2021), fluid-pressure sensing (Becker et al., 2017), monitoring of well integrity (Raab et al., 2019), and borehole decommissioning operations (Ricard et al., 2019). Because temperature variations can occur in the same frequency band, they can distort low-frequency seismic records.

Understanding the effect of temperature changes on the strain rate measured by DAS can help to compensate for this effect in the data.

Manuscript received by the Editor 20 August 2021; revised manuscript received 29 December 2021; published ahead of production 31 January 2022; published online 11 March 2022.
[1]Centre for Exploration Geophysics, Curtin University, Kensington, Perth 6151, Australia and CO2CRC Ltd., Melbourne 3053, Australia. E-mail: evgenysidenko@gmail.com (corresponding author); konstantin.Tertyshnikov@curtin.edu.au; R.Pevzner@curtin.edu.au.
[2]Centre for Exploration Geophysics, Curtin University, Kensington, Perth 6151, Australia. E-mail: M.Lebedev@exchange.curtin.edu.au.

DOI:10.1190/geo2021-0524.1

However, the temperature response on DAS should not be always treated as noise. In some situations, for example, when there are no separate temperature measurements, such as distributed temperature sensing (DTS), DAS can be used for relative temperature monitoring as well (Koyamada et al., 2009; Bao and Wang, 2021).

There are two main aspects of how DAS amplitudes can be affected by the temperature change: thermal expansion and refractive index change (thermo-optic effect). Phase-based DAS interrogators measure the phase difference of the backscattered light. From Bakku (2015) and Fang et al. (2012), amplitude dependence on temperature change can be expressed as

$$\Delta\Phi = \Phi\Delta T(\alpha_T + \xi), \tag{1}$$

where $\Delta\Phi$ is the amplitude of the DAS signal (change of optical phase), Φ is the optical phase, ΔT is the temperature change, α_T is the thermal expansion coefficient, and ξ is the thermo-optic effect coefficient. Thermal expansion effect manifests itself as an induced strain, whereas thermo-optic effect changes the refractive index of the fiber. Both of these phenomena have the same effect on DAS measurements because they both change the traveltime of the laser pulse in the fiber. For a silica fiber, the thermal expansion coefficient is $0.5 \cdot 10^{-6}{}^{\circ}\mathrm{C}^{-1}$ (Roy et al., 1989; Feng et al., 2010), and the thermo-optic coefficient is approximately $0.68 \cdot 10^{-5}{}^{\circ}\mathrm{C}^{-1}$ (Palik, 1997; Adamovsky et al., 2012; Gao et al., 2018). These values demonstrate that the temperature effect on DAS is mainly defined by the change of the refractive index (thermo-optic effect). However, different cable designs and ways of cable deployment can behave differently under changing thermal conditions because different materials and compositions will expand/compress differently in response to temperature changes. Thus, DAS response to the changing temperature is likely to depend on a particular cable setup.

To study the temperature effect on DAS in a controlled environment, we first run a series of experiments in Curtin University/National Geosequestration Laboratory (NGL) well and Curtin's rock-physics laboratory. First, to estimate the order of the temperature effect on DAS measurements in the seismically quiet environment (borehole), we conducted the experiment in a research well on the Curtin University campus. Then, to study temperature response on different cables, we conducted an experiment at the Curtin rock-physics laboratory where we organized a heating/cooling setup which allowed us to control the temperature variations. The findings of these controlled experiments are then applied to multiwell DAS observations during water injections performed as part of the Otway CO2 Geosequestration Project. Overall, two different fibers were tested in the laboratory and one cable, which is installed behind the casing in the Curtin/NGL well, was examined at the research facility site. After that, we analyzed passive DAS and DTS field data recorded during water injections within the Otway CO2 geosequestration project.

All experiments show that DAS is sensitive to long-period temperature changes and its strain rate is proportional to the time derivative of temperature. All our tests show a linear dependency of DAS strain-rate response to the temperature time derivative. However, our results show that different cables and different installation designs behave differently under the changing temperature conditions.

Using the linear trend estimated from the data, temperature effect on DAS measurements can be predicted and separated from signals related to purely mechanical deformations. However, different DAS acquisition setups can have different responses to the changing temperature and should be calibrated/tested separately. In addition, our study reveals possible low-frequency equipment-related noise that should be removed from data before low-frequency signal analysis.

BOREHOLE EXPERIMENT: CURTIN/NGL RESEARCH FACILITY

Data acquisition

For the borehole experiment, we acquired data at the Curtin/NGL research facility located at Curtin University main campus in Perth, Western Australia. We used an iDASv2 (Silixa Ltd) interrogator and a BandWeaver DTS (Bandweaver) connected to an FO cable cemented behind the casing of the 900 m deep Curtin/NGL well. The cemented FO cable is a nonmetallic armored loose-tube cable carrying single and multimode fibers, which are housed in individual plastic buffer tubes filled with gel. Figure 1a shows the location of the NGL well facility on the map. DTS and DAS units were placed in the NGL equipment room.

Figure 1b shows the schematic of the NGL well experiment. To explore the effect of a temperature change, we drop 50 kg of ice into the well. The ice stayed at a water level approximately 30 m deep. The ice melted and cooled the borehole water, which caused the temperature decrease of the well's casing and the FO cable cemented behind it. Figure 2 shows the DTS and DAS data recorded during this experiment. Figure 2a and 2b shows four days of DTS data and the time derivative. DTS recording uses 1 m channel spacing. Figure 2c shows 24 h of DAS data decimated to 5 m channel spacing. The vertical dotted black lines in Figure 2a and 2b indicate the start and end times of the DTS record shown in Figure 2c. The temperature anomaly

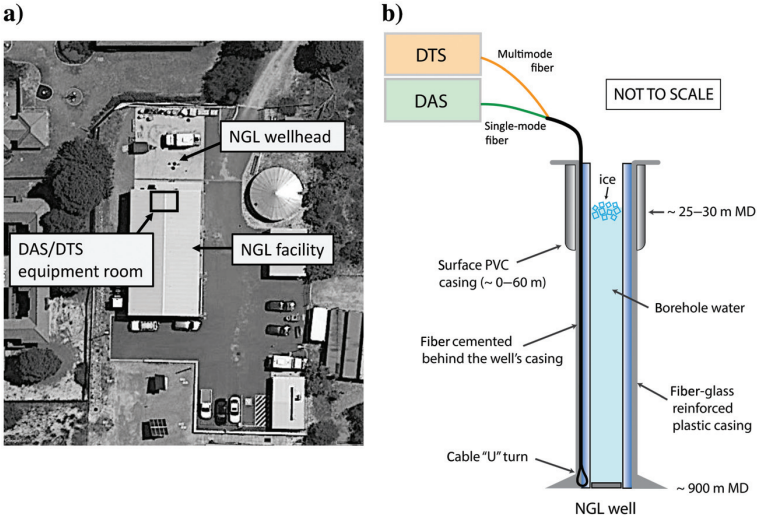

Figure 1. Schematic of NGL well experiment. (a) Satellite image of Curtin NGL well facility; (b) schematic of NGL well experiment.

is clearly visible on DTS and DAS data recorded on 08 July 2020 at the same depth level of approximately 25–30 m.

DTS data are shown in Figure 2a as a temperature change with respect to the baseline (ambient-temperature distribution) temperature. DAS and DTS data in Figure 2 are shown after subtraction of a background trend related to diurnal temperature changes in the room housing the acquisition unit (as described in "Correction of measurements" section). The response from the introduced ice can be traced on DTS data over 2–3 days. DAS measurements demonstrate a shorter visible response of only approximately 3–4 h. From Figure 2, it is clear that the DAS response corresponds to the temperature derivative. This happens because DTS measures the temperature along the fiber, whereas DAS measures the strain rate, which is proportional to the time derivative of temperature. Thus, DAS primarily reacts to the temperature gradient.

Correction of measurements

Besides the signal related to the temperature change and high-frequency random noise, DAS and DTS recordings contain low-frequency periodic common-mode noise of unknown origin (shown by the black arrows in Figure 3). It has been observed (e.g., Wang et al. [2018] Figure 3 and accompanying text) that DAS systems exhibit a small sensitivity to vibration of the interrogator that results in an easily estimated common signal present on all of the DAS traces. It seems that a sensitivity similar to environmental temperature changes occurs and can be remediated in the same way. The form of this noise, its consistency along the fiber, its periodicity, and temporal coincidence on DAS and DTS suggests that it is most likely related to the changing ambient-temperature conditions in the acquisition room housing DAS and DTS interrogators. This temperature change signal can be attributed to the working regime of an air conditioning unit in the room.

To confirm this hypothesis, we ran a separate test in which we logged the temperature in the acquisition room over a few days with a portable temperature logger. The accuracy of the logger is 0.5°C, which is enough to track the temperature trend in the acquisition room. Comparison of the temperature logger data and continuous DAS record is presented in Figure 4. Figure 4a shows the low-frequency DAS signal (strain rate) recorded with the FO cable cemented in the well. It is clear that the DAS signal is changing with time, not with depth. Figure 4b shows the averaged DAS response along the 0–800 m depth interval in the well (the black line) and logged room temperature (the orange line). Comparison of the DAS strain-rate response and temperature log shows that the oscillation period of the temperature logger signal coincides with that of the low-frequency component of the DAS response, which suggests that they are of the same origin. Positive DAS values correspond to the room's decreasing temperature, and vice versa (note that the ice in the borehole caused negative DAS values). The black and orange curves do not have to perfectly match each other because the DAS unit has its own built-in cooling system, so the temperature inside the interrogator can differ from the ambient one. Nevertheless, this test indicates that the presented low-frequency common-mode signal in DAS and DTS recordings is not related to changing conditions in the borehole and should be filtered out or suppressed for further analysis.

To separate the signal of interest (response from the ice) from ambient-temperature-related noise (common-mode noise), we estimated a noise trace for DAS and DTS by averaging the recorded data over the depth range of 600–800 m. Figure 5 shows DAS data before (Figure 5a and 5b) and after (Figure 5c) common-mode noise removal. The horizontal dashed lines in Figure 5a indicate the depth interval used to estimate the DAS common-mode noise. Then, the estimated trace is subtracted from the data. After the noise subtraction, only the signal related to the temperature change is observed on the traces from the "ice" interval and no signal outside the ice interval.

This calibration allowed us to highlight the response of DAS and DTS to the temperature change caused by the ice placed in the borehole. Figure 3 shows DAS and DTS recordings before and after noise subtraction for two different depths in the NGL well. Figure 3a and 3c shows DTS response at the depth of 26 and 847 m, respectively; Figure 3b and 3d shows the DAS response at the same depth points. The depth of 26 m corresponds to the ice level; the depth of 847 m corresponds to the interval with no expected temperature change. (The signal should be constant for DAS and DTS.) All four plots (Figure 3a–3d) present two traces: before and after acquisition noise removal. The black arrows in Figure 3 indicate the acquisition (room) noise. The amplitude of this noise in DAS data is comparable with the temperature response signal. DAS data also are complicated by strong "random" spikes that are related to vibrational (acoustic) signals. For DTS data, the level of the acquisition noise is significantly lower than the signal level. After removal of the acquisition noise, there is no visible signal at 847 m in DAS and DTS data, and, at 26 m depth, DAS and DTS signals are clearer.

Figure 6 shows the trace-to-trace comparison of DAS and DTS response at the ice level after data correction. Figure 6a shows DAS strain rate (black) and DTS time derivative (orange), and Figure 6b shows DAS strain (black) and DTS (orange). The temperature strain rate on DAS is clearly evident and proportional to the temperature (DTS) time derivative. Figure 6b demonstrates an excellent match between strain and temperature. However, the calculated strain has some deviations caused by the integration of DAS data (strain rate) containing high-amplitude spikes. Overall, both plots in Figure 6 suggest that there can be a linear relationship between two time series (strain and temperature change). Simultaneously, obtained

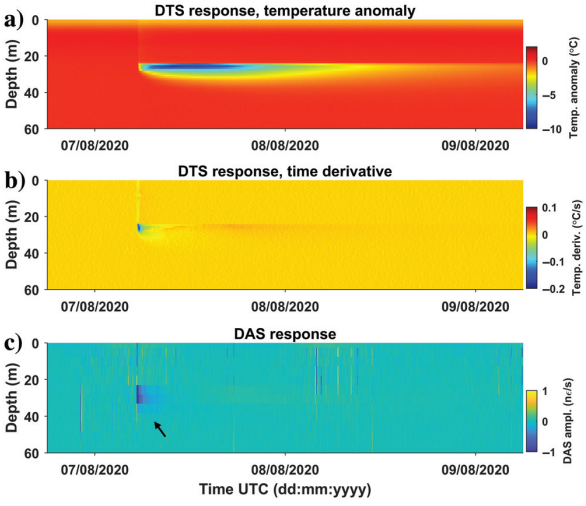

Figure 2. DTS and DAS response to the temperature change in the Curtin/NGL well. (a) DTS response after temperature baseline subtraction, (b) DTS time derivative, and (c) DAS strain-rate response.

DAS and temperature recordings can be used to estimate DAS strain-rate response to the temperature change for a particular acquisition system as demonstrated next.

LABORATORY EXPERIMENT

To study the effect of changing temperature on DAS measurements in controlled temperature conditions, we designed a heating/cooling laboratory setup. We conducted a series of experiments in the Curtin rock-physics laboratory to estimate this effect as well as to gain insights on the influence of different FO cables on such temperature response. The laboratory setup is schematically shown in Figure 7.

We used the same iDASv2 interrogator (exactly the same unit as in the borehole experiment), a water bath coupled with a water heater/cooler, a temperature logger, testing fibers (the fiber submerged in the water bath), and two pieces of reference fibers (coiled fiber connected before and after the water bath). The experiments were done with a bare single-mode fiber and a tight-buffered single-mode fiber. We used the coiled bare single-mode fiber as a reference fiber unaffected by water temperature (spliced to the testing fiber

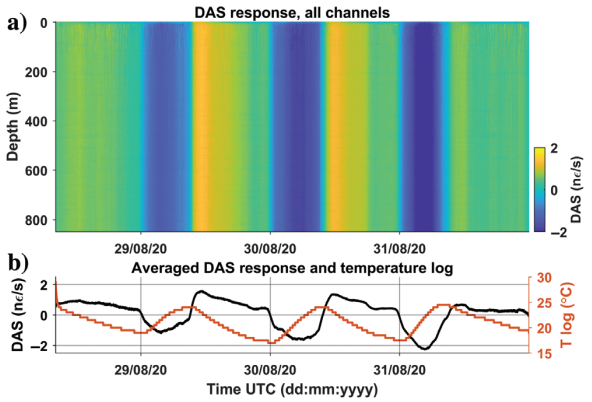

Figure 4. DAS strain-rate response (common-mode noise) to changing room temperature. (a) DAS signal in the NGL well and (b) DAS averaged signal and temperature recorded in the acquisition room.

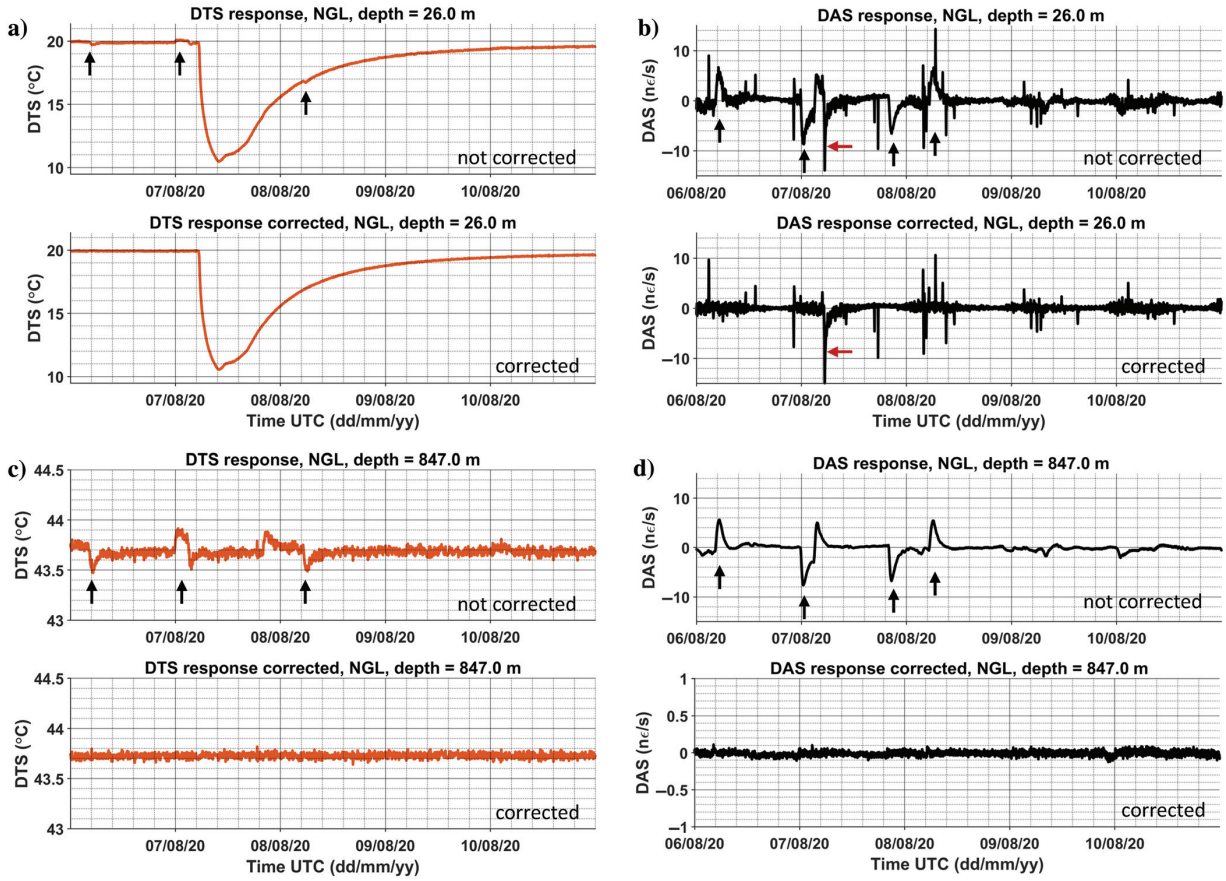

Figure 3. DTS and DAS before and after common-mode noise removal. Common-mode noise is indicated by the black arrows. The red arrows indicate DAS strain-rate response to the temperature change. (a) DTS signal at 26 m depth before and after common-mode noise removal, (b) DAS signal at 26 m depth before and after common-mode noise removal, (c) DTS signal at 847 m depth before and after common-mode noise removal, and (d) DAS signal at 847 m depth before and after common-mode noise removal.

before and after the water bath). Both experiments were conducted with several cycles of heating and cooling.

Figures 8 and 9 show the results of the laboratory test with bare and tight-buffered fibers, respectively. Figures 8a and 9a show the filtered (moving average smoothing) DAS strain-rate response for all DAS channels. The dashed white lines outline margins between three pieces of coiled fibers shown in Figure 7 (two reference coils and a coil in the bath). DAS channels corresponding to the fiber in the water bath show a clear response to the temperature change: the yellow color indicates heating cycles; the blue color corresponds to cooling periods. The temperature logs are shown in the orange color in Figures 8c and 9c, and the time derivatives of temperature are shown in Figures 8b and 9b (the orange color). The black curves in Figure 8b and 8c and Figure 9b and 9c correspond to averaged DAS responses (average trace computed for the channels between two black lines in Figures 8a and 9a) and strain values calculated from DAS strain-rate amplitudes using integration, respectively.

In the bare fiber test, the DAS strain-rate response is very close to the temperature derivative (Figure 8b), whereas the strain calculated from the DAS strain rate looks similar to the temperature log (Figure 8c). These observations indicate a linear dependency between strain and temperature change. Results from the test with a tight-buffered fiber also demonstrate a good correspondence between DAS response and temperature change (Figure 9b and 9c). However, in the tight-buffered fiber test, the correlation between strain and temperature (or strain rate and temperature derivative) is not as strong as for the bare fiber. The estimated values of the Pearson correlation coefficient (Freedman et al., 2007) between the temperature time derivative (dT/dt) and the DAS response (strain rate, $d\varepsilon/dt$) are 0.975 for the bare fiber and 0.93 for the tight-buffered fiber. It seems that the presence of a tight coating in a cable design can cause deviation from linear strain-temperature dependence for a particular DAS-cable combination. To analyze this in more detail, later in the paper, we estimate this dependency between strain and temperature change for both laboratory tests and for the borehole ice experiment.

WATER INJECTIONS AT THE OTWAY SITE

CO2CRC Otway site

CO2CRC Otway Project is a pilot research project focused on the geologic sequestration of CO_2 gas in a deep formation in the Australian State of Victoria (Cook, 2014). The current stage of the project is focused on borehole-based monitoring of a small (15 kt) injection of supercritical CO_2 into a saline aquifer through the CRC-3 well (Jenkins et al., 2017; Isaenkov et al., 2021). This vertical injection well and four slightly deviated monitoring wells (CRC-4, 5, 6, and 7) are being used for seismic, temperature, and pressure monitoring. Figure 10 shows the Otway site map with overlaid monitoring well trajectories. All five wells are equipped with FO sensing equipment: FO cables are cemented behind the casings and connected to DAS (Silixa Carina systems) and DTS (Silixa Ultima DTS) interrogators. A

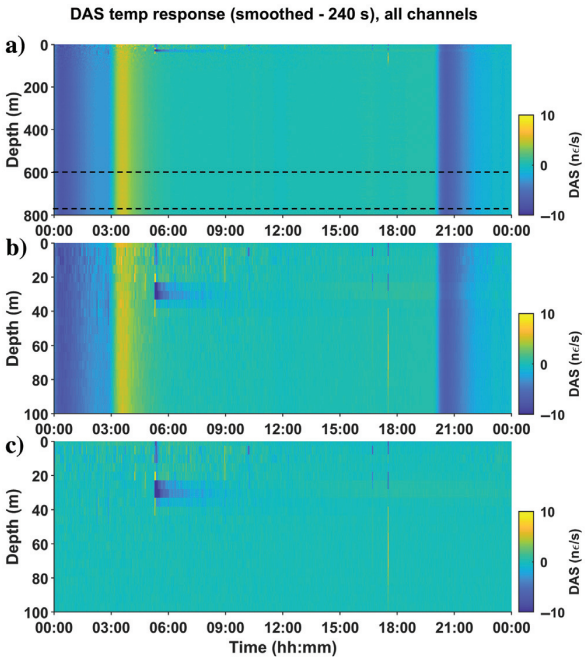

Figure 5. Ice response on DAS data. (a) The whole well interval before the common-mode noise removal, (b) first 100 m of the well before the common-mode noise removal, and (c) first 100 m of the well after the common-mode noise removal. The dashed line in (a) shows the depth interval used to estimate the DAS common-mode noise.

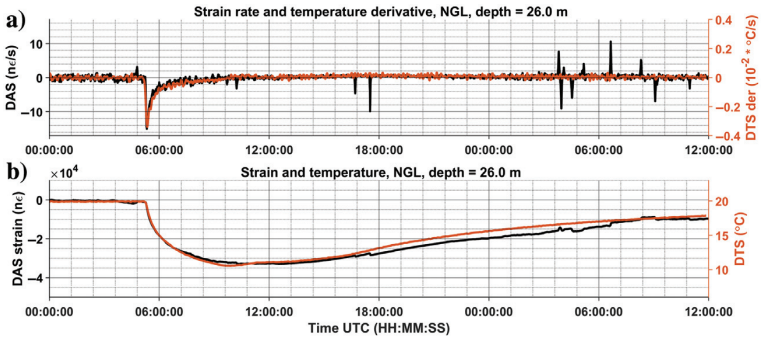

Figure 6. Comparison of DAS and DTS responses. (a) DAS strain-rate response (the black curve) and time derivative of temperature/DTS (the orange curve) and (b) strain (the black curve) calculated from DAS strain rate and DTS response (the orange curve).

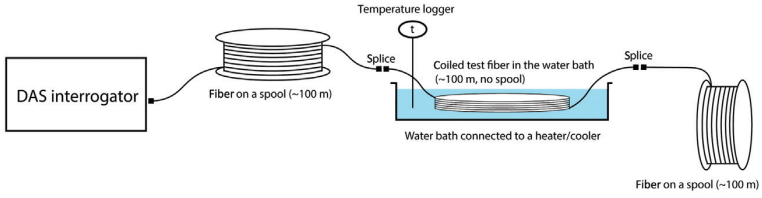

Figure 7. Schematic of the laboratory setup for DAS temperature test.

simplified schematic of FO cable deployment for the CRC-6 and CRC-7 wells is shown in Figure 11. The CRC-6 and CRC-7 wells share the same FO cable for DAS acquisition. Such acquisition design allows the use of a single DAS interrogator for two wells. The cable covers the CRC-7 well first (standard single-mode fiber downhole and engineering fiber uphole) and then CRC-6 (engineering fiber downhole only). DTS data are being acquired separately for both wells using a downhole-uphole cable loop design. Similar to CRC-7 and CRC-6, CRC-4 and CRC-3 share the same DAS cable connected to the same interrogator (CRC-4 first, CRC-3 second). The cable that collects data from CRC-5 well is connected to another DAS unit, which also records surface cable data (follows the CRC-5 well). Detailed description of the Otway project stage-3 setup can be found in Isaenkov et al. (2021).

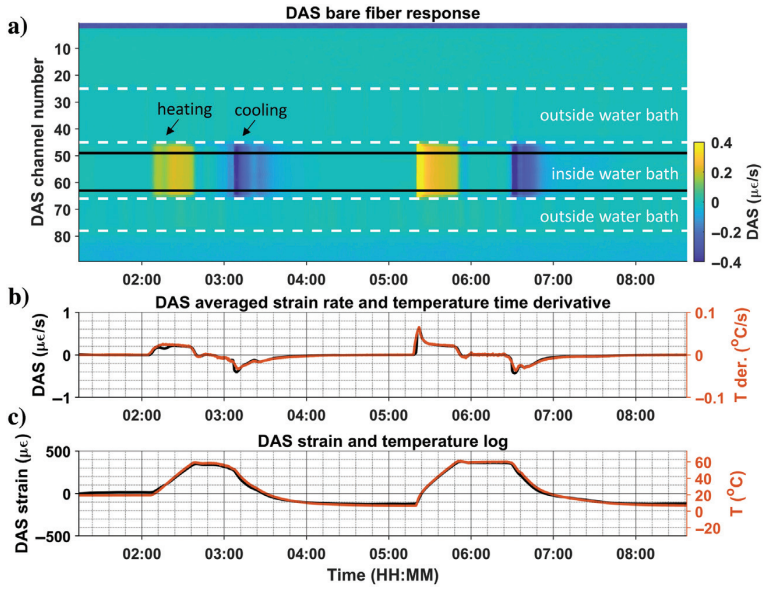

Figure 8. Laboratory test on a bare fiber: (a) DAS strain-rate response over all channels, (b) DAS averaged strain-rate trace (the black curve) and temperature time derivative (the orange curve), and (c) DAS converted to strain (the black curve) and temperature log (the orange curve).

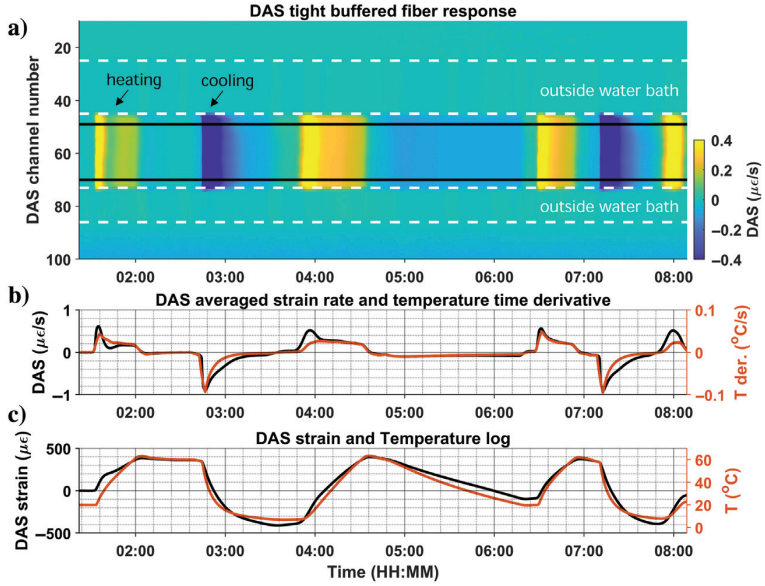

Figure 9. Laboratory test on a tight-buffered fiber: (a) DAS strain-rate response over all channels, (b) DAS averaged strain-rate trace (the black curve) and temperature time derivative (the orange curve), and (c) DAS converted to strain (the black curve) and temperature log (the orange curve).

The CRC-6 and CRC-7 (as well as CRC-4 and CRC-5) wells are slightly deviated (not shown in Figure 11) from approximately 700 m measured depth (MD) to the bottom. The CRC-6 and CRC-7 wells are perforated approximately 1500 m MD and equipped with downhole pressure-temperature gauges installed above perforations. Pressure-temperature gauges are single-point receivers and can be used as a reference for FO sensing data recorded at the same depth.

Water injections

The Otway monitoring design includes pressure tomography, which involves periodic water injections. The first series of water injections were performed in June–July 2020. Water was injected in all wells, except the CRC-3 well. During the injection, water from a surface water tank comes down a borehole and pushes the borehole fluid down along the well. As a result, the temperature is changing (decreasing) at each depth along the borehole due to the borehole fluid (which is initially in thermal equilibrium with the surrounding rocks) being replaced with colder water from the surface. Examples of borehole pressure (black) and temperature (orange) variations recorded by borehole gauges are shown in Figure 12a and 12b. The temperature decrease can reach as much as 25°C. Pressure and temperature changes shown in Figure 12a and 12b clearly indicate the start and end of water injections in the CRC-6 and CRC-7 wells, respectively.

To examine the DAS strain-rate response to the temperature change, we extracted passive DAS data recorded in the CRC-6 and CRC-7 wells during the first water injection in July 2020. Figure 12c and 12d shows spectral density calculated for both wells for a single DAS channel located right above the perforation interval. Corresponding borehole pressure and temperature gauge responses are shown in Figure 12a and 12b.

The spectrograms in Figure 12 show the change of the frequency content in the range of 0.008–10 Hz over time. The frequency band between 0.1 and 1–1.2 Hz mainly contains the signal from secondary oceanic microseisms

(Bromirski, 2002; Nishida, 2017; Glubokovskikh et al., 2021). The dashed ellipses show the temperature response on DAS spectrograms during the water injection in the CRC-6 well. The temperature response can be observed mainly in the frequency range below 0.1 Hz over the time interval that corresponds to the temperature change in the borehole. The cooling down process corresponds to the water injection (pump is on — the pressure is increasing), and the warming up process corresponds to the temperature equilibration process (pump is off — the pressure is returning back to its hydrostatic value). The low-frequency DAS response to the water injection occurs at the same time in both wells (highlighted by the dashed ellipses). However, there is no evidence (Figure 12b) of temperature change in the CRC-7 well during injection in CRC-6 (and vice versa). Thus, the anomaly in the adjacent CRC-7 well is artificial and can be explained with the measurement calibrations inside the DAS interrogator that acquires monitoring data from the CRC-6 and CRC-7 wells simultaneously via the same cable. Besides the low-frequency temperature response, there are strong broadband events that can be mainly observed around the perforation interval and mostly in the injection well. These events can probably be treated as artifacts and could be caused by a direct (strong) temperature impact on the cemented FO cable. Injection in the CRC-7 well started 24 h after the start of the water injection in the CRC-6 well. Similar to the first injection, there is a response in the data from both wells; broadband events are primarily associated with the injector well. A few strong broadband events can be observed on the CRC-6 spectrogram during the injection in the CRC-7 well. However, those events are most likely associated with the previous injection in the CRC-6 well.

Joint DAS/DTS analysis and data calibration

To quantitatively estimate the relationship between DAS measurements and temperature for the water injection effect described in the previous section, we performed a time-domain analysis of DAS and DTS data recorded in the CRC-6 and CRC-7 wells. Figure 13 shows DAS and DTS data recorded during the water injection in the CRC-6 well. Figure 13a shows DTS data: the temperature change in the CRC-6 well. Figure 13b shows DAS data from the CRC-7 well. Figure 13c and 13d shows DAS data from the CRC-6 well before and after correction, respectively. All data in Figure 13 are shown after the removal of the high-frequency component using a moving average filter. Thus, here we are dealing only with low-frequency signals.

DTS data recorded in the CRC-6 well indicate a temperature decrease of more than 20°C (Figure 13a). This value matches the information recorded by the borehole temperature gauge in the well (Figure 12a). Because water is being injected into the formation through the perforated interval of approximately 1500 m MD, there is no evidence of the temperature change below the perforated interval. (Only convectional heat exchange is possible.) The start and stop of the water injection can be easily tracked on DTS data as a temperature decrease at 21:00 and an increase at 03:00.

As expected, CRC-6 DAS data (Figure 13c) recorded above the perforation depth correspond to temperature variations recorded by DTS. The DAS strain-rate signal responds to the time derivative (rate of change) of the temperature. Thus, there is a clear change of polarity along the time vector when the temperature derivative changes the sign from negative to positive. Besides the temperature strain-rate response recorded by DAS, there are series of strong continuous periodic events that occur mainly around the perforation depth. These events correspond to broadband spikes on the DAS spectrogram (Figure 12c). They are most probably related to deformations of the cable or movements that can be caused either by slippage of the fiber core inside the gelled loose tube or by the cable relaxation due to strong direct impact of injected water on the cable at the perforation interval.

The signal on DAS below the perforation depth in the CRC-6 well perfectly repeats the CRC-7 DAS signal, which is uniform

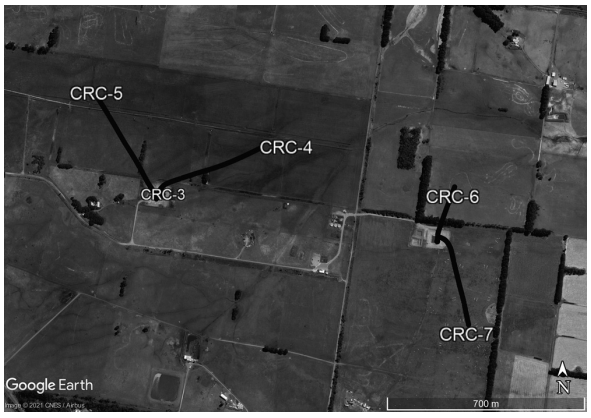

Figure 10. Otway site map. The black lines show projections of monitoring wells' trajectories (CRC-4, -5, -6, and -7) on the surface. The CRC-3 well is a subvertical injection well.

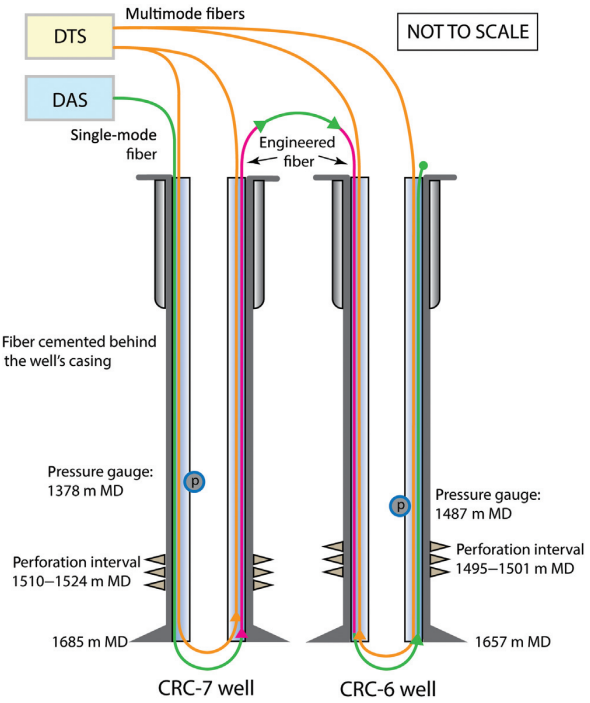

Figure 11. Schematic of the configuration of borehole FO monitoring equipment in the CRC-6 and CRC-7 wells.

along the entire length of the well (Figure 13b). Because there is no evidence of temperature change either in the CRC-6 or CRC-7 well below the perforation, there should be no physical reason that could cause this effect on DAS measurements in the borehole (CRC-7). As such, this signal can be treated as an artificial acquisition noise. The existence of this noise in each well can be explained by the fact that DAS data in both wells are being recorded simultaneously by different parts of the single cable connected to a single interrogator (Figure 11). Because most of the data in CRC-6 are dominated by the presence of the temperature signal, the observed artificial noise results from possible common-mode compensation inside the DAS unit. Nevertheless, this noise can be estimated for each time sample as a truncated mean value over the entire length of the CRC-7 well and then subtracted from the entire CRC-6–CRC-7 data set (Figure 13d). After the subtraction, there is no low-frequency signal related to the temperature change below the perforation interval.

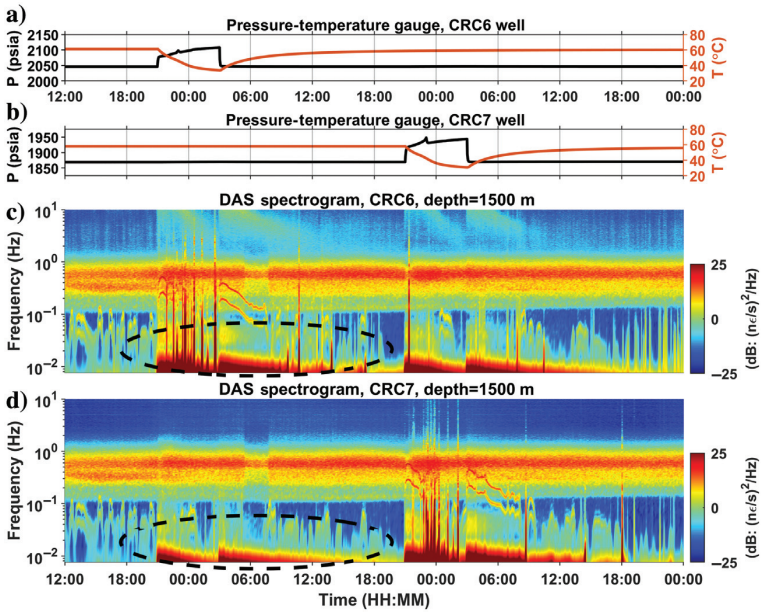

Figure 12. The DAS and pressure-temperature gauge responses to water injections in the CRC-6 and CRC-7 wells. (a and b) Pressure and temperature gauge responses in the CRC-6 and CRC-7 wells, respectively, and (c and d) spectrograms showing low-frequency strain-rate response from water injections in the CRC-6 and CRC-7 wells, respectively.

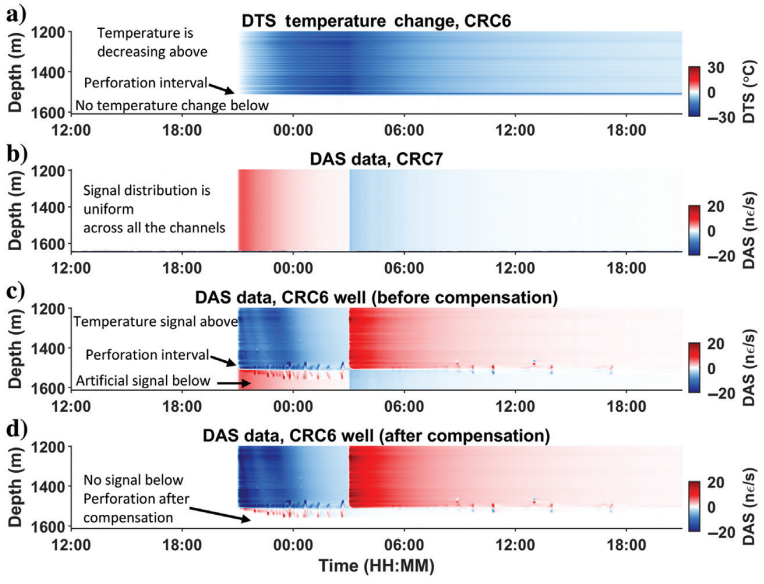

Figure 13. The DTS and DAS data recorded during water injection in the CRC-6 well. (a) The DTS data recorded in the CRC-6 well, (b) DAS data recorded in the CRC-7 well, and (c and d) CRC-6 DAS data before and after signal compensation, respectively.

Figure 14 shows an example of DAS and DTS data recorded during water injections in the CRC-5 well. Similar to the injection in CRC-6, DTS shows no temperature change below the perforation interval (Figure 14a), and the part of the DAS cable buried on the surface (outside the CRC-5 well) has a signal (Figure 14b) similar to CRC-5 below the perforation (Figure 14c). After subtraction of the artificial noise estimated outside the injector well, the signal below perforation disappears (Figure 14d).

QUANTITATIVE DATA ANALYSIS

Simultaneously, recorded temperature data (DTS or temperature logger) and DAS strain-rate data converted to strain (for all previously described acquisitions) allow us to estimate the overall coefficient for a particular FO cable or DAS acquisition setup for all previously described sets of data. To this end, we explore whether this coefficient differs between different cables depending on the installation design. To estimate thermal coefficients for all setups, we build crossplots between strain estimated from DAS amplitudes and temperature change relative to the starting point (baseline value). Crossplots for the NGL well and laboratory experiments are shown in Figure 15. To build these plots, we take a single channel DAS data and temperature responses. Figure 15a shows the strain-temperature relation for the Curtin/NGL well experiment with ice dropped in the borehole; Figure 15b and 15c shows results from the laboratory measurements with a bare fiber and tight-buffered fiber, respectively.

To estimate thermal coefficients (microstrain per degree celsius) for the Curtin/NGL well experiment and laboratory test with the bare fiber, we use linear regression. Crossplots for these two experiments clearly demonstrate the linear relationship between strain and temperature change. Estimated linear trends are shown in orange (Figure 15a) and green (Figure 15b) colors.

The estimated strain-temperature change coefficient for cable cemented in the NGL well is 2.9 and 9.1 με/°C for the bare fiber tested in the laboratory. Each coefficient represents the overall thermal effect for a particular tested cable. Both estimated coefficients are of the same order of magnitude. The estimated coefficient for the bare fiber is close to a thermo-optic coefficient of silica ($dn/dT = \xi * n_{\text{eff}} \approx 10^{-5}$, where n_{eff} is the refractive index of silica). At the same time, it is not clear why the coefficient is lower for the fiber in a gel-fitted loose tube (cable in the well). A similar observation of a low apparent thermal coupling coefficient in a loose-tube optical cable was made by Miller and Coleman (2018). They suggest that the anomaly might be caused by the combined thermal response of the steel tube and its contents (gel and fiber). If the steel tube of the cable expands uniformly (circumferentially and axially), to a greater extent than the gel, the result would be a volume deficit for the gel, which could cause a net axial contracting force applied to the fibers inside.

The trend for the tight-buffered cable (Figure 15c) is not perfectly linear. Significantly, different behavior can be observed from temperature-strain plots in Figure 8b and 8c and Figure 9b and 9c. Figure 8b and 8c shows a much clearer similarity between DAS and temperature time series. At the same time, the experiment with the tight-buffered fiber (Figure 9b and 9c) shows a clear deviation of DAS measurements from the temperature log for rapid heating/cooling intervals. Most likely, the deviation from the linear trend is caused by the presence of a tight coating (acrylate layer), which is firmly bound to the plastic fiber layer and experiences too rapid heating and cooling. Relatively fast temperature variations cause quite complicated interaction between the acrylate coating and the fiber itself due to the different thermal characteristics of these two materials (two orders of magnitude higher for acrylate than glass: 75 versus 0.55 με/°C). In addition, the thermal expansion coefficient and stiffness of plastic coating depend on the temperature that also can cause nonlinear dependence between strain and temperature change at low temperatures, as plastic becomes stiffer. Nevertheless, the right part of the crossplot in Figure 15c shows linear behavior (the blue line). The linear coefficient for this part is 10.5 με/°C, which is slightly higher than the thermal coefficient obtained for the bare fiber (9.1 με/°C). The higher value for the tight-buffered fiber can be explained by the influence of the tight plastic coating, which can result in a larger cumulative thermal effect. However, in the linear segments, the estimated values for both tested fibers are close and comparable to the thermo-optic coefficient for silica (≈10 με/°C).

Figure 16 shows crossplots between DTS temperature change and DAS strain for four different injections (wells). Figure 16a–16d shows

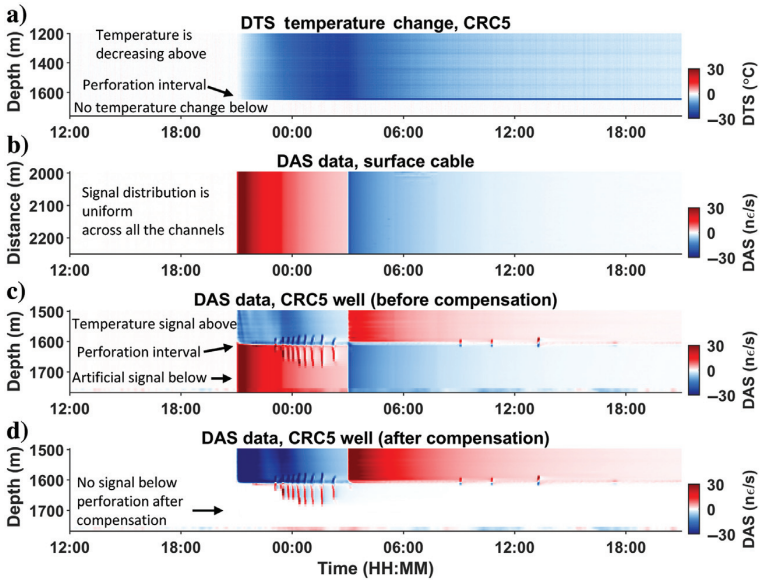

Figure 14. DTS and DAS data recorded during water injection in the CRC-5 well. (a) DTS data recorded in the CRC-5 well, (b) DAS data recorded along the surface part of the DAS cable, and (c and d) CRC-5 DAS data before and after signal compensation.

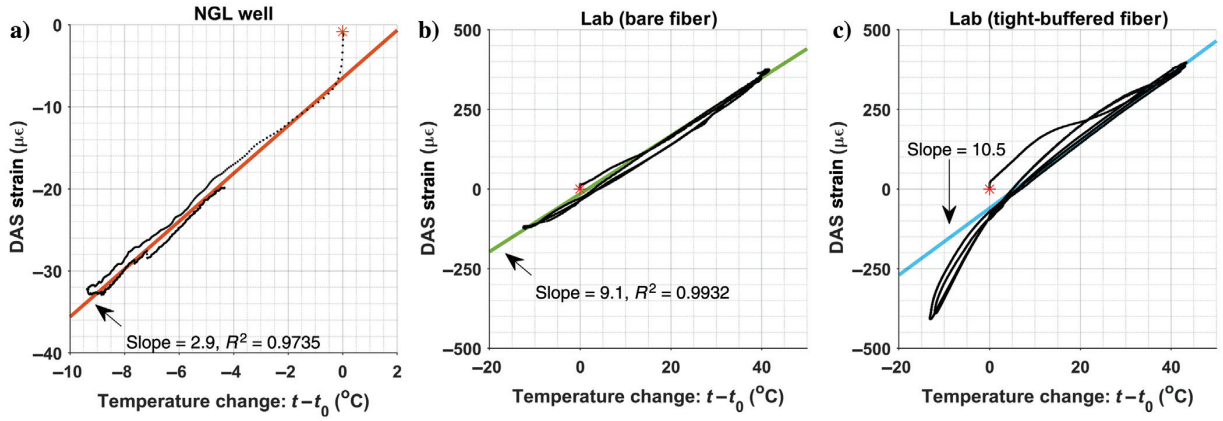

Figure 15. Crossplots between DAS strain and temperature change for the NGL well and laboratory experiment: (a) NGL well (ice level 26 m); (b) bare fiber in water bath (averaged); and (c) tight-buffered fiber in water bath (averaged).

DOI:10.1190/geo2021-0524.1

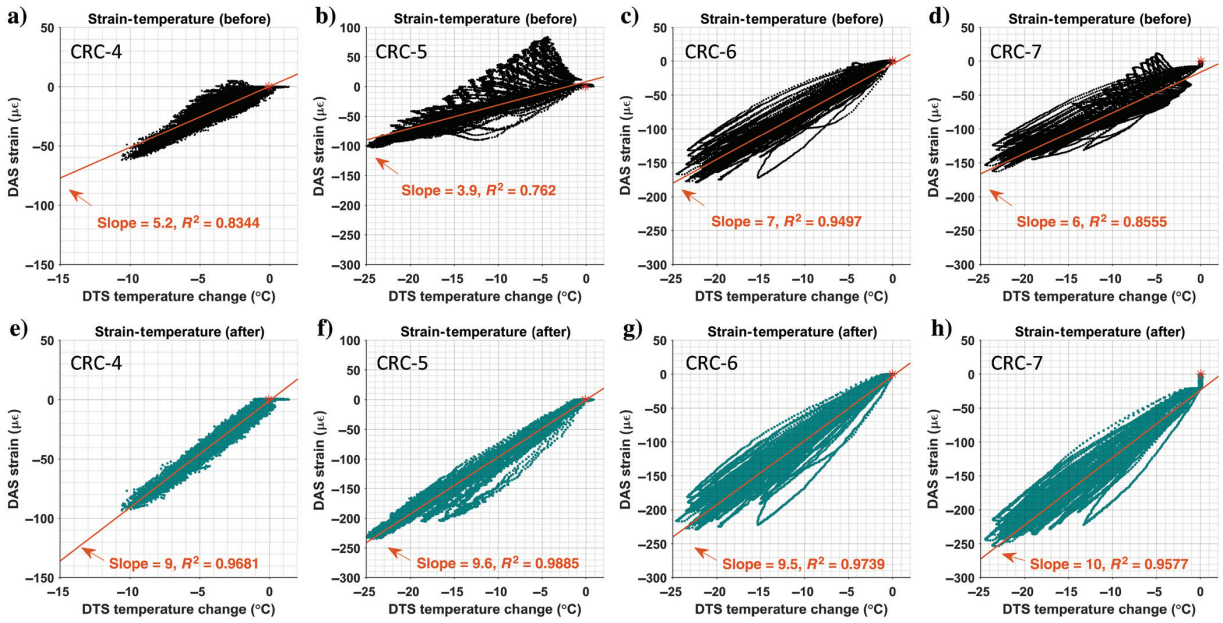

Figure 16. Strain-temperature crossplots between DAS and DTS data recorded during water injections at Otway site. The black plots show relation between temperature change and strain before compensation of acquisition noise; the blue plots show data after compensation of the acquisition noise. (a and b) Water injection in CRC-4, (c and d) water injection in CRC-5, (e and f) water injection in CRC-6, and (g and h) water injection in CRC-7.

DAS-DTS values relationship before signal compensation and Figure 16e–16h shows corresponding data after the signal compensation. The crossplots include data recorded at 10 m intervals from 100 to 1500 m MD (only above the perforation). The orange lines in Figure 16 show a linear regression estimated for each data set. Estimated linear coefficients (slopes) correspond to the strain-temperature dependencies specific for each borehole setup.

Figure 16a–16d demonstrates linear dependency between induced DAS response and temperature change. However, quite strong deviations from a linear trend can be observed for some depths (especially in Figure 16b and 16d). Estimated strain-temperature coefficients change from 3.9 με/°C for the CRC-5 well to 7 με/°C for the CRC-6 well.

Corrected data shown in Figure 16e–16h demonstrate much clearer linearity between DAS and DTS and higher estimations for strain-temperature coefficients. Higher coefficients for the corrected data (Figure 16e–16h) indicate that the applied signal compensation is a valid operation that helps to retrieve more accurate DAS measurements. Increased strain-temperature coefficients (9.5 με/°C on average) are close to the estimation made in the laboratory experiment for a bare fiber (Figure 15b) despite different DAS interrogators used in these two studies.

CONCLUSION

To examine DAS strain-rate response and its sensitivity to changing temperature conditions, we performed three separate tests using the following setups: research NGL well with the FO cable cemented behind the casing, controlled laboratory measurements with two different fibers, and field borehole FO recordings of water injections in four wells at the Otway site. Phase-based DAS is sensitive to temperature time derivative and is able to register very low-frequency signals (<0.01 Hz). Our results demonstrate a linear relationship between DAS response and temperature change. The proportionality constant in these linear relationships has different values for different types of DAS cables and installations, but it is all of the same order of magnitude (from 2.9 to 10.5 με/°C).

The rapid temperature change has a significant effect on DAS measurements and must be taken into account in time-lapse DAS seismic monitoring applications and especially in passive monitoring with the usage of low frequencies.

Knowing a linear dependency between strain and temperature, we can potentially remove low-frequency temperature-related noise from DAS data or use DAS records to estimate temperature variations along the FO cable. Thus, DAS can be potentially used to track temperature changes in the absence of DTS or other direct temperature measurements. However, the usage of DAS and DTS together can be very beneficial because it would allow estimating the thermal effect on DAS measurements and can help separate the temperature effect from the acoustic (seismic) signal.

The data analysis shows that DAS measurements can be affected by the artificial equipment-related noise that should be removed from data before low-frequency data analysis. It is caused by temperature variations in the room housing the acquisition unit and affects the interrogator itself (shown in Curtin/NGL well experiment and iDASv2). This noise appears as a common-mode signal, which is closely correlated with the room temperature. Similar equipment-related noise was observed during water injections in Otway (iDASv3). We observed a weakened temperature signal for the cable section that was affected by the cold water and an artificial signal for the section that was not affected by any temperature variation (adjacent borehole). Thus, this noise possibly appears because

of internal measurements processing (common-mode subtraction). The described noise can be estimated using a reference (not affected by any signals) piece of fiber and subtracted from the data.

Many other aspects such as DAS acquisition parameters (gauge length and pulse length), types of interrogators, type of cable, cable installation designs, etc. influence the DAS measurements. Overall, it is apparent that the combination of a particular FO cable, specific interrogator unit, and deployment strategy should be considered, assessed, and operated as a single acquisition system in which each component has its own contribution to the data quality.

ACKNOWLEDGMENTS

The authors wish to acknowledge assistance provided through ANLEC R&D, supported by Low Emission Technology Australia and the Australian Government through the Department of Industry, Science, Energy and Resources; the Victorian Government, BHP, the Commonwealth Government via the EIF, and the CO2CRC members who have committed their time and support to the Stage 3 Project. CO2CRC wishes to acknowledge the Otway International Test Centre landowners, community, Moyne Shire Council, and regulatory bodies that have supported the site over the past decade of operation. We would like to acknowledge L. Ricard for the help with the DTS data set. E. Sidenko is grateful to C. Otto and the Curtin University Oil and Gas Innovation Centre for providing the Ph.D. stipend. In addition, we would like to thank J. Correa for the idea for this study. Special thanks to B. Gurevich (Curtin University) for his useful advice and help with the manuscript preparation.

DATA AND MATERIALS AVAILABILITY

Some data associated with this research are available and can be obtained by contacting the corresponding author.

REFERENCES

Adamovsky, G., S. F. Lyuksyutov, J. R. MacKey, B. M. Floyd, U. Abeywickrema, I. Fedin, and M. Rackaitis, 2012, Peculiarities of thermo-optic coefficient under different temperature regimes in optical fibers containing fiber Bragg gratings: Optics Communications, **285**, 766–773, doi: 10.1016/j.optcom.2011.10.084.

Ajo-Franklin, J. B., S. Dou, N. J. Lindsey, I. Monga, C. Tracy, M. Robertson, V. Rodriguez Tribaldos, C. Ulrich, B. Freifeld, T. Daley, and X. Li, 2019, Distributed acoustic sensing using dark fiber for near-surface characterization and broadband seismic event detection: Scientific Reports, **9**, 1–14, doi: 10.1038/s41598-018-36675-8.

Bakku, S. K., 2015, Fracture characterization from seismic measurements in a borehole: Massachusetts Institute of Technology, 227.

Bakku, S. K., M. Fehler, P. Wills, J. Mestayer, A. Mateeva, and J. Lopez, 2014, Vertical seismic profiling using distributed acoustic sensing in a hydrofrac treatment well: 84th Annual International Meeting, SEG, Expanded Abstracts, 5024–5028, doi: 10.1190/segam2014-1559.1.

Bao, X., and Y. Wang, 2021, Recent advancements in Rayleigh scattering-based distributed fiber sensors: Advanced Devices & Instrumentation, **2021**, 1–17, doi: 10.34133/2021/8696571.

Becker, M., T. Coleman, C. Ciervo, M. Cole, and M. Mondanos, 2017, Fluid pressure sensing with fiber-optic distributed acoustic sensing: The Leading Edge, **36**, 1018–1023, doi: 10.1190/tle36121018.1.

Becker, M. W., C. Ciervo, and T. Coleman, 2019, Laboratory testing of low frequency strain measured by distributed acoustic sensing: International Exposition and Annual Meeting, SEG 2018, 4963–4966, doi: 10.1190/segam2018-2997900.1.

Becker, M. W., and T. I. Coleman, 2019, Distributed acoustic sensing of strain at earth tide frequencies: Sensors (Switzerland), **19**, 1975, doi: 10.3390/s19091975.

Bromirski, P. D., 2002, The near-coastal microseism spectrum: Spatial and temporal wave climate relationships: Journal of Geophysical Research, **107**, 2166, doi: 10.1029/2001JB000265.

Cook, P., 2014, *G*eologically storing carbon: Learning from the Otway Project experience: CSIRO Publishing.

Fang, Z., K. K. Chin, R. Qu, and H. Cai, 2012, Fundamentals of optical fiber sensors: John Wiley & Sons, Inc.

Feng, X., C. Sun, X. Zhang, and F. Ansari, 2010, Determination of the coefficient of thermal expansion with embedded long-gauge fiber optic sensors: Measurement Science and Technology, **21**, 065302, doi: 10.1088/0957-0233/21/6/065302.

Feo, G., J. Sharma, D. Kortukov, W. Williams, and T. Ogunsanwo, 2020, Distributed fiber optic sensing for real-time monitoring of gas in riser during offshore drilling: Sensors (Switzerland), **20**, 267, doi: 10.3390/s20010267.

Freedman, D., R. Pisani, and R. Purves, 2007, Statistics, 4th ed.: Norton.

Gao, H., Y. Jiang, Y. Cui, L. Zhang, J. Jia, and L. Jiang, 2018, Investigation on the thermo-optic coefficient of silica fiber within a wide temperature range: Journal of Lightwave Technology, **36**, 5881–5886, doi: 10.1109/JLT.2018.2875941.

Glubokovskikh, S., R. Pevzner, E. Sidenko, K. Tertyshnikov, B. Gurevich, S. Shatalin, A. Slunyaev, and E. Pelinovsky, 2021, Downhole distributed acoustic sensing provides insights into the structure of short-period ocean-generated seismic wavefield: Journal of Geophysical Research, Solid Earth, **126**, e2020JB021463, doi: 10.1029/2020JB021463.

Isaenkov, R., R. Pevzner, S. Glubokovskikh, S. Yavuz, A. Yurikov, K. Tertyshnikov, B. Gurevich, J. Correa, T. Wood, B. Freifeld, M. Mondanos, S. Nikolov, and P. Barraclough, 2021, An automated system for continuous monitoring of CO2 geosequestration using multi-well offset VSP with permanent seismic sources and receivers: Stage 3 of the CO2CRC Otway Project: International Journal of Greenhouse Gas Control, **108**, 103317, doi: 10.1016/j.ijggc.2021.103317.

Jenkins, C., S. Marshall, T. Dance, J. Ennis-King, S. Glubokovskikh, B. Gurevich, T. La Force, L. Paterson, R. Pevzner, E. Tenthorey, and M. Watson, 2017, Validating subsurface monitoring as an alternative option to surface M&V — The CO2CRC's Otway Stage 3 Injection: Energy Procedia, **114**, 3374–3384, doi: 10.1016/j.egypro.2017.03.1469.

Jin, G., and B. Roy, 2017, Hydraulic-fracture geometry characterization using low-frequency DAS signal: The Leading Edge, **36**, 975–980, doi: 10.1190/tle36120975.1.

Karrenbach, M., S. Cole, A. Ridge, K. Boone, D. Kahn, J. Rich, K. Silver, and D. Langton, 2019, Fiber-optic distributed acoustic sensing of microseismicity, strain and temperature during hydraulic fracturing: Geophysics, **84**, no. 1, D11–D23, doi: 10.1190/geo2017-0396.1.

Karrenbach, M., A. Ridge, S. Cole, K. Boone, J. Rich, K. Silver, and D. Langton, 2017, DAS microseismic monitoring and integration with strain measurements in hydraulic fracture profiling: Unconventional Resources Technology Conference, SEG, Global Meeting Abstracts, 1316–1330, doi: 10.15530/urtec-2017-2670716.

Koyamada, Y., M. Imahama, K. Kubota, and K. Hogari, 2009, Fiber-optic distributed strain and temperature sensing with very high measurand resolution over long range using coherent OTDR: Journal of Lightwave Technology, **27**, 1142–1146, doi: 10.1109/JLT.2008.928957.

Lindsey, N. J., T. Craig Dawe, and J. B. Ajo-Franklin, 2019, Illuminating seafloor faults and ocean dynamics with dark fiber distributed acoustic sensing: Science, **366**, 1103–1107, doi: 10.1126/science.aay5881.

Mateeva, A., J. Lopez, H. Potters, J. Mestayer, B. Cox, D. Kiyashchenko, P. Wills, S. Grandi, K. Hornman, B. Kuvshinov, W. Berlang, Z. Yang, and R. Detomo, 2014, Distributed acoustic sensing for reservoir monitoring with vertical seismic profiling: Geophysical Prospecting, **62**, 679–692, doi: 10.1111/1365-2478.12116.

Miller, D. E., and T. Coleman, 2018, DAS and DTS at Brady Hot Springs: Observations about coupling and coupled interpretations: Stanford Geothermal Workshop, 1–13.

Nishida, K., 2017, Ambient seismic wave field: Proceedings of the Japan Academy, Series B, **93**, 423–448, doi: 10.2183/pjab.93.026.

Palik, E. D., 1997, Handbook of optical constants of solids: Five-volume set, *in* G. C. Ghosh, ed., Handbook of thermo-optic coefficients of optical materials with applications: Elsevier Science.

Raab, T., T. Reinsch, S. R. Aldaz Cifuentes, and J. Henninges, 2019, Real-time well-integrity monitoring using fiber-optic distributed acoustic sensing: SPE Journal, **24**, 1997–2009, doi: 10.2118/195678-PA.

Ricard, L., R. Pevzner, E. Sidenko, K. Tertyshnikov, S. Sharma, D. Van Gent, and R. Isaenkov, 2019, Transforming an abandoned well into a permanent downhole receiver array: Harvey-3 case study: ASEG Extended Abstracts, 1–4.

Roy, R., D. K. Agrawal, and H. A. McKinstry, 1989, Very low thermal expansion coefficient materials: Annual Review of Materials Science, **19**, 59–81, doi: 10.1146/annurev.ms.19.080189.000423.

Sharma, J., T. Cuny, O. Ogunsanwo, and O. Santos, 2021, Low-frequency distributed acoustic sensing for early gas detection in a wellbore: IEEE Sensors Journal, **21**, 6158–6169, doi: 10.1109/JSEN.2020.3038738.

Sharma, J., O. L. A. Santos, G. Feo, O. Ogunsanwo, and W. Williams, 2020, Well-scale multiphase flow characterization and validation using distributed fiber-optic sensors for gas kick monitoring: Optics Express, **28**, 38773, doi: 10.1364/OE.404981.

Titov, A., Y. Fan, G. Jin, A. Tura, K. Kutun, and J. Miskimins, 2020, Experimental investigation of distributed acoustic fiber-optic sensing in production logging: Thermal slug tracking and multiphase flow characterization: Presented at the Annual Technical Conference and Exhibition, SPE.

Wang, H. F., X. Zeng, D. E. Miller, D. Fratta, K. L. Feigl, C. H. Thurber, and R. J. Mellors, 2018, Ground motion response to an ML 4.3 earthquake using co-located distributed acoustic sensing and seismometer arrays: Geophysical Journal International, **213**, 2020–2036, doi: 10.1093/gji/ggy102.

Biographies and photographs of the authors are not available.

2.4 DAS signature of reservoir pressure changes caused by a CO2 injection: experience from the CO2CRC Otway Project.

International Journal of Greenhouse Gas Control 119 (2022) 103735

Contents lists available at ScienceDirect

International Journal of Greenhouse Gas Control

journal homepage: www.elsevier.com/locate/ijggc

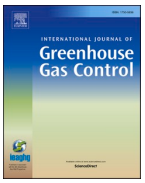

DAS signature of reservoir pressure changes caused by a CO_2 injection: Experience from the CO2CRC Otway Project

Evgenii Sidenko [a,b,*], Konstantin Tertyshnikov [a,b], Boris Gurevich [a,b], Roman Pevzner [a,b]

[a] Centre for Exploration Geophysics, Curtin University, Kensington, Perth 6151, Australia
[b] CO2CRC Ltd., Melbourne 3053, Australia

ARTICLE INFO

Keywords:
Monitoring of CO_2 injection
CO_2 geosequestration
Reservoir pressure monitoring
Distributed fibre-optic sensing
Pressure response on DAS
Borehole geophysics

ABSTRACT

Distributed Acoustic Sensing (DAS) is a fast-developing technology and is being actively used in geophysical monitoring applications. DAS technology is based on continuous measurements along a fibre-optic cable and can record seismic waves/signals that induce axial strain in the cable. Most DAS systems are designed to measure signals higher than 1 Hz; however some DAS systems are sensitive to low-frequency (< 1 Hz) signals such as reservoir pressure variations.

At the time of CO2 injection within the CO2CRC Otway Project, pressure related strain-rate DAS signals were observed in two monitoring wells. These signals are highly correlated with the pressure signals measured by borehole pressure gauges above the perforations in monitoring wells.

Comparison of DAS measurements and pressure measurements shows a linear relationship between the two datasets. Analysis of data shows that DAS is able to detect reservoir pressure variations higher than 10^{-4} psi/s. Analysis of pressure variations and strain calculated from DAS strain rate values allows estimation of the elastic modulus of the reservoir formation.

Obtained results show that DAS systems can be utilised not only as seismic sensors, but also as continuous pressure sensors that can help track possible CO_2 leakages into the overburden. In contrast to traditional pressure gauges, DAS is also capable of tracking the pressure profile along the entire well. DAS pressure sensing capabilities open up many new applications to complement subsurface reservoir pressure monitoring, CCUS and hydrogeological studies.

1. Introduction

Monitoring of the injected CO_2 is one of the key components of Carbon Capture Utilisation and Storage (CCUS) technology, as it allows the prediction, monitoring and tracking of the CO_2 plume. It can also detect possible CO_2 leakages into the overlying strata or along the injection/monitoring well. Monitoring in CCUS often includes borehole pressure monitoring and borehole-based seismic monitoring (Jenkins et al., 2017a). Borehole pressure monitoring is usually implemented with downhole pressure gauges (transducers), which work as point sensors and provide precise measurements of pressure and temperature inside boreholes. Borehole seismic monitoring increasingly uses Distributed Acoustic Sensing (DAS) technology, which provides measurement along the fibre-optic cable along the entire wellbore.

DAS technology is designed to measure and record perturbations that induce strain in the fibre-optic cable. DAS can be utilised in seismic monitoring applications as a continuous borehole vibrational sensor instead of traditional geophones or hydrophones (Parker et al., 2014). As one DAS cable can replace hundreds of geophones, this technology is becoming increasingly popular in reservoir monitoring and vertical seismic profiling (VSP) applications (Correa et al., 2017; Daley et al., 2013; Isaenkov et al., 2021; Mateeva et al., 2014).

Another advantage of DAS compared to geophones is its very broad frequency range. Lindsey et al. (2019) showed that subsea DAS cables can record different types of signals below 1 Hz (such as secondary microseisms, tide bores, sediment transport), which can be used for ocean dynamics studies. Glubokovskikh et al. (2021) demonstrated that borehole-based DAS can be utilised for in-depth characterisation of ambient seismic wavefield generated by ocean waves. Lindsey et al. (2017) and Ajo-Franklin et al. (2019) showed that telecommunication DAS arrays can be used for a broadband seismic monitoring of earthquakes (broadband seismic event detection).

* Corresponding author at: Centre for Exploration Geophysics, Curtin University, 26 Dick Perry Ave, Kensington, WA, 6151, Australia.
E-mail address: evgenysidenko@gmail.com (E. Sidenko).

https://doi.org/10.1016/j.ijggc.2022.103735
Received 24 January 2022; Received in revised form 10 July 2022; Accepted 17 July 2022
Available online 29 July 2022

Being sensitive to slow strain variations, DAS can be utilised for monitoring reservoir temperature (Karrenbach et al., 2019; Miller and Coleman, 2018) and pressure (Becker et al., 2017). In particular, Becker et al. (2017) showed in their experimental study that fibre-optic cables can be utilised to measure oscillating pressure signals at mHz frequencies. In the later study Becker and Coleman (2019) demonstrated that DAS is able to record signals at Earth tide frequencies (down to μHz). Low-frequency DAS is also used for characterisation of induced fractures in geological reservoirs. Becker et al. (2017) also showed that a DAS cable attached to a borehole wall is able to record fracture displacements caused by pressure variations of less than 20 Pa. Jin and Roy (2017) demonstrated examples of using low-frequency DAS to constrain hydraulic fracture geometry. Furthermore, low-frequency capabilities of DAS allow it to be used as a real-time monitoring tool for early detection of gas (kick detection) and for flow characterisation in a wellbore (Feo et al., 2020; Sharma et al., 2021, 2020). Capability of pressure sensing indicates that DAS can be potentially utilised as a distributed sensing tool in harmonic pulse method for leakage detection (Sun et al., 2015). A recent study by Ekechukwu and Sharma (2021) demonstrated that DAS technology can be effectively used for automatic downhole pressure prediction.

Despite the cited research on DAS sensors, their full pressure sensing capabilities are not yet fully understood. The lack of real project demonstrations does not allow the DAS technology to be recognised as a continuous pressure sensor that can be efficiently utilised in different areas such as CO_2 injection monitoring, hydrogeological studies, borehole leakage detection.

The most straightforward fibre-optic technique for monitoring stress variations caused by pressure changes is Distributed Strain Sensing (DSS). However, the CO2CRC Otway project monitoring system is primarily designed for seismic monitoring of the injected CO_2, and does not include DSS measurements. Nevertheless, rapid pressure changes can still be monitored using dynamic (strain rate) measurements with DAS. This is a situation in many field projects, and therefore it is important to understand how effective this method is, its accuracy and limitations. These issues are investigated in this paper.

In this study we explore the capabilities of DAS technology as a continuous pressure sensor in an active CCUS project. To this end, we describe the DAS strain rate response to reservoir pressure changes during CO_2 injection at the CO2CRC Otway injection site. We analyse DAS data and borehole pressure gauge data recorded in monitoring and injection wells. Analysis of low-frequency DAS response indicates a linear relationship between pressure-induced strain rate (time derivative of strain) and pressure variation. Sensitivity of DAS to reservoir pressure change suggests that DAS can be utilised for CO_2 monitoring not only as a seismic sensor, but also as a continuous pressure sensor that can help detect and accurately locate CO_2 leakages.

2. Data: CO2CRC Otway project

The data were acquired in the scope of CO2CRC Otway Project, a pilot research initiative of onshore CO_2 geosequestration in Australia (Cook, 2014). Stage 3 of the Otway project is focused on borehole-based monitoring of a small (15 kt) injection of supercritical CO_2 into a saline aquifer through the CRC-3 (Isaenkov et al., 2021; Jenkins et al., 2017a, b). This injection well and four monitoring wells (CRC-4, 5, 6, 7) are being used for the seismic, temperature and pressure monitoring. Fig. 1 shows the well trajectories (black lines) in plane (a) and 3D (b) views (Glubokovskikh et al., 2016).

All the wells are equipped with fibre-optic sensing equipment: fibre-optic cables are cemented behind casings and connected to DAS (Silixa Carina systems) and DTS (Silixa Ultima DTS) interrogators. A simplified schematic of the fibre-optic cable deployment for CRC-3, CRC-4 and CRC-5 is shown in Fig. 2. The CRC-3 and CRC-4 share the same fibre-optic cable for DAS acquisition. This acquisition design allows the use of a single DAS interrogator for simultaneous data acquisition in several wells. The cable covers the CRC-4 first (standard single-mode fibre downhole and engineering fibre uphole) and then CRC-3 (engineering fibre downhole only). DAS data from CRC-5 is acquired with a separate interrogator, which collects data from the CRC-5 well and along a surface line also using a single continuous fibre-optic cable. Temperature data is acquired with two different DTS units for the CRC-3 and CRC-4; however, the CRC-4 shares the continuous multimode cable with the CRC-5 (Fig. 2). A more detailed description of the Otway project Stage 3 setup can be found in (Isaenkov et al., 2021).

As shown in Fig. 1b, both CRC-4 and CRC-5 are slightly deviated (not shown in Fig. 2) from approximately 700 m measured depth (MD) to the bottom. All the wells are perforated at the Paaratte formation depth interval and equipped with downhole pressure-temperature gauges installed above perforations. CRC-3 has two downhole pressure/temperature gauges installed below and above perforation. These pressure-temperature gauges are single point receivers and can be used as a reference for fibre-optic sensing data recorded at the same depth.

3. Low-frequency pressure signal on DAS passive recordings

Injection of supercritical CO_2 within the CO2CRC Otway Project provided an opportunity to analyse the pressure response of DAS using

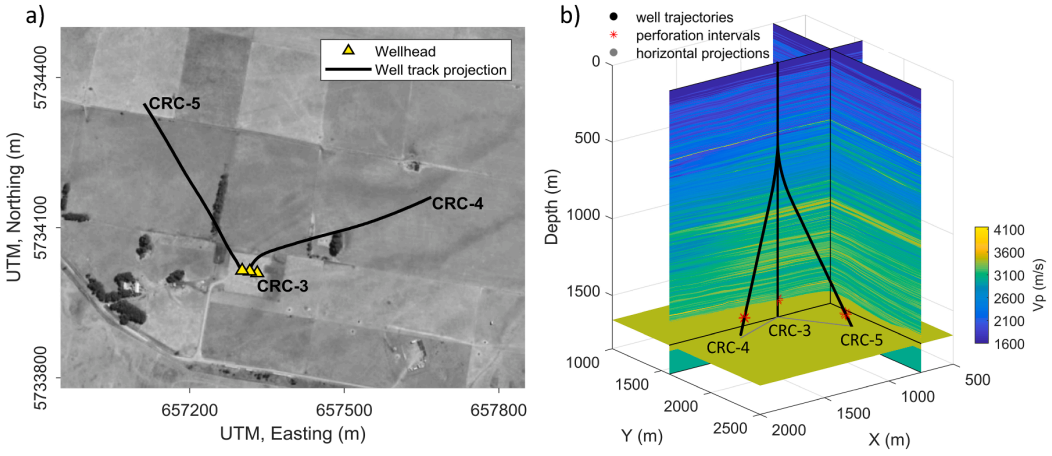

Fig. 1. Otway site map (a) and well trajectories overlaid with Otway site velocity model (b). Black lines show projections of monitoring wells trajectories (CRC-3, CRC-4 and CRC-5) on the surface. CRC-3 is a subvertical injection well.

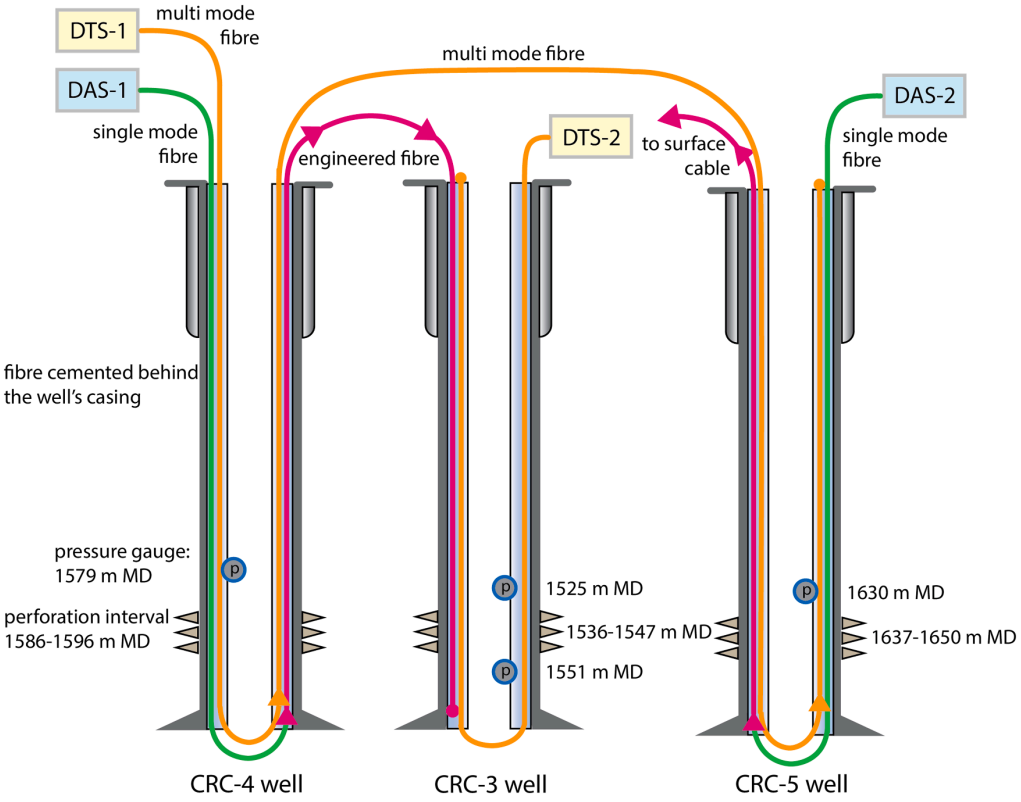

Fig. 2. Schematic of DAS and DTS setup in CRC-3, CRC-4 and CRC-5 wells.

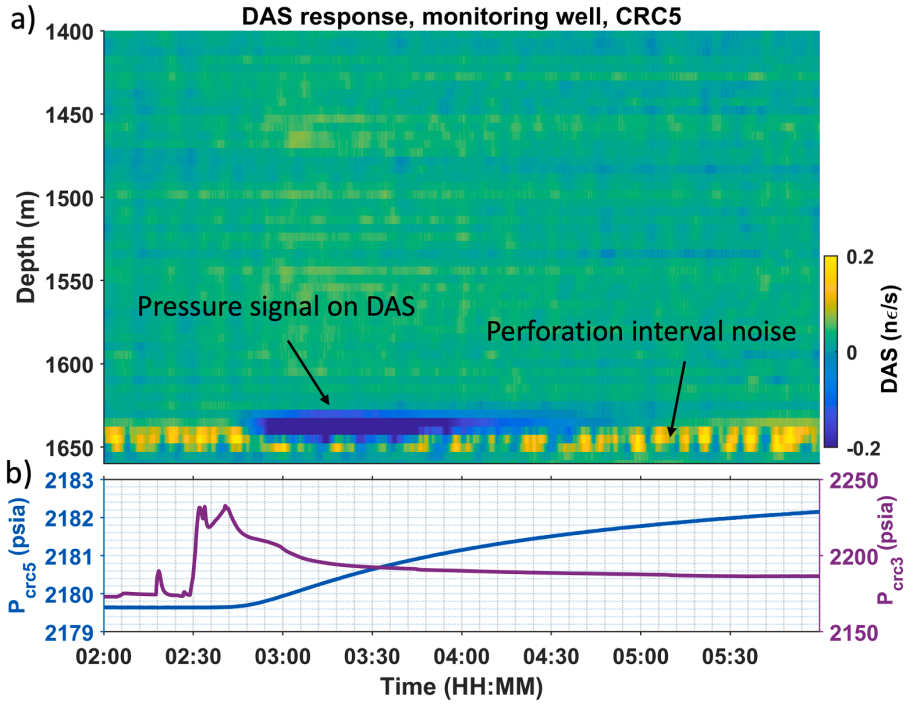

Fig. 3. DAS response to the pressure change in the CRC-5 during CO_2 injection in CRC-3. (a) – DAS response: blue colour corresponds to the increasing pressure; (b) – pressure change recorded by borehole pressure gauges in CRC-3 (purple, right y-axis) and CRC-5 (blue, left y-axis).

data from borehole pressure gauges and data recorded by DAS cables cemented in monitoring and injection wells. The DAS response to pressure changes has been observed in CRC-4 and CRC-5 during the CO_2 injection in CRC-3. As mentioned earlier, CRC-3 and CRC-4 are connected to the same DAS unit via the same fibre-optic cable, while CRC-4 and CRC-5 are connected to the same DTS unit via the same cable (Fig. 2). Low-frequency DAS measurements in a particular borehole can be affected by signals (artificial noise) from another borehole if they are being acquired using the same continuous cable connected to the same DAS interrogator. Thus, comparison of pressure responses between CRC-3 and CRC-5 is more appropriate as these wells are monitored using different DAS interrogators. More details about this issue can be found in the Discussion section and in Sidenko et al. (2021).

Fig. 3 shows DAS response to a pressure change in the CRC-5. Fig. 3a shows DAS data recorded in the 1400 – 1650 m MD interval. The data were smoothed by a moving average filter in 800 s time window. A yellow signal above 1650 m MD indicates noise at the perforation interval of the CRC-5 (1637 – 1650 m). This noise can be possibly related to some filtration processes through the perforation. A blue signal matches the pressure change in CRC5 and corresponds to the strain-rate signal caused by the pressure change in the reservoir. The pressure signal on DAS is present only at the top of the perforation interval and slightly above. Fig. 3b shows hydrostatic pressure recorded in CRC-3 (purple curve) and CRC-5 (blue curve) wells. Note that pressure for CRC-3 and CRC-5 shown in different vertical scales indicated on the right and left axes, respectively. Fig. 3b shows the significant pressure increase in the CRC-3 around 2:30 am UTC due to the CO_2 injection into the formation. Approximately at 2:50 am, pressure starts to increase in the CRC-5 as recorded by the borehole pressure gauge installed right above the perforation interval at 1630 m MD (Fig. 2). The interval between 3:00 and 4:00 am UTC corresponds to the maximum pressure change (dp/dt) in the CRC-5. During this time interval, the DAS response shows a strong signal in the upper part and slightly above the perforation interval. The DAS pressure signal begins to decrease after 4:00 am and disappears after 4:30 am UTC as the pressure change (dp/dt) is significantly decreasing. These observations indicate that DAS is sensitive to the pressure change (pressure time derivative, dp/dt) and can be utilised to monitor pressure distribution (relative pressure change) along the well or/and to detect any potential leakages along the well.

To analyse the DAS pressure response in more detail, in Fig. 4 we show continuous DAS recordings made during an inconsistent working regime of the compressor (pump), when the injection pressure (recorded by a pressure sensor in CRC-3) rose and dropped periodically within a 48 hours' time interval.

Fig. 4c shows the pressure and temperature response recorded in CRC-5 by the borehole pressure/temperature gauge installed at 1630 m MD. The blue line indicates periodic pressure variations in the CRC-5. The maximum pressure variation (difference between highest and lowest pressure) reached almost 3 psi in CRC-5. The orange line shows the temperature variation. It is clear that the temperature in CRC-5 is virtually constant (observed variation < 0.05 °C). Thus, there should not be a temperature related DAS strain rate signal (Sidenko et al., 2021). Fig. 4a shows a smoothed DAS response to the pressure change. The periodic DAS signal in Fig. 4a shows a good match with the pressure change shown in Fig. 4c. The strongest response can be observed at 1635–1640 m MD interval, which corresponds to the top of the perforation interval. Fig. 4b shows a comparison between the DAS strain rate at 1635 m MD (black line) and pressure time derivative dp/dt (blue curve) corresponding to the DAS channel at 1635 mMD indicated by the thin horizontal black line in Fig. 4a. The DAS strain rate response repeats most of the features of the pressure time derivative curve. This indicates that there is a near-linear relationship between strain rate recorded by

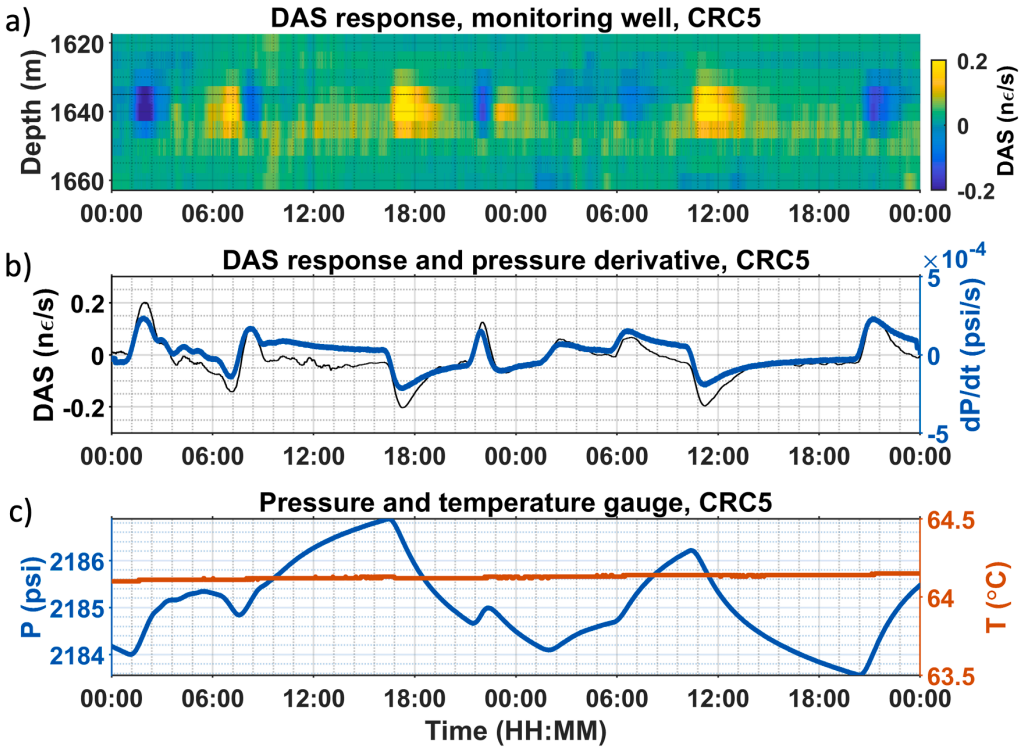

Fig. 4. CRC-5 pressure response to CO_2 injection in CRC-3. (a) - low-frequency DAS response around the perforation interval; (b) - DAS strain rate (black curve) and CRC-5 pressure time derivative (blue curve) comparison (strain rate response corresponds to the DAS channel at 1635 m MD indicated by the thin horizontal black line in plot "a"); (c) – pressure (blue) and temperature (orange) recorded by the borehole pressure gauge installed in CRC-5.

DAS and pressure time derivative. Comparison of the strain rate and pressure data recorded in CRC-5 well indicates that DAS in CRC-5 can accurately record pressure change signals at or above $1 \bullet 10^{-4}$ psi/s.

4. Measurements analysis

The effect of fluid pressure on the DAS response can be quantified by stress-strain relations for a porous rock, which for an isotropic rock can be written as (e.g., Detournay and Cheng (1993), eq. (105); Jaeger et al. (2007), eq. (7.42))

$$\sigma_{ij} + \alpha p \delta_{ij} = 2\mu * \varepsilon *_{ij} + \lambda * \varepsilon * \delta_{ij}. \quad (1)$$

where σ_{ij} is the total stress tensor, $*\varepsilon *_{ij}$ the strain tensor of the solid frame, $*\varepsilon * = *\varepsilon *_{kk} = *\varepsilon *_{xx} + *\varepsilon *_{yy} + *\varepsilon *_{zz}$ the volumetric strain, p the fluid pressure, λ and μ the Lamé constants of the frame (so-called drained moduli), α the Biot effective stress coefficient, and δ_{ij} the Kronecker delta. Injection of fluid into a layer of reservoir rock results in the change of the fluid pressure p, which, according to Eq. (1) results in deformation of the rock. According to the strain convention, a positive normal stress corresponds to tension (Detournay and Cheng, 1993). In contrast, pressure is usually defined as positive in compression: $p = -(\sigma^f_{xx} + \sigma^f_{yy} + \sigma^f_{zz})/3$, where σ^f_{ij} is the (diagonal) stress tensor in the fluid. For a laterally confined (or laterally infinite) reservoir, the horizontal strains are zero, $*\varepsilon *_{xx} = *\varepsilon *_{yy} = \mathbf{0}$ and hence $*\varepsilon * = *\varepsilon *_{zz}$ Then, Eq. (1) for the vertical stress σ_{zz} reduces to

$$\sigma_{zz} + \alpha p = (\lambda + 2\mu) * \varepsilon *_{zz}, \quad (2)$$

cf. Jaeger et al. (2007), eq. (7.100). For a horizontally layered earth, the vertical total stress is the lithostress resulting from the weight of the overburden layers, and is thus independent of the injection pressure, so that $\sigma_{zz} = 0$. Then, Eq. (2) reduces to

$$\alpha p = (\lambda + 2\mu) * \varepsilon *_{zz} \quad (3)$$

or

$$\varepsilon_{zz} = \frac{\alpha}{\lambda + 2\mu} p, \quad (4)$$

where $\lambda + 2\mu$ is the P-wave modulus of the dry frame. For a monomineralic rock (for example, quartz sandstone) with a mineral bulk modulus K_m,

$$\alpha = 1 - \frac{K}{K_m}, \quad (5)$$

where $K = \lambda + 2\mu/3$ is the drained bulk modulus (Detournay and Cheng, 1993; Jaeger et al., 2007). From Caspari et al. (2015), the dry bulk modulus K of core samples from the reservoir level are about 8 GPa. Together with the quartz bulk modulus $K_m = 37$ GPa, Eq. (5) gives $\alpha \approx 0.8$. Note that for such high-porosity rocks, α is relatively insensitive to K.

The strain induced in the fibre-optic cable should be inversely proportional to the P-wave elastic modulus. The strain rate measured by DAS should then be proportional to the effective pressure change:

$$\frac{d\varepsilon_{zz}}{dt} = \frac{dp}{dt}\left(\frac{\alpha}{\lambda + 2\mu}\right) \quad (6)$$

Such linear proportionality between DAS strain rate and pressure time derivative is shown in Fig. 4.

From these plots, the ratio of the induced pressure to DAS strain is about 8 GPa. According to Eq. (6), the corresponding theoretical value from the measured moduli (Caspari et al., 2015) is $(\lambda + 2\mu)/\alpha = (K + 4\mu/3)/\alpha \approx 23$ GPa, i.e., three times higher. Note that theoretical values are derived from measured compressional and shear wave velocities, and thus correspond to so-called dynamic moduli, whereas the ratio of pressure to strain corresponds to static moduli, which are relevant for geomechanical observations. Dynamic moduli are typically higher than static. The factor of 3 difference between dynamic and static moduli is reasonable for soft sandstones (Cheng and Johnston, 1981) and is usually attributed to the contribution of plastic deformation.

There may be some confusion with the use of the terms static and dynamic. As discussed earlier, DAS responds to the strain rate, and in this sense, is a dynamic measurement in contrast to strain sensing, which is (quasi-)static. However, in rock mechanics, the term "dynamic moduli" refers to moduli obtained from elastic-wave velocities (seismic, acoustic or ultrasonic), while moduli obtained from explicit measurements of stress and strain are called static. In this sense, the moduli obtained from DAS and pressure-gauge measurements are static.

5. Discussion

DAS systems are primarily designed to record vibrational signals at frequencies commonly used in seismic exploration. Therefore, not every DAS system can provide reliable measurements below 1 Hz. Nevertheless, some DAS systems are sensitive to far lower frequencies than 1 Hz; however, their sensitivity does decline with decreasing frequency. Thus, DAS is mostly expected to be sensitive to short but strong signals (Becker et al., 2017). In this sense, ideally Distributes Strain Sensing (DSS) systems would be the best method for such a study. But in the absence of that, strain rate DAS can provide reliable measurements for relatively rapid pressure changes (up to several hours). The strain is reconstructed from strain rate by integrating the DAS response, and thus is only known subject to an integration constant or a slow trend.

Indeed, DAS strain rate responds to dynamic pressure change (pressure time derivative). However, as pressure variation drops with the distance from the injector, the ability to detect dynamic pressure changes over large distances depends on the geological setting. In the Otway setup, DAS detected no obvious pressure-related signals in CRC-6 or CRC-7 wells, which are ~1 km away from the injection CRC3 well.

Traditional borehole pressure gauges can provide more precise pressure estimates in the borehole environment and can be used for inter- or cross-well communication detection, leakage detection, pressure monitoring and tomography (Jenkins et al., 2015). However, traditional pressure gauges are usually based on electrical transducers that may fail in harsh environments with high-pressure and/or high temperature (Becker et al., 2017). Borehole gauges also require calibrations and are prone to rate measurement errors and long-term drift (Unneland et al., 1998). Moreover, borehole gauges provide measurement only at a few points along the wellbore. In contrast, DAS uses a fibre-optic cable, which does not have electrical parts, is insensitive to electro-magnetic signals and can withstand harsh borehole environment conditions. In addition, DAS provides continuous measurements along the entire length of the cable.

As mentioned earlier, CRC-3 and CRC-4 are connected to the same DAS unit via the same fibre-optic cable (Fig. 2). Low-frequency DAS measurements in a particular borehole can be affected by signals from another borehole if they are acquired using the same continuous cable connected to the same DAS interrogator (Sidenko et al., 2021). In this case DAS data can be distorted by additional artificial signal that arises perhaps because of the compensation of common-mode signal related to temperature variations. For instance, this can be an issue for "two wells – one interrogator" acquisition setup. Water or CO_2 injection in one of the wells creates a temperature decrease along the entire borehole. This temperature variation causes a strong signal on DAS measurements (almost uniform along the entire fluid injection path) which are proportional to the rate of temperature change. Some DAS interrogators can have build-in compensation algorithms, which can eliminate common-mode temperature effect (by estimating and subtracting the mean value along the entire fibre-optic cable). However, for the acquisition setup described in this study, such common-mode noise compensation can result in artificial signal in the second borehole not

affected by any temperature variation (Sidenko et al., 2021). Thus, in our experiment, comparison of pressure responses between CRC-3 and CRC-5 is more appropriate as these wells are monitored using separate DAS interrogators, and hence, DAS data recorded in CRC-5 should not be distorted by the presence of the equipment/artificial noise caused by CO_2 injection in CRC-3. iDASv3 systems (Silixa Carina systems), utilised in CO2CRC Otway Project, have a fixed Gauge length of 10 m, which is defined during the manufacturing process. Thus, we were not able to test other gauge lengths. It is hard to predict what measurement would look like for different gauge length without field tests. This large gauge length may be a limitation of the study. However, since the reservoir interval is relatively homogeneous, the DAS measurement is probably an adequate estimate of average strain within the interval.

6. Conclusions

Results of our study show that DAS can accurately and continuously record local pressure changes in a dynamic borehole environment. During the Stage 3 of Otway Project we recorded a pressure response on DAS in two monitoring wells from CO_2 injection in the injection well.

Comparison of pressure gauge and DAS data shows that the DAS response is proportional to pressure time derivative and is sensitive to pressure variations as low as 10^{-4} psi/s. Capability of DAS to record such minor pressure deviations opens up a perspective to utilize DAS for CO_2 monitoring not only as a seismic sensor, but as a continuous pressure sensor, which can help track possible CO_2 leakages into the overlying formations (leakage detection). While borehole pressure gauges provide response only from certain depth points, DAS is capable of tracking the pressure profile along the entire well (at 1 m spacing).

The data analysis of strain-pressure relationship provided an estimation of the ratio of the induced pressure to DAS strain of about 8 GPa. The corresponding theoretical value from the measured moduli is 23 GPa, i.e., three times higher. The theoretical values are derived from measured velocities and correspond to the dynamic moduli. Dynamic moduli are typically higher than static, and the observed difference is reasonable for soft sandstones.

Pressure sensing capabilities open up many new applications for DAS technology in subsurface reservoir pressure monitoring, CCS and hydrogeological studies. As the DAS system examined in this study responds to pressure change (pressure time derivative), its sensitivity can be limited by the rate of pressure variations, thus, it can be insensitive to very small and long period signals. This is the major limitation of DAS compared to traditional borehole pressure gauges. Nevertheless, DAS can be utilised in monitoring systems and setups that are not designed to have a dense pressure gauge coverage. In such situations DAS can be used to interpolate pressure data between high sensitivity pressure sensors.

CRediT authorship contribution statement

Evgenii Sidenko: Software, Formal analysis, Investigation, Conceptualization, Data curation, Writing – original draft, Visualization. **Konstantin Tertyshnikov:** Conceptualization, Methodology, Formal analysis, Resources. **Boris Gurevich:** Conceptualization, Formal analysis, Supervision, Writing – original draft. **Roman Pevzner:** Conceptualization, Methodology, Software, Formal analysis, Investigation, Resources, Data curation, Supervision, Project administration.

Declaration of Competing Interest

The authors declare that they have no known competing financial interests or personal relationships that could have appeared to influence the work reported in this paper.

Acknowledgements

The authors wish to acknowledge financial assistance provided through Australian National Low Emissions Coal Research and Development. ANLEC R&D is supported by Low Emission Technology Australia (LETA) and the Australian Government through the Department of Industry, Science, Energy and Resources. Evgenii Sidenko is grateful to Professor Claus Otto and The Curtin University Oil and Gas Innovation Centre for providing the PhD stipend.

References

Ajo-Franklin, J.B., Dou, S., Lindsey, N.J., Monga, I., Tracy, C., Robertson, M., Rodriguez Tribaldos, V., Ulrich, C., Freifeld, B., Daley, T., Li, X., 2019. Distributed acoustic sensing using dark fiber for near-surface characterization and broadband seismic event detection. Sci. Rep. 9 (1), 1–14. https://doi.org/10.1038/s41598-018-36675-8.

Becker, M., Ciervo, C., Cole, M., Coleman, T., Mondanos, M., 2017a. Fracture hydromechanical response measured by fiber optic distributed acoustic sensing at milliHertz frequencies. Geophys. Res. Lett. 44 (14), 7295–7302. https://doi.org/10.1002/2017GL073931.

Becker, M., Coleman, T., Ciervo, C., Cole, M., Mondanos, M., 2017b. Fluid pressure sensing with fiber-optic distributed acoustic sensing. Lead. Edge 36 (12), 1018–1023. https://doi.org/10.1190/tle36121018.1.

Becker, M., Coleman, T.I., 2019. Distributed acoustic sensing of strain at earth tide frequencies. Sensors (9), 19. https://doi.org/10.3390/s19091975.

Caspari, E., Pevzner, R., Gurevich, B., Dance, T., Ennis-King, J., Cinar, Y., Lebedev, M., 2015. Feasibility of CO 2 plume detection using 4D seismic: CO2CRC Otway Project case study — Part 1: Rock-physics modeling. Geophysics 80 (4), B95–B104. https://doi.org/10.1190/geo2014-0459.1.

Cheng, C.H., Johnston, D.H., 1981. Dynamic and static moduli. Geophys. Res. Lett. 8 (1), 39–42.

Cook, P. (2014). *Geologically Storing carbon: Learning from the Otway Project Experience*. CSIRO PUBLISHING.

Correa, J., Egorov, A., Tertyshnikov, K., Bona, A., Pevzner, R., Dean, T., Freifeld, B., Marshall, S., 2017. Analysis of signal to noise and directivity characteristics of DAS VSP at near and far offsets — a CO2CRC Otway Project data example. Lead. Edge 36 (12). https://doi.org/10.1190/tle36120994a1.1, 994a991-994a997.

Daley, T.M., Freifeld, B.M., Ajo-Franklin, J., Dou, S., Pevzner, R., Shulakova, V., Kashikar, S., Miller, D.E., Goetz, J., Henninges, J., Lueth, S., 2013. Field testing of fiber-optic distributed acoustic sensing (DAS) for subsurface seismic monitoring. Lead. Edge 32 (6), 699–706. https://doi.org/10.1190/tle32060699.1.

Detournay, E., & Cheng, A.H.D. (1993). Fundamentals of poroelasticity. In C. Fairhurst (Ed.), *Analysis and Design Methods* (pp. 113–171). Pergamon. https://doi.org/https://doi.org/10.1016/B978-0-08-040615-2.50011-3.

Ekechukwu, G.K., Sharma, J., 2021. Well-scale demonstration of distributed pressure sensing using fiber-optic DAS and DTS. Sci. Rep. 11 (1), 1–18. https://doi.org/10.1038/s41598-021-91916-7.

Feo, G., Sharma, J., Kortukov, D., Williams, W., Ogunsanwo, T., 2020. Distributed fiber optic sensing for real-time monitoring of gas in riser during offshore drilling. Sensors (1), 20. https://doi.org/10.3390/s20010267.

Glubokovskikh, S., Pevzner, R., Dance, T., Caspari, E., Popik, D., Shulakova, V., Gurevich, B., 2016. Seismic monitoring of CO2geosequestration: CO2CRC Otway case study using full 4D FDTD approach. Int. J. Greenh. Gas Control 49 (2016), 201–216. https://doi.org/10.1016/j.ijggc.2016.02.022.

Glubokovskikh, S., Pevzner, R., Sidenko, E., Tertyshnikov, K., Gurevich, B., Shatalin, S., Slunyaev, A., 2021. Downhole distributed acoustic sensing provides insights into the structure of short-period ocean-generated seismic wavefield. J. Geophys. Res. 126 https://doi.org/10.1029/2020JB021463.

Isaenkov, R., Pevzner, R., Glubokovskikh, S., Yavuz, S., Yurikov, A., Tertyshnikov, K., Gurevich, B., Correa, J., Wood, T., Freifeld, B., Mondanos, M., Nikolov, S., Barraclough, P., 2021. An automated system for continuous monitoring of CO2 geosequestration using multi-well offset VSP with permanent seismic sources and receivers: stage 3 of the CO2CRC Otway Project. Int. J. Greenh. Gas Control 108 (December 2020). https://doi.org/10.1016/j.ijggc.2021.103317, 103317-103317.

Jaeger, J.C., Cook, N.G., & Zimmerman, R. (2007). Fundamentals of Rock Mechanics J.C. Jaeger, N.G.W. Cook, and R.W. Zimmerman (4th. ed.). Malden, MA: Blackwell Pub.

Jenkins, C., Chadwick, A., Hovorka, S.D., 2015. The state of the art in monitoring and verification—ten years on. Int. J. Greenh. Gas Control 40, 312–349. https://doi.org/10.1016/j.ijggc.2015.05.009.

Jenkins, C., Marshall, S., Dance, T., Ennis-King, J., Glubokovskikh, S., Gurevich, B., La Force, T., Paterson, L., Pevzner, R., Tenthorey, E., Watson, M., 2017a. Validating subsurface monitoring as an alternative option to surface M&V - The CO2CRC's Otway Stage 3 injection. Energy Procedia 114 (November 2016), 3374–3384. https://doi.org/10.1016/j.egypro.2017.03.1469.

Jenkins, C., Marshall, S., Dance, T., Ennis-King, J., Glubokovskikh, S., Gurevich, B., La Force, T., Paterson, L., Pevzner, R., Tenthorey, E., Watson, M., 2017b. Validating subsurface monitoring as an alternative option to surface M&V - the CO2CRC's Otway Stage 3 injection. Energy Procedia 114 (November 2016), 3374–3384. https://doi.org/10.1016/j.egypro.2017.03.1469.

Jin, G., Roy, B., 2017. Hydraulic-fracture geometry characterization using low-frequency DAS signal. Lead. Edge 36 (12), 975–980. https://doi.org/10.1190/tle36120975.1.

Karrenbach, M., Cole, S., Ridge, A., Boone, K., Kahn, D., Rich, J., Silver, K., Langton, D., 2019. Fiber-optic distributed acoustic sensing of microseismicity, strain and temperature during hydraulic fracturing. Geophysics 84 (1), D11–D23. https://doi.org/10.1190/geo2017-0396.1.

Lindsey, N.J., Craig Dawe, T., Ajo-Franklin, J.B., 2019. Illuminating seafloor faults and ocean dynamics with dark fiber distributed acoustic sensing. Science 366 (6469), 1103–1107. https://doi.org/10.1126/science.aay5881.

Lindsey, N.J., Martin, E.R., Dreger, D.S., Freifeld, B., Cole, S., James, S.R., Biondi, B.L., Ajo-Franklin, J.B., 2017. Fiber-optic network observations of earthquake wavefields. Geophys. Res. Lett. 44 (23), 11. https://doi.org/10.1002/2017GL075722, 792-711,799.

Mateeva, A., Lopez, J., Potters, H., Mestayer, J., Cox, B., Kiyashchenko, D., Wills, P., Grandi, S., Hornman, K., Kuvshinov, B., Berlang, W., Yang, Z., Detomo, R., 2014. Distributed acoustic sensing for reservoir monitoring with vertical seismic profiling. Geophys. Prospect. 62 (4), 679–692. https://doi.org/10.1111/1365-2478.12116.

Miller, D.E., Coleman, T., 2018. DAS and DTS at BradyHot springs: observations about coupling and coupled interpretations. Stanf. Geotherm. Workshop (March 2016), 1–13.

Parker, T., Shatalin, S., Farhadiroushan, M., 2014. Distributed Acoustic Sensing – a new tool for seismic applications. First Break 32 (2010), 61–69. https://doi.org/10.3997/1365-2397.2013034.

Sharma, J., Cuny, T., Ogunsanwo, O., Santos, O., 2021. Low-frequency distributed acoustic sensing for early gas detection in a wellbore. IEEE Sens J 21 (5), 6158–6169. https://doi.org/10.1109/JSEN.2020.3038738.

Sharma, J., Santos, O.L.A., Feo, G., Ogunsanwo, O., Williams, W., 2020. Well-scale multiphase flow characterization and validation using distributed fiber-optic sensors for gas kick monitoring. Opt. Express 28 (26). https://doi.org/10.1364/OE.404981, 38773-38773.

Sidenko, E., Pevzner, R., Tertyshnikov, K., 2021. Compensation of the temperature effect on low-frequency DAS measurements: case study of the water injection at the Otway site. In: First International Meeting for Applied Geoscience & Energy Expanded Abstracts.

Sun, A.Y., Lu, J., Hovorka, S., 2015. A harmonic pulse testing method for leakage detection in deep subsurface storage formations. Water Resour. Res. 51 (6), 4263–4281. https://doi.org/10.1002/2014WR016567.

Unneland, T., Manin, Y., Kuchuk, F., 1998. Permanent gauge pressure and rate measurements for reservoir description and well monitoring: field cases. SPE Reserv. Eng. 1 (3), 224–230. https://doi.org/10.2118/38658-pa.

Appendices

Appendix A

Statements of co-authors

Paper 1.

Sidenko, E., Tertyshnikov, K., Bona, A., & Pevzner, R. (2021). DAS-VSP interferometric imaging:

CO2CRC Otway Project feasibility study. *Interpretation, 9*(4), SJ1-SJ12.

Authors	**Conception and design**	**Acquisition of data**	**Data processing**	**Data analysis**	**Paper writing**	**Paper review**
Evgenii Sidenko			x	x	x	x
I acknowledge that these represent my contribution to the above research output Signed:						
Konstantin Tertyshnikov		x				x
I acknowledge that these represent my contribution to the above research output Signed:						
Andrej Bona	x	x		x		x
I acknowledge that these represent my contribution to the above research output Signed:						
Roman Pevzner	x	x		x		x
I acknowledge that these represent my contribution to the above research output Signed:						

Paper 2.

Sidenko, E., Tertyshnikov, K., Gurevich, B., Isaenkov, R., Ricard, L.P., Sharma, S., Van Gent, D. and Pevzner, R., 2022. Distributed fiber-optic sensing transforms an abandoned well into a permanent geophysical monitoring array: A case study from Australian South West. *The Leading Edge, 41*(2), pp.140-148.

Authors	**Conception and design**	**Acquisition of data**	**Data processing**	**Data analysis**	**Project administration**	**Supervision**	**Paper writing**	**Paper review**
Evgenii Sidenko		x	x	x			x	x
I acknowledge that these represent my contribution to the above research output Signed:								
Konstantin Tertyshnikov	x	x			x			x
I acknowledge that these represent my contribution to the above research output Signed:								
Boris Gurevich				x			x	x
I acknowledge that these represent my contribution to the above research output Signed:								
Isaenkov Roman		x						x
I acknowledge that these represent my contribution to the above research output Signed:								
Ludovic Ricard	x	x	x					x
I acknowledge that these represent my contribution to the above research output Signed:								
Sandeep Sharma	x	x				x		x
I acknowledge that these represent my contribution to the above research output Signed:								
Dominique Van Gent		x			x	x		x
I acknowledge that these represent my contribution to the above research output Signed:								
Roman Pevzner	x	x	x	x	x		x	x
I acknowledge that these represent my contribution to the above research output Signed:								

Paper 3.

Sidenko, E., Tertyshnikov, K., Lebedev, M., & Pevzner, R. (2022). Experimental study of temperature change effect on distributed acoustic sensing continuous measurements. *Geophysics, 87*(3), D111-D122.

Authors	**Conception and design**	**Acquisition of data**	**Design of laboratory setup**	**Data processing**	**Data analysis**	**Paper writing**	**Paper review**
Evgenii Sidenko	x	x	x	x	x	x	x
I acknowledge that these represent my contribution to the above research output Signed:							
Konstantin Tertyshnikov	x	x					x
I acknowledge that these represent my contribution to the above research output Signed:							
Lebedev Maxim	x	x	x				x
I acknowledge that these represent my contribution to the above research output Signed:							
Roman Pevzner	x	x	x		x		x
I acknowledge that these represent my contribution to the above research output Signed:							

Paper 4.

Sidenko, E., Tertyshnikov, K., Gurevich, B., & Pevzner, R. (2022). DAS signature of reservoir pressure changes caused by a CO2 injection: Experience from the CO2CRC Otway Project. *International Journal of Greenhouse Gas Control, 119*, 103735.

Authors	Conception and design	Acquisition of data	Data processing	Data analysis	Paper writing	Paper review
Evgenii Sidenko	x	x	x	x	x	x
I acknowledge that these represent my contribution to the above research output Signed:						
Konstantin Tertyshnikov		x				x
I acknowledge that these represent my contribution to the above research output Signed:						
Boris Gurevich	x			x	x	x
I acknowledge that these represent my contribution to the above research output Signed:						
Roman Pevzner	x	x				x
I acknowledge that these represent my contribution to the above research output Signed:						

Appendix B

Copyright Information

1. Sidenko, E., Tertyshnikov, K., Bona, A. and Pevzner, R. (2021). DAS-VSP interferometric imaging: CO2CRC Otway Project feasibility study. *Interpretation, 9*(4), SJ1-SJ12.

2. Sidenko, E., Tertyshnikov, K., Gurevich, B., Isaenkov, R., Ricard, L.P., Sharma, S., Van Gent, D. and Pevzner, R. (2022). Distributed fibre-optic sensing transforms an abandoned well into a permanent geophysical monitoring array: a case study from Australian South West. *The Leading Edge, 41*(2), 140-148.

3. Sidenko, E., Tertyshnikov, K., Lebedev, M. and Pevzner, R. (2022). Experimental study of temperature change effect on distributed acoustic sensing continuous measurements. *Geophysics, 87*(3), D111-D122.

SEG copyright information can be found here:
https://library.seg.org/page/policies/open-access

SEG allows authors to reuse all or part of their papers in a thesis or dissertation that authors write and are required to submit to satisfy criteria of degree-granting institutions.

Traditional publication (including green open access)

- No author publication charge (APC) is levied, although payment of mandatory page charges are assessed and payment of voluntary charges is requested. Relief from mandatory charges may be requested under SEG's hardship relief policy.
- Copyright is transferred to SEG.
- Authors/employers retain proprietary rights such as the right to patentable subject matter and the right to make oral presentation of the work with full citation and proper copyright acknowledgment.
- Authors/employers enjoy the right to prepare and hold copyright in derivative publications based on the paper provided that the derivative work is published subsequent to the official date of the original paper's publication by SEG.
- Authors/employers may post a final accepted version of the manuscript or the final SEG-formatted version (book chapters excluded) on authors' personal websites, employers' websites, or in institutional repositories operated and controlled exclusively by authors' employers provided that:
  1. the SEG-prepared version is presented without modification;
  2. copyright notice and a full citation appear with the paper;
  3. a link to the SEG version of record in the SEG Library using the digital object identifier (DOI) and a permalink is provided;
  4. the posting is noncommercial in nature, and the paper is made available to users without charge; and
  5. that notice be provided that use is subject to SEG terms of use and conditions.
- Authors/employers may not post their articles in an institutional repository or other site in which the content is required to carry or is implied as carrying a license contrary to SEG copyright and terms of use and terms of this policy.
- Authors of articles, conference proceedings, and book chapters reporting research funded by UK Research & Innovation (UKRI) may post a final accepted version of the manuscript in any institutional or subject repository (e.g., EarthArXiv) without embargo. Manuscripts may be deposited immediately upon acceptance under Creative Commons Attribution 4.0 International (CC BY 4.0) license terms.
- Authors may reuse all or part of their papers published with SEG in a thesis or dissertation that authors write and are required to submit to satisfy criteria of degree-granting institutions.
- Authors/employers have the nonexclusive right, after publication by SEG, to give permission to third parties to republish print versions of the paper, or excerpts therefrom, without obtaining permission from SEG, provided that:
  1. the SEG-prepared version is not used for this purpose;
  2. the paper is not republished in another journal or book; and
  3. the third party does not charge a fee. Permission must be obtained from SEG for other republication of the paper.

4. Sidenko, E., Tertyshnikov, K., Gurevich, B. and Pevzner, R. (2022). DAS signature of reservoir pressure changes caused by a Co2 injection: experience from the CO2CRC Otway Project. *International Journal Of Greenhouse Gas Control, 119*, 10373

Elsevier copyright information can be found here:

https://www.elsevier.com/about/policies/copyright

Elsevier allows authors to use and share their work for scholarly purposes, including for a thesis or dissertation, if they are not published commercially.

Author rights

The below table explains the rights that authors have when they publish with Elsevier, for authors who choose to publish either open access or subscription. These apply to the corresponding author and all co-authors.

Author rights in Elsevier's proprietary journals	Published open access	Published subscription
Retain patent and trademark rights	√	√
Retain the rights to use their research data freely without any restriction	√	√
Receive proper attribution and credit for their published work	√	√
Re-use their own material in new works without permission or payment (with full acknowledgement of the original article): 1. Extend an article to book length 2. Include an article in a subsequent compilation of their own work 3. Re-use portions, excerpts, and their own figures or tables in other works.	√	√
Use and share their works for scholarly purposes (with full acknowledgement of the original article): 1. In their own classroom teaching. Electronic and physical distribution of copies is permitted 2. If an author is speaking at a conference, they can present the article and distribute copies to the attendees 3. Distribute the article, including by email, to their students and to research colleagues who they know for their personal use 4. Share and publicize the article via Share Links, which offers 50 days' free access for anyone, without signup or registration 5. Include in a thesis or dissertation (provided this is not published commercially) 6. Share copies of their article privately as part of an invitation-only work group on commercial sites with which the publisher has a hosting agreement	√	√
Publicly share the preprint on any website or repository at any time.	√	√
Publicly share the accepted manuscript on non-commercial sites	√	√ using a CC BY-NC-ND license and usually only after an embargo period (see Sharing Policy for more information)
Publicly share the final published article	√ in line with the author's choice of end user license	×
Retain copyright	√	×